patients improved their renal function (creatinine range, 99-155 μmol/L; mean follow-up 6 months). Creatinine however remained well above the previous baseline range of 65-77 μmol/L.
Conclusions: IgA-PIGN was mostly found in non-diabetic patients in this study, in contrast with some previous studies showing strong association with diabetic nephropathy. We confirm that IgA-PIGN is often associated with SA and MRSA infections and for the first time we found an association with CMRSA-10. Although renal function improved in all non-diabetic patients, full recovery was not seen in any of the patients during the follow-up.

1549 Genetic Modulation of Anti-Myeloperoxidase Induced Murine Crescentic Glomerulonephritis

H Xiao, YW Zeng, F Pardo-Manuel De Villena, D Ciavatta, R Falk, JC Jenette. University of North Carolina, Chapel Hill, NC.
Background: Anti-neutrophil cytoplasmic autoantibodies (ANCA), including anti-myeloperoxidase (MPO), are associated with crescentic glomerulonephritis (GN). Similar GN is induced in mice by injecting anti-MPO IgG. Patients have a spectrum of ANCA GN severity, whereas the inbred mouse strain that was initially used as a model (C57BL/6) has a narrow range of severity. The experiments reported here demonstrate that anti-MPO IgG causes GN of different severity in genetically different mice that is regulated primarily by differences in leukocyte responsivity to anti-MPO.
Design: Crescentic glomerulonephritis was induced in mice by iv injection of 50 μg/g anti-MPO IgG. Mice were sacrificed on day 6. Anti-MPO was given to: 1) 129S6 mice and C57BL/6 (B6) mice, 2) F1 mice from B6 x 129S6 mice, 3) F2 mice generated by B6 x 129S6 F1 intercross. 4) 129S1 mice, 5) chimeric mice with genetic differences between 129S6 or B6 donor bone marrow (BM) . To test the functional effects of genetically determined differences in disease severity, in vitro activation by anti-MPO IgG was evaluated in neutrophils from B6, 129S6 and 129S mice. Neutrophils were primed with 10ng/ml TNFa, stimulated with anti-MPO IgG, and superoxide generation measured.
Results: After injection of anti-MPO IgG: 1) B6 mice (n=17) developed an average 9% crescents, whereas 129S6 mice (n=13) developed 69% crescents. 2) F1 (B6 x 129S6) mice developed 13.5% crescents. 3) Of 60 F2 mice, 30 had < 10%, 24 10-25 %, 5 26-50% and 1 >50% crescents. 4) 129S1 developed 21% crescents and thus had less disease than 129S6 mice. 5) Rag2-/- B6 mice (n=4) that received BM from 129S6 mice had 79% crescents similar to 129S6 mice; however, Rag2-/-129S6 mice (n=6) that received BM from B6 mice had 17% crescents more similar to B6 mice. In the functional assays, anti-MPO IgG caused more activation of neutrophils from 129S6 mice than neutrophils from B6 or 129S1 mice.
Conclusions: 1) pathogenic events in this model of ANCA disease are influenced by genetic factors, 2) this genetic influence acts primarily through modulation of the responsivity of bone marrow derived cells (e.g. neutrophils) to activation by ANCA, 3) identification of the genes responsible for this modulation should reveal genes and gene products that have important roles in pathogenesis of ANCA disease, and could be markers of disease activity and outcome, as well as targets for therapy.

1550 Phosphorylated Mammalian Target of Rapamycin Is Upregulated in Both Cytoplasm and Nuclei along Cystic Epithelium of Adult Type Polycystic Kidney Disease

PL Zhang, RE Brown, SK Hicks, W Li. William Beaumont Hospital, Royal Oak, MI; University of Texas Health Science Center, Houston, TX.
Background: Mammalian target of rapamycin pathway (mTOR) is a dominant growth pathway in development of polycystic kidney disease (PKD) in both animal models and human adults, since the mutated polycystin-1 gene activated this pathway (PNAS 2006; 103:5466-5471). It is known that phosphorylated form of mTOR complexes with either raptor (to form mTORC1 for activating its downstream signals p70S6K and elF4E to stimulate cell proliferation) or rictor (to form mTORC2, a rapamycin-insensitive complex, for mediating its downstream targets including PKCα). mTORC1 mainly stays in the cytoplasm and mTORC2 is chiefly located in nuclei. In this study, we stained p-mTOR and one of its main down stream signals p-p70S6K in adult type PKD (autosomal dominant) and compared the stain intensity with unremarkable renal tubules.
Design: 10 cases of human adult type of PKD and 10 cases of unremarkable renal parenchyma (from nephrectomy for tumors) were stained for p-mTOR (Ser 2448) and p-p70S6K (Thr 389) (from Cell Signaling Technology), using a Dako Autostainer. Chromogenic cytoplasmic and nuclear staining was assessed and categorized into four grades: 0 (background), 1+ (weak), 2+ (moderate), or 3+ (strong) based on intensity of staining.
Results: In our recent study, we found that all cystic lining stained positively for cytokeratin 7, confirming that the cystic lining of PKD was originated from the distal nephron tubules. In all cases (10/10) of the current study, p-mTOR showed strong (3+) staining in both nuclear and cytoplasmic cellular compartments of both residual distal nephron tubules and cystic lining compared to moderate (2+) cytoplasmic staining of p-mTOR in the normal distal nephron tubules without significant nuclear staining. However, the p-p70S6K showed moderate (2+) nuclear intensity in approximal 50% of cystic lining, similar to the distal nephron tubular epithelium.
Conclusions: In the cystic epithelium and residual distal nephron tubules of PKD, upregulated p-mTOR in both cytoplasm and nuclei may enhance formation of both mTORC1 and mTORC2 . Unchanged expression of p-p70S6K of mTORC1 branch in cystic epithelium implies that p-p70S6K may only partially contribute to cystic formation, whereas the other branch of mTORC1 via elF4E is still under investigation. In contrast, mTORC2 branch may play a major role in the cystic formation of PKD.

1551 The Balance of Thymosin β4 and Its Metabolite Ac-SDKP Modulates Activity of Profibrotic Factors

Y Zuo, SA Potthoff, H-C Yang, L-J Ma, AB Fogo. Vanderbilt University, Nashville, TN.
Background: We have previously shown that the G-actin sequestering protein thymosin β4 (Tβ4) is dramatically upregulated in the obstructed kidney in the unilateral ureteral obstruction (UUO) model of tubulointerstitial fibrosis. Tβ4, which is postulated to have profibrotic effects, is degraded by prolyl oligopeptidase (POP) to Ac-SDKP, a peptide with anti-fibrotic actions. Our previous study further revealed that inhibition of POP altered the balance of Tβ4 and Ac-SDKP and exacerbated fibrosis in obstructed kidneys. We now investigated whether the balance of Tβ4 vs Ac-SDKP also affects kidneys without injury.
Design: Adult male C57BL/6 wild type mice underwent UUO and were divided into five groups: UUO without treatment, UUO+POP inhibitor (S17092, 40mg/kg per day, by gavage), UUO+Tβ4 (150μg/d, i.p.), UUO+combination (POP inhibitor and Tβ4), and UUO+Ac-SDKP (1.6 mg/kg/d, delivered by minipump, starting 5 days before the surgery). Mice were sacrificed 5 days after UUO and the contralateral non-injured kidneys were studied.
Results: POP activity was significantly lower in the contralateral kidneys of mice treated with POP inhibitor, combination or Ac-SDKP (POP inhibitor, 12.7±1.3; combination, 18.3±1.4; Ac-SDKP 25.4±2.6; vs untreated UUO, 40.1±3.0 pmol/min*mg tissue, all $p<0.05$). The Ac-SDKP level in the contralateral kidneys was remarkably increased only in the group receiving Ac-SDKP (Ac-SDKP, 4.06±0.34; untreated UUO, 2.14±0.30 pmol/mg tissue, $p<0.05$). Compared to untreated UUO, plasminogen activator inhibitor (PAI-1) and Tβ4 expression in the contralateral kidneys assessed by real time PCR were dramatically reduced by Ac-SDKP treatment, but not affected by POP inhibitor with or without Tβ4. There was no difference in transforming growth factor (TGF)-β1 mRNA among these five groups.
Conclusions: Our study suggests that exogenous Ac-SDKP may have negative feedback to decrease POP enzyme activity, thus potentially decreasing endogenous Ac-SDKP production. However, in the non-injured contralateral kidney, exogenous administration of Ac-SDKP inhibits profibrotic factors. We propose that Ac-SDKP is a crucial molecule in determining fibrosis.

Liver & Pancreas

1552 Looking for Recipient Cells in Donor Tissue: Do Recipient Cells Transform To Become Hepatocytes in Allograft Liver?

OA Adeyi, M Selzner, N Selzner, D Grant. University Health Network, Toronto, ON, Canada.
Background: If the recipient uncommitted stem cells were shown to assist with regeneration/repopulation of hepatocytes post-transplant, some marginal organs would be more easily acceptable as a solution to organ shortage. Studies from bone marrow transplant patients, although inconclusive, suggest donor cells differentiate to mature hepatocytes, but no evidence exists that recipient bone marrow cells contribute to liver allograft hepatocellular regeneration. This study aims at investigating this concept using Fluorescent in-situ hybridization (FISH) methods.
Design: Male-female mismatched recipients were identified in the Toronto General Hospital liver transplant record. FISH staining was performed on the most recent post-transplant biopsy for X-Y chromosome markers. HepPar-1 staining was superimposed on FISH to identify hepatocytes. Working on the concept that X/Y-carrying hepatocytes in male recipients of female organ implies contribution by recipient cells in post-transplant hepatocyte repopulation, 200-500 hepatocytes were evaluated per specimen.
Results: Study set includes native liver biopsies, one each from one male (N-M) and one female (N-F) patients; 9 allograft biopsies from male recipients of female (whole or split liver) organs (F-M); and one allograft biopsy from a female recipient of female organ (F-F). The native biopsies confirm specificity of the FISH method, F-N showing only X chromosomes while M-N shows both X and Y chromosomes in hepatocytes. The studied F-M and F-F biopsies were performed 6-102 months post-transplant, and all show only X chromosomes in hepatocytes confirming donor origin. Non-hepatocyte cells (HepPar-1 negative) however show both X and Y chromosomes in M-F samples.

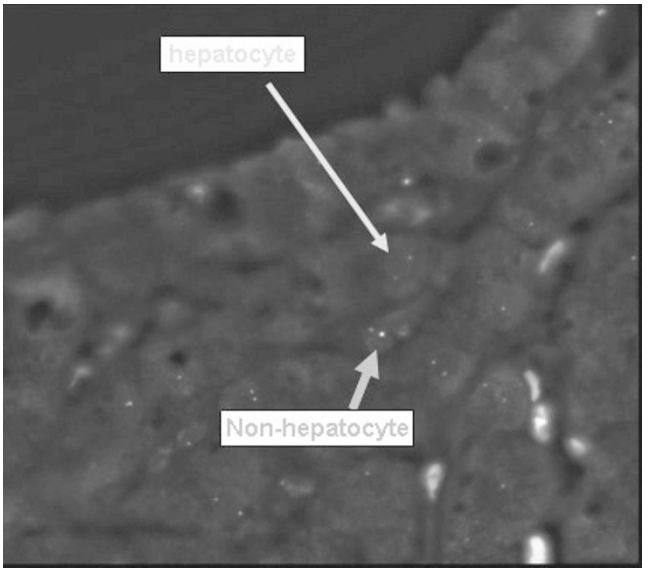

Conclusions: Recipient non-parenchymal cells expectedly infiltrate liver grafts post-transplant but there is no evidence based on X-Y chromosomal study that these cells differentiate into hepatocytes in whole liver grafts up to 8½ years post-transplant.

1553 Humoral Rejection of Liver

RM Agni, P Wai, AM D'Alessandro, D Lorentzen, LA Sebree, SA Drew, BJ Voss, GE Leverson, LA Fernandez, JD Mezrich, DP Foley, MR Lucey, A Musat. University of Wisconsin School of Medicine and Public Health, Madison, WI; Wisconsin School of Medicine and Public Health, Madison, WI.

Background: To study antibody-mediated injury of liver allografts, we applied established criteria used to recognize humoral rejection in kidney allografts, along with therapeutic intervention and outcome.

Design: Records were reviewed of 43 recipients of ABO compatible donor livers who had post-transplant biopsies to evaluate abnormal liver tests, biopsy staining with C4d, and donor-specific class I/II HLA antibodies (HLA-Ab) determination by Luminex. HLA-Ab specificities were considered positive when MFI>500. The C4d stain was considered positive if staining of the portal stromal connective tissue or capillaries was present in 50% or more of portal tracts. Endothelial staining of any site in the biopsy was recorded as focal or diffuse to study correlation with HLA-Ab). HR was considered only in patients who had C4d staining plus HLA-Ab positivity (C4d/HLA-Ab).

Results: 17/43 (40%) patients had C4d/HLA-Ab. Portal venular staining in > 50% tracts was seen in a 11/17 cases. Sinsusoidal staining focal was seen in 3. Compared to C4d/HLA-Ab negative subjects, C4d/HLA-Ab positive subjects had: 1) a higher incidence of acute cellular rejection (ACR) 15/17 vs. 13/26 (88% vs 50%), p= 0.02;; 2) higher incidence of steroid resistant ACR 7/17 vs 5/26 (41% vs19%), p=0.03. In the patient-group with liver biopsies <90 days post transplant (n=17) there were 11 cases of ACRall with bile duct damage but only in 1 of the 6 patients without ACR. C4d/HLA-Ab was found in 4/ 7 (57%) with steroid resistant rejection, and in 3/ 4 cases of steroid responsive rejection. Two of the cases of steroid resistant ACR progressed to severe cholestasis and ductopenia resistant to thymoglobulin, and required plasma pheresis (PP), IVIG and splenectomy. ACR was seen in 17/26 patients >90 days post transplant and 5 had chronic rejection (2 positive for C4d/HLA-Abs). C4d/HLA-Abs were positive in 47% ACR cases, one of which required PP and IVIG.

Conclusions: Humoral rejection mediated by HLA-Abs is found in about 50% cases of ACR. In some of these cases humoral rejection may predominate and lead to rapid development of severe ductopenia, necessitating treatment directed at antibody removal and suppression.

1554 Pancreatic and Duodenal Homeobox 1 (PDX-1) Expression in Primary Pancreatic Endocrine Neoplasia

R Alvarez, SM Hastings, J-H Chen. Indiana University School of Medicine, Indianapolis, IN.

Background: Pancreatic and duodenal homeobox-1 (PDX-1) is a pancreas-specific transcription factor associated with the development and maintenance of endocrine cells. It is expressed in islets as well as in pancreatic neoplasms, and its detection in metastatic endocrine carcinoma is suggestive of spread from a pancreatic origin. However, an evaluation of PDX-1 expression in primary pancreatic endocrine neoplasms has not been performed.

Design: 124 pancreatic endocrine neoplasms from 112 pancreatic specimens are retrieved from the pathology archives of Indiana University. The clinical findings and pathology material are reviewed. The cases are classified according to the current WHO classification of pancreatic endocrine tumors. Immunohistochemical staining for PDX-1 is performed on formalin-fixed paraffin-embedded sections. Nuclear staining intensity for PDX-1 is scored from 0 (negative) to 3+ (strong), with 3+ staining intensity in islet cells serving as an internal reference.

Results: The neoplasms are composed of 25 microadenomas, 70 endocrine tumors, including 35 with uncertain behavior, and 39 endocrine carcinomas (33 well differentiated, 3 poorly differentiated, and 3 mixed exocrine-endocrine carcinomas). 21 tumors are hormonally functioning (15 insulinoma, 5 gastrinoma, and 1 VIPoma) and the remainder non-functioning, including 1 pancreatic polypeptide (PP)-cell neoplasm (PPoma). 25/25 microadenomas exhibit 0 to 1+ PDX-1 staining intensity (average 0.5). PDX-1 expression in pancreatic endocrine tumor and carcinoma was variable and ranged from 0 to 3+. Of these, 3+ PDX-1 staining was observed in 15/15 insulinomas, while its expression is variably diminished in the remaining endocrine tumors and carcinomas (average 0.8 and 1.1, respectively).

Conclusions: Whereas PDX-1 is strongly expressed in pancreatic islets, its expression in pancreatic endocrine neoplasia is variable. PDX-1 staining is strong in insulinomas, supportive of its preserved function in neoplastic beta cells. However, its expression is markedly decreased in endocrine microadenomas, and variably diminished in pancreatic tumor and carcinoma. These results suggest that differential PDX-1 expression and signaling may contribute to the biology and physiology of pancreatic endocrine neoplasia.

1555 Antiproliferative Effects of Bombesin and Neurotensin on Oval Cells in Exprerimental Biliary Obstruction in Rats

S Assimakopoulos, AC Tsamandas, C Georgiou, C Vagianos, CD Scopa. University of Patras, Patras, Greece.

Background: Oval cells (OC) are liver stem cells involved in organ's regeneration following diverse types of injury, while their numbers increase in direct proportion with liver injury severity. This study investigates the effect of the neuropeptides bombesin (BBS) and neurotensin (NT) on OC proliferation in the cholestatic rat liver.

Design: Seventy male Wistar rats were randomly divided into 5 groups: controls, sham operated, bile duct ligated (BDL), BDL+BBS (10μg/kg/d), BDL+NT (300μg/kg/d). After 10 days, rats were sacrificed and total bilirubin and ALT levels were determined. Liver tissue samples were evaluated for expression of alpha-fetoprotein (AFP) mRNA (in situ hybridization), CK19 and Ki67 antigen expression (immunohistochemistry) and apoptosis (TUNEL). Cells with morphologic features of OC that were CK19(+) and AFP mRNA(+) were scored in morphometric analysis and their proliferation (Ki67+ OC) was recorded. Also, proliferation, apoptosis were evaluated in hepatocytes and cholangiocytes. Hepatic oxidative stress was estimated on liver homogenates by measurements of lipid peroxidation and glutathione redox state.

Results: The neuropeptides BBS and NT significantly attenuated cholestatic liver injury as evidenced by reduction of ALT activity and hepatic oxidative stress. Both agents exerted similar and cell type-specific effects on OC, hepatocytes and cholangiocytes: (a) as table shows OC proliferation and accumulation in the cholestatic liver was attenuated, (b) hepatocyte proliferation was increased along with a decreased rate of their apoptosis ($p<0.001$ in each case) and (c) cholangiocyte proliferation was attenuated and their apoptosis was increased ($p<0.001$ in each case).

Table: Oval cell presence and proliferation

Markers	Control (I) (n=10)	Sham (II) (n=15)	BDL (III) (n=15)	BDL+BBS (IV) (n=15)	BDL+NT (V) (n=15)
CK19	1.72±0.43	1.71±0.44	50.76±2.80*	30.05±2.27*	29.23±2.78*
AFPmRNA	1.22±0.48	1.16±0.37	44.58±3.32*	23.25±3.41*	22.71±4.14*
Ki67	1.17±0.39	1.21±0.39	46.14±2.79*	28.17±1.91*	26.37±2.46*

*p<0.001 versus sham, *p<0.001 versus BDL. BDL, bile duct ligation; BBS, bombesin; NT, neurotensin; AFP; alpha fetoprotein

Conclusions: BBS and NT exert a significant antiproliferative effect on oval cells in experimental biliary obstruction along with improvement of hepatocytes' regenerative response, prevention of ductular hyperplasia and reduction of hepatic oxidative stress. This observation might be of potential value in patients with extrahepatic cholestasis.

1556 Well-Differentiated Hepatocellular Neoplasms in Adult Women with Congenital Hepatic Fibrosis

DW Azar, A Shabaik, MR Peterson. University of California, San Diego, La Jolla, CA.

Background: Congenital hepatic fibrosis (CHF) is a genetic disorder associated with autosomal recessive polycystic kidney disease (ARPKD), characterized by portal based fibrosis and anastomosing bile ducts, and leading to hepatomegaly and portal hypertension. Rare cases of hepatic mass lesions including adenomatous hyperplasia (1 case), hepatocellular carcinoma (1 case), and dysplastic nodule (1 case) have been reported in patients with CHF. We here report two cases of well differentiated hepatocellular neoplasms with features intermediate between adenoma and hepatocellular carcinoma arrising in adult women with CHF.

Design: The first patient was a 22 year old female with known ARPKD in whom two hepatic masses were identified via routine screening, a 3.4 cm segment II mass and a 5.2 cm right lobe mass. The second patient was a 34 year old female presenting with asymptomatic AST/ALT elevations found to have an 8.5 cm mass in the caudate lobe. Neither patient was taking oral contraceptives at the time of diagnosis. Both patients underwent partial hepatectomy.

Results: Features consistent with CHF were confirmed in non-neoplastic liver parenchyma in both patients. Both resected tumors were characterized by sheets of uniform, well differentiated hepatocytes with low N/C ratios and low mitotic indices. The second tumor was also extensively steatotic. Wide fibrous bands extended through both tumors, but biliary structures were entirely absent from the mass lesions. Focal areas of large-cell dysplasia were identified in the second tumor. Reticulin staining showed areas of both tumors with loss of reticulin fibers. CD34 immunostaining on both tumors revealed patchy sinusoidal positivity, in contrast to the background liver parenchyma. Glypican-3 immunostaining on the second tumor showed faint granular cytoplasmic reactivity.

Conclusions: We present two cases of well-differentiated hepatocellular neoplasms developing in young adult female patients with congenital hepatic fibrosis. While both tumors exhibited features of hepatic adenoma, the clinical presentations are atypical for hepatic adenoma and both demonstrated atypical features, including areas of reticulin framework loss, CD34 sinusoidal positivity, and large cell dysplasia (one case). These cases add to the limited reports of hepatocellular neoplasms arising in CHF. While the

atypical features raise concern for malignancy, only long-term follow-up and expanded case volume will attest to the prognosis of such lesions.

1557 Applicability and Prognostic Relevance of Ampullary Carcinoma Histologic Typing as Pancreatobiliary Versus Intestinal

S Balci, GE Kim, N Ohike, T Tajiri, I Coban, A Krasinskas, S Bandyopadhyay, O Basturk, A Dolgun, D Kooby, C Staley, NV Adsay. Hacettepe U, Ankara, Turkey; UCSF, CA; Emory U, GA; Showa U, Yokohama, Japan; U of Pittsburgh, PA; WSU, MI; NYU, NY.

Background: Ampullary carcinomas (ACs) show cell-lineage towards the epithelial lining located in this region. A lineage-based classification as pancreatobiliary (PB) or intestinal (IN) has been proposed, and treatment protocols are being designed accordingly; however, the applicability and prognostic relevance of this system has yet to be verified.

Design: 5 observers independently classified 232 stringently-defined invasive ACs, based on their resemblance to pancreatic or colonic carcinomas, as: ***pure*** *PB,* ***pure*** *IN, mixed (MX)* and others (*OT*). *MX* group was further divided, based on the predominant pattern, as *MXPB vs MXIN*. For incidence and prognostic analysis, 3 of 5 were considered as consensus diagnosis.

Results: The incidences of cases that were classified as ***pure*** *PB* and ***pure*** *IN* was 32% and 6%; remainder were *MX* (41%) or *OT* (12%). Agreement among the observers for these categories was "**fair**" (Kappa=0.3850; Z score=28.80; p<0.001), with only 23% agreed by all 5. The high incidence of *MX* category was attributed to tumor heterogeneity, mostly along the advancing carcinoma edge that often displayed PB pattern in an otherwise IN tumor. However, when **the predominant-pattern based** classification was evaluated (by combining *MXPBs* to *pure PB* and *MXINs* to *pure IN*), "**moderate**" agreement was obtained (Kappa=0.4402; Z=28.09; p<0.0001) with 59% classified as *PB*, 25% as *IN* and 15% as *OT*. The PB-predominant (*pure PB + MXPB*) group had a significantly lower median survival (41 mos) than that of IN-predominant (*pure IN+MXIN*) tumors (80 mos; p=0.026) with a 1.78 times higher risk of death (p=0.028). However, this survival correlation was not independent of established prognostic parameters in multivariate analysis.

Conclusions: As a transitional region, ACs often show hybrid phenotypes between PB and IN epithelium, producing substantial subjectivity of histologic type designation. Tumor heterogeneity is common, particularly along the advancing edge with morphologic transformation. If the predominant-pattern approach is employed, PB *vs* IN classification has moderate agreement and good prognostic value; however, the differences in survival is by no means analogous to that of pancreatic *vs* colonic adenocarcinoma. Other prognosticators are necessary to appropriately stratify ACs.

1558 Pancreatobiliary Osteoclastic-Giant Cell Carcinomas (OGCCs) Are Often Characterized by Intraductal Growth and Polypoid Pattern Similar to Sarcomatoid Carcinomas (SCs) of Other Organs

O Basturk, I Coban, S Bandyopadhyay, K Jang, J Sarmiento, NV Adsay. NYU, NY; Emory U, GA; WSU, MI; Samsung MC, Seoul, Korea.

Background: Pancreatobiliary OGCCs are very rare tumors (the largest pathologically analyzed series, 7 cases), regarded as a distinct form of SCs, and associated with striking chemotaxis of OGCs. Biologic nature of these tumors has yet to be determined. Here, we present our observations on common intraductal growth of OGCCs, which may have implications on their biology.

Design: 6 OGCCs, 4 of which we had personally dissected, were analyzed.

Results: *Clinic:* F/M=5. Mean age=67(51-86). Presentation symptoms: Back pain(4/6), weight loss(3/6), jaundice(1/6) and diarrhea(2/6). *Gross:* 3 tumors were localized in the head, 3 in tail. Mean size=5.7 cm(2-10). Those 4 dissected by the authors were polypoid, smooth-surfaced, focally hemorragic lesions within the ducts, 1 with cyst formation. *Microscopy:* All cases showed intraductal/intracystic growth. 3 different cells were noted: **I.**OGCs **II.**Relatively small, ovoid-spindle histiocyte-like cells(HLCs) **III.**Pleomorphic giant cells(PGCs). 5 cases were associated with an ordinary inv ductal adenocarcinoma(DA). DA component ranged from microscopic to 80% of the tumor(mean, 30%). 1 also had IPMN, 2 had multifocal PanIN-3. 2 contained osteoid. *F/U:* 1 patient who had extensive DA died(25 mos), 3 are alive(19-27 mos).

	CK	CD68	Ki67	p53
OGCs	0/4	4/4	0/4	0/4
HLCs	1/4, Focal	4/4*	4/4; 20-40%	2/4; 70%
PGCs	0/4	1/4, Focal	4/4; 30-50%	2/4; >80%

* In contrast with the literature. In-built controls staining appropriately.

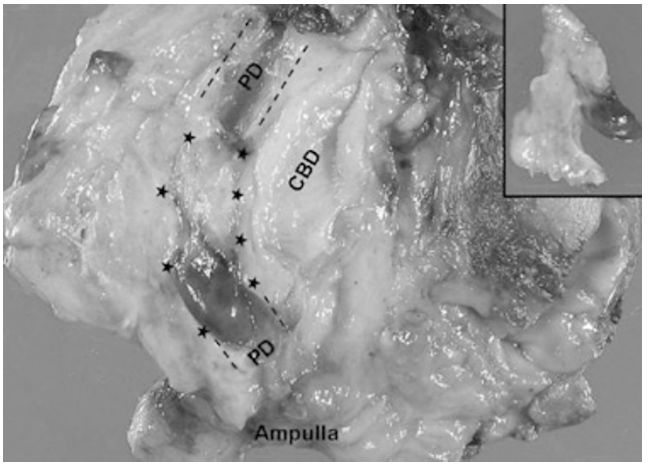

Conclusions: Careful macroscopic examination/microscopic correlation discloses that pancreatobiliary OGCCs often have prominent intraductal growth, a finding previously not fully appreciated in the literature. This may not be surprising, considering that SCs occurring in other sites also often form polypoid lesions with pushing-border infiltration. It may be important to document relative amount of OGCC and DA patterns, because our limited F/U suggests that OGCC-predominant cases may not be as aggressive. Further studies are warranted on larger number of cases.

1559 Value of Immunohistochemistry of Hepatocellular Adenomas: A Series of 79 Cases

C Bazille, M Karanian- Philippe, B Alkofer, N Le Stang, L Chiche, P Rousselot, F Galateau-Salle. CHU Caen, Caen, France.

Background: A large series of hepatocellular adenomas (HA) was reviewed to compare their morphological and immunohistochemical (IHC) phenotypes and evaluate the usefulness of IHC.

Design: 79 resected HA, including 25 adenomatosis, collected from 1992 to 2009 were classified according to morphology and immunohistochemistry – Liver Fatty Acid Binding Protein (LFABP), SAA, Glutamin Synthetase (GS) and β-catenin (BC) antibodies. Results were validated by molecular biology in some frozen samples.

Results: Median age was 39 years (range 14-66) with a M/F ratio of 1/8. 72% of women received oral contraception with mean duration of 19 years. Morphologically there were 21 steatotic (26.6%), 35 inflammatory (44,3%), 2 atypical (2,5%) and 21 unclassified (26,6%) HA. IIHC analysis of 79 cases gave 4 subtypes: HNF1a-mutated HA (LFABP neg), n=25 (31,6%); BC-activated HA (SAA -ve, GS high, BC +ve, n=1 (1,3%); inflammatory HA (SAA +ve), n=39 (49,4%) including 3 inflammatory with BC-activated HA (SAA+ve, GS high, BC +ve); and non-specific immunophenotype HA (LFABP +ve, SAA -ve, GS low), n=14 (17,7%). 20/25 (80%) of HNF1α-mutated HA and 30/39 (77%) of inflammatory HA are correctly classified according to morphology only. 7/21 (33%) of non-specific HA and 18/79 (22,8%) of HA were reclassified after IHC, notably IHC detected 2/4 of BC-activated HA without significant atypia. Men comprised 82% of inflammatory HA. Two patients developed hepatocellular carcinoma (1 inflammatory and 1 unclassified). Adenomatosis cases were divided up by 15 HNF1α-mutated, 7 inflammatory and 3 unclassified HA.

Conclusions: Clinico-pathological results of our series correlated with the literature. IHC analysis is helpful for HA subtyping in case of non-specific features and particularly for BC-activated HA with a high risk of malignant transformation.

1560 Cell Cycle Arrest in Fibrosing Cholestatic Hepatitis – C (FCH-C)

NT Beaubier, JH Lefkowitch. Columbia University Medical Center, New York, NY.

Background: FCH is an uncommon but severe form of post-transplantation liver injury associated with marked hepatic reinfection by either hepatitis B virus (HBV) or hepatitis C virus (HCV) in the setting of immunosuppression. FCH-C shows cytopathic hepatocellular injury and portal/periportal fibrosis associated with a prominent ductular reaction (DR). DR in FCH is likely due to progenitor cell activation due to severe hepatocellular injury and impaired regeneration. The cyclin-dependent kinase inhibitor p21WAF1/CIP1 (p21), an effector of cell cycle arrest when induced by p53, is known to be expressed in liver parenchyma following various insults including toxins, viruses and steatohepatitis. We investigated the possible role of cell cycle arrest in cases of FCH-C after liver transplantation.

Design: 13 liver biopsies (bxs) showing FCH-C and 7 control bxs with cholestasis and DR due to large bile duct obstruction (LBDO) were immunostained for p21, a marker of cell cycle arrest, for p53, an inducer of p21, and for Ki-67, a marker of dividing cells. All three proteins have nuclear expression; the samples were therefore graded according to the percentage of positive nuclei. Cytokeratin 7 (CK7) immunostain was also applied in order to assess the DR.

Results: p21 was highly expressed in the parenchyma of the FCH-C cases: 10 of 13 cases showed p21 expression in >60% of hepatocytes while only 1 case of LBDO had > 60% expression (p = 0.0072, Fisher's exact test). p53 was also more highly expressed in FCH-C (p = 0.0012). The FCH-C bxs showed a much lower level of Ki-67 positivity (1-20% of cells). There was no statistical difference between the DR of FCH-C and LBDO as assessed by CK7 immunohistochemistry (p = 0.64), thus making LBDO an appropriate control. These data are consistent with ongoing parenchymal attempts at cell division in FCH-C being ineffective because of large numbers of cells in replicative arrest.

Conclusions: In FCH-C the extensive cholestatic liver parenchymal damage and HCV replication are associated with widespread cell cycle arrest as measured by p21 expression (also supported by the elevated levels of p53 expression, the upstream inducer of p21.) The p53-p21 pathway therefore may represent a final common pathway for several types of liver injury, including FCH-C, in which hepatic regeneration is impaired.

1561 Molecular Profiling of Pancreatic Cancer Stroma

JR Brody, J Kline, CJ Yeo, S Peiper, P McCue, AK Witkiewicz. Thomas Jefferson University, Philadelphia, PA.

Background: Treatment strategies targeting epithelial cells in pancreatic ductal adenocarcinoma (PDA) have yielded disappointing results. Since the bulk of PDA tumor volume consists of stroma, investigating the stromal cells may elucidate pathways responsible for PDA aggressiveness and lead to the identification of new treatment targets. A characteristic of prior studies of gene expression in the stromal compartment of human PDA is that these studies have focused on a limited number of genes identified by serial analysis of gene expression as highly expressed in invasive pancreatic cancer tissues but not in pancreatic cancer cell lines. The goal of our study was to perform global gene expression analysis of PDA associated stroma, obtained thorough laser microdissection (LCM), from frozen PDA tissue.

Design: Qiagen RNAeasy Micro kit (Qiagen, Inc., Valencia, CA). The purity of the obtained stromal RNAs was confirmed by quantitative RT-PCR for epithelial marker keratin 18. RNA amplification and labeling was performed by the WT-Ovation Pico RNA amplification system (NuGen Technologies, Inc.). Expression analysis was carried out using Affymetrix gene chip human Gene 1.0 ST array (Affymetrix, Santa Clara, CA). Background correction and normalization was done using Robust Multichip Average (RMA) with Genespring V 10.0 software (Agilent, Palo Alto, CA, USA). Selected genes showing > 3 fold difference ($p<0.001$) were validated by Q RT-PCR and immunohistochemistry (IHC).

Results: showed significant changes in a subset of genes with 49 genes showing > 5 and 260 genes >3 fold difference when compared to normal cultured fibroblasts ($p<0.01$) Ingenuity Pathway Analysis showed that differentially expressed genes were involved in "Cell Death, Immunological Response and Post-Translational Modification" (score 53), "Cell signaling, actin cytoskeleton remodeling/ signaling and cell adhesion" (score 43) and 'Lipid Metabolism, Molecular Transport, Small Molecule Biochemistry (score 31). Three up regulated (UIMC1, SPARCL1, NCOR2) and three downreagulated genes (CAV-1, LDHB, MMP1) were validated by QRT-PCR using amplified and unamplified RNA. Additionally we demonstrated expression of SPARCL1 in stroma and lack of Caveolin-1 expression by IHC.

Conclusions: Our preliminary results show that a number of genes and pathways are specifically altered in PDA associated stroma and may lead into greater insight into pathophysiology of PDA.

1562 Squamous Cell and Adenosquamous Carcinomas of the Gallbladder: Clinicopathologic Analysis of 34 Cases

A Cakir, O Tapia, JC Roa, N Dursun, I Coban, O Basturk, T Jazaerly, D Akdemir, J Sarmiento, NV Adsay. Emory U, GA; U de La Frontera, Temuco, Chile; NYU, NY; WSU, MI; Ohio Northern U, OH.

Background: The information in the literature on squamous cell (*SCCs*) and adenosquamous carcinomas (*ASCs*) of the gallbladder (GB) is highly limited. This study, which comprises the largest number of patients to date, was undertaken to better define the clinicopathologic characteristics of these tumors.

Design: 606 resected invasive GB carcinomas were reviewed. 41 cases (6.7%) showed squamous differentiation. Those without any identifiable glandular-type invasive component was classified as *pure SCCs* (8 cases) and those with the squamous component constituting 25-99% of the tumor as *ASCs* (26 cases). Remainders were excluded as *carcinoma with focal squamous change* (7 cases).

Results: **Clinical Features:** F/M=4.3 (*vs* 3.8 in ordinary carcinomas; OCs). Mean age=65 (*vs* 64 in OCs). **Pathology:** Mean tumor size=3.1 cm (*vs* 2.7 cm in OCs). 65% (17/26) of *ASCs* had focal keratinization, while others were poorly differentiated; however, 90% (7/8) of *pure SCCs* had substantial keratinization including pearl formation and dyskeratotic cells. 32% (11/34) of all cases also revealed squamous change in the adjacent mucosa. 6 cases had sarcamotoid appearance, 5 comedo-like necrosis; 5 focal clear cell change (1 with renal cell carcinoma-like pattern); 3 microcyst formation; 1 sebaceous differentiation and 1 goblet cell change. Tumor giant cells were identified in 29% of *ASCs/pure SCCs* (*vs* 10% in OCs; p=0.02). Peritumoral eosinophils were also more common in *pure SCCs* (51% *vs* 6% in OCs; p=0.001). The incidence of vascular and perineural invasion were 76% and 32%, respectively (*vs* 72% and 48% in OCs). 5 of 7 metastatic lymph nodes available for our examination had squamous areas (3 *ASCs* and 2 *pure SCCs*.) **Outcome:** Follow-up was available in 31 patient: 25 died of disease (median=5, range: 0-20 mos), 6 were alive (median=64, range: 5-112.5 mos). Overall median survival (5.4 mos) was worse than that of OCs (11.4 mos, p=0.01).

Conclusions: Squamous differentiation is noted in 6.7% of GB carcinomas. The incidence of *ASC* (defined as 25-99% of the tumor being squamous) is 4.3%, and that of *pure SCC* (without any documented invasive glandular component) is 1.3%. *Pure SCCs* often show prominent keratinization. The overall prognosis of ASC/SCC appears to be even worse than that of OCs. Most patients die within a few months; however, those few alive beyond 2 years might experience long term survival.

1563 Cytokeratin 8 Immunohistochemistry Distinguishes Chronic Hepatitis C from Steatohepatitis

JP Cantor, JL Farber. Thomas Jefferson University Hospital, Philadelphia, PA.

Background: Chronic hepatitis C (CHC) is frequently accompanied by varying degrees of steatosis, owing to the direct effects of HCV genotype 3, as well as the prevalence of obesity and alcohol abuse in these patients. The degree of steatosis is predictive of the rate of progression to cirrhosis and the response to therapy. Thus, the steatosis itself, rather than the immune response to HCV, may be a major cause of chronic injury in CHC. In searching for Mallory bodies in cases of steatohepatitis, we observed that both steatotic and ballooned hepatocytes lack the normal, membranous immunohistochemical reactivity for CK8. The present study sought to determine whether CK8 reactivity could serve to differentiate the relative contributions of the persistent virus infection and steatosis to the progression of CHC.

Design: 10 biopsies from each of the following 2 groups were stainined immunohistochemically for CK8: 1) CHC with an HAI score of at least 6 but with less than 10% steatotic hepatocytes; 2) steatohepatitis with a NASH score of at least 4.

Results: In all group 1 biopsies (CHC), the hepatocytes stained diffusely for CK8 (top). By contrast, in all group 2 biopsies (steatohepatitis alone), CK8 staining of the hepatocytes was markedly decreased or absent (bottom).

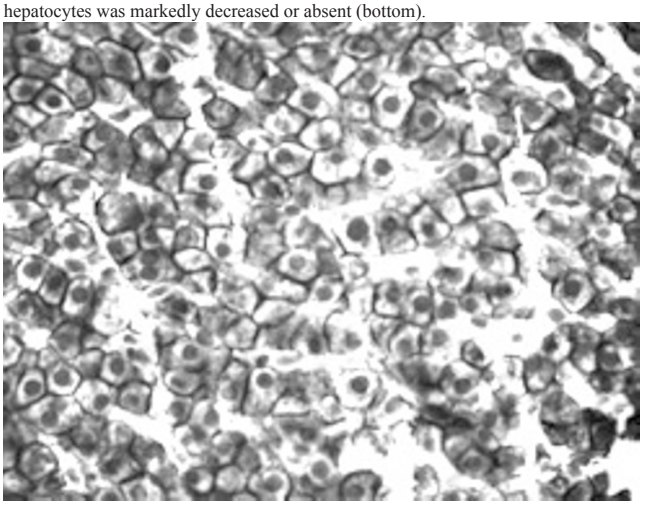

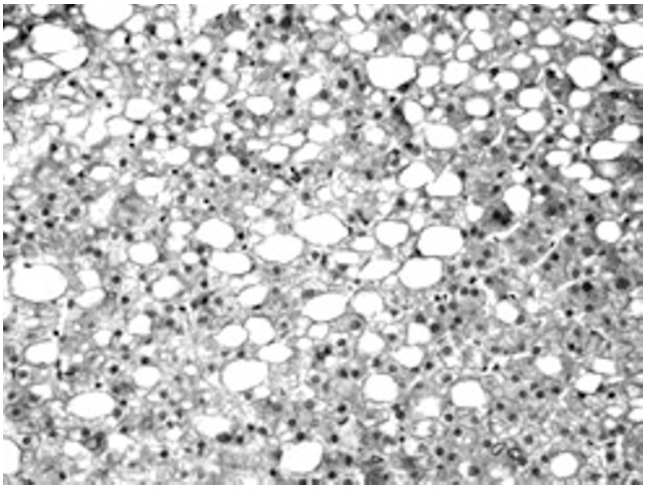

Conclusions: CK8 immunostaining was lost from steatotic hepatocytes. By contrast, CHC was characterized by retention of CK8. Thus, CK8 reactivity may provide an effective marker to differentiate the relative contributions of the persistent virus infection and steatosis to the ongoing liver cell injury in CHC.

1564 Recurrence of Non Alcoholic Fatty Liver Disease Following Liver Transplantation

FL Chang, J Mellinger, P Dureja, G Avey, A D'Alessandro, J Mezrich, A Said, R Agni. University of Wisconsin School of Medicine and Public Health, Madison, WI.

Background: Non alcoholic liver disease (NAFLD) is a common reason for liver transplantation. The current study is undertaken to study recurrence of NAFLD in a large cohort of adult liver transplant recipients and assess recurrence-related factors

Design: Consecutive patients transplanted for NAFLD / cryptogenic cirrhosis from 1993 to 2005 were studied. NAFLD recurrence was defined histologically with radiological confirmation Liver biopsies were assessed by two blinded pathologists for steatosis, steatohepatitis, and fibrosis using NASH-CRN scoring and Brunt system.

Results: 88 consecutive transplant recipients met selection criteria, including 50 males and 38 females, with an average age of 58 years. Pretransplant diabetes was present in 39 (45%) and in 62 (71%) posttransplant. Biopsy recurrence of NAFLD was documented in 29 of 47 patients (62%). Of the 29, steatosis alone was present in 19 (65%), with steatohepatitis in 10. Hepatic fibrosis was at stage 1 in 3 of 29 (10%), stage 2 in 7 (24%) and stage 3-4 in 2. Post transplant survival was similar among those with NAFLD recurrence and those without (P=0.33). The most significant factors associated with post-transplant NAFLD recurrence were pre-transplant diabetes (OR 5.26, 95% CI 1.25-22.2, P=0.03) and post-transplant diabetes (OR 4.41, 95% CI 1.20-16.14, P=0.03). Other predictors of recurrence included high triglyceride levels at 6 (P=0.01) and 12 months (P=0.02) ; average triglyceride levels at 12 months were 328 mg/dl in recipients

with NAFLD recurrence and 189 mg/dl in those without NAFLD recurrence. Prednisone dose at 6 months was higher in patients with NAFLD recurrence (11.8 mg/day) than in patients without recurrence (7.7 mg/day), P=0.03. Pre or post transplant hypertension, non-triglyceride lipids, insulin dose and post transplant choice of calcineurin inhibitor were not associated with NAFLD recurrence

Conclusions: Post-transplant recurrent NAFLD is common. However it is mild in most patients and does not lead to reduced survival. Pretransplant diabetes, post transplant diabetes, high triglyceride levels and higher average steroid doses are associated with NAFLD recurrence.

1565 Histopathologic Features of Extensive Hepatic Vascular Malformations

S Cho, V Paradis, R Pai, P Bioulac-Sage, V Alves, T Souza, H Makhlouf, P Schirmacher, K Evason, L Ferrell. Univ Calif, San Francisco; Hospital Beaujon, Clichy, France; Wash Univ, St Louis; Hospital Pellegrin, Bordeaux, France; Univ Sao Paulo, Sao Paulo, Brazil; Hospital Alianca, Salvador, Brazil; AFIP, Washington, DC; Univ Hospital, Heidelberg, Germany.

Background: Hepatic vascular malformations (HVM), often occurring in the setting of hereditary hemorrhagic telangiectasia (HHT, or Osler-Weber-Rendu syndrome) are increasingly recognized by imaging studies. While the clinical manifestations of HHT are well known, the histopathology of HVMs has not been studied extensively. We aim to characterize these rare diagnostically challenging lesions.

Design: Specimens (10) ranged from wedge biopsies (2/10) to partial (1/10) and total hepatectomies (7/10). H&E, elastic, reticulin, CD34, SMA, and D2-40 stains were performed to characterize the vascular types and effects/changes in the background liver.

Results: 7 patients have a clinical diagnosis of HHT; 3 patients lack a definitive diagnosis of HHT. Histologic examination shows a wide spectrum of complex changes. Some cases (4/10) show exclusively venous alterations, while others have arterial changes ranging from isolated arteries (1/10) and focal thick-walled arteries (2/10) to arteriovenous malformation-like areas (3/10). Mild/early changes consist of abnormal portal vessels and central veins with periportal telangiectases, sinusoidal dilation, and periduct fibrosis. The larger abnormal vessels show irregularly thickened walls with an irregular or fragmented elastic lamina and increased smooth muscle, as well as focal recent to organizing thrombi. The periportal telangiectases lack organized elastic fibers but demonstrate increased SMA and patchy CD34 positivity. Moderate/later changes include periportal fibrosis and greater degree of sinusoidal dilation with increased SMA and CD34 staining, with foci resembling cavernous hemangioma. Severe/end-stage changes demonstrate extensive sinusoidal fibrosis with widened hepatic plates often 3-5 cells thick, nodular regenerative hyperplasia or focal nodular hyperplasia-like lesions (7/10), and bile duct alterations, including ectasia, cysts, fistulas, stones, infarcts, and infections. Late stage lesions are also associated with cardiac failure and sepsis.

Conclusions: HVMs of the liver demonstrate changes that likely reflect progression of abnormal vascular flow over time, and recognition of this wide spectrum of pathologic changes should enhance our diagnosis of these problematic lesions.

1566 Tumor Budding Is an Independent Prognostic Parameter in Ampullary Adenocarcinomas

I Coban, N Ohike, G Kim, T Morohoshi, A Krasinskas, O Basturk, S Bandyopadhyay, M Goodman, NV Adsay. Emory, GA; UCSF, CA; Showa, Tokyo, Japan; U of Pittsburg, PA; NYU, NY; WSU, Detroid.

Background: Tumor budding (BUD) confers a worse prognosis and correlates significantly with nodal metastasis in colorectal cancer but has not been evaluated in ampullary adenocarcinoma (AAC).

Design: 244 surgically resected stringently defined invasive AAC were analyzed for BUD, defined as an isolated single cell or a cluster composed of <5 cells. The presence of any focus with >5 BUDs per 20X (0.785 mm^2) was considered as "positive", and if there were ≥3 BUD-"positive" foci, the case was regarded as *BUD-high*. Accordingly, BUD-negative cases and those with <3 BUD-positive foci were regarded as *BUD-low*.

Results: 194 AAC cases were *BUD-high*, and 50 were *BUD-low* (29 with 1-2 positive foci, and 21 negative). BUD-high cases correlated significantly with non-intestinal type histology, higher lymph node metastasis, higher T-stage tumors, and more aggressive behavior. Furthermore, in stepwise multivariable Cox regression model, tumor budding was found to be an independent predictor of survival (p=0.0051), impacting prognosis (hazards ratio of 2.9) more than that of T-stage and LN metastasis (2.0 and 1.9, respectively).

	Case #	Histologic Subtype (IN/non-IN)	T stage (T1+T2 / T3+T4)	LN Met (%)	Mean Survival (mos)	3-yr Survival (%)
BUD-high	194	55/139	112/82	44	31	40
BUD-low	50	27/23	45/5	17	44	93
p-value		<0.01	<0.01	<0.01	<0.05	<0.01

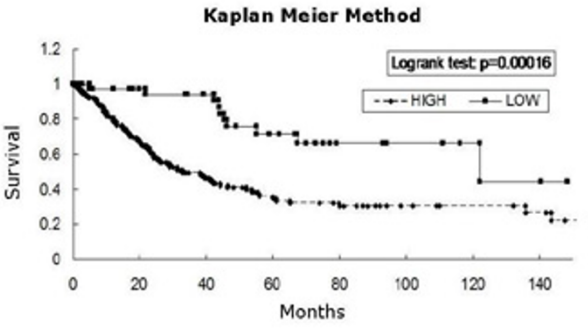

Conclusions: Tumor budding is frequently encountered in ACC. High budding is a strong independent predictor of overall survival, with a prognostic correlation stronger than established parameters of T-stage and lymph node metastasis. Therefore, budding should be incorporated into surgical pathology reports for AAC.

1567 Centrilobular Fibrosis Is Not a Specific Feature of Steatohepatitis in the Setting of Chronic Hepatitis C Infection

JF Coleman, R Lopez, A Pillai, IA Hanouneh, NN Zein. Cleveland Clinic, Cleveland, OH.

Background: Coexistent steatohepatitis (SH) can occur in patients infected with hepatitis C virus (HCV), but study of these patients is complicated by the fact that HCV can cause metabolic derangements including hepatic steatosis. Although steatosis and lobular inflammation are nonspecific findings, the presence of hepatocellular ballooning degeneration and centrilobular fibrosis (CLF) have been proposed as markers of SH in the setting of HCV. We hypothesize that CLF is not specific, however, and may be seen in HCV without superimposed SH.

Design: Patients with HCV and two liver biopsies between 1997 and 2006 were identified with the electronic medical record. Biopsies were scored by two pathologists for necroinflammation (modified HAI), fibrosis (Ishak, stages 0-6), steatosis (%), and CLF (0 absent, 1 mild, 2 marked). Patients with combined hepatocellular ballooning degeneration, steatosis, and CLF at baseline were excluded for a possible diagnosis of SH. Patients were also excluded for insufficient biopsy tissue (< 10 portal tracts) and incomplete clinical data. Patients were divided into groups of those with (56) and without (15) CLF at baseline. Age and BMI were compared with student's t-tests, histology scores with Wilcoxon rank sum tests and categorical factors (sex, race, ethanol, tobacco, diabetes mellitus, antiviral therapy and sustained virologic response) with Fisher's Exact tests. Fibrosis progression-free rates were compared with a Kaplan-Meier plot and log-rank test.

Results: CLF was seen in 56 of 71 patients (79%) at baseline. These subjects had higher inflammation and modified staging scores than those without CLF (P<0.05). There were no other significant differences between the groups, including BMI, history of diabetes mellitus, alcohol abuse, and subsequent development of SH. In addition, the rate of fibrosis progression was not significantly different between patients with and without CLF at baseline.

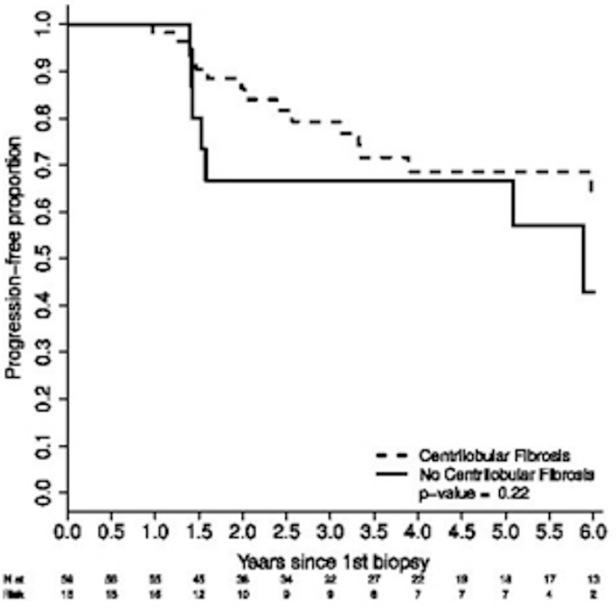

Conclusions: CLF is found in HCV patients without other findings of SH and does not correlate with BMI, history of diabetes mellitus, or alcohol use. The presence of CLF does not predict more rapid progression of fibrosis or subsequent development of steatohepatitis.

1568 Frequent Activation of the mTOR Pathway in Adenocarcinoma of the Ampulla of Vater

CD Crowder, OH Iwenofu, AM Bellizzi, WL Frankel. The Ohio State University Medical Center, Columbus, OH; Brigham & Women's Hospital, Boston, MA.

Background: Mammalian target of rapamycin (mTOR) is a key serine/threonine kinase that exerts a central regulatory effect on metabolism, cell growth, proliferation and cell cycle progression. Constitutive activation of the PI3K/Akt/mTOR pathway has been described in the carcinogenesis of various organs. Previous studies have demonstrated loss of PTEN function (a tumor suppressor interacting with the pathway) and amplification of Akt (a kinase directly upstream of mTOR) and S6rp (a major downstream effector of mTOR and component of the 40S ribosomal subunit) in pancreatic ductal adenocarcinomas. To our knowledge, the activation of this pathway has not yet been demonstrated in ampullary adenocarcinoma (AdCa). We utilized immunohistochemistry for p-S6rp, PTEN and p-Akt to assess the status of the mTOR pathway in ampullary AdCas.

Design: Tissue microarrays were constructed from 40 ampullary AdCas; 1.5 mm duplicate cores were taken from each tumor. Slides were stained with antibodies to p-Akt, p-S6rp and PTEN, and cases were scored as follows: p-S6rp (0, 1+ modest intensity in ≥ 5%, 2+ strong intensity in ≥ 5%); PTEN and p-Akt (positive ≥ 5% staining, negative). Normal pancreatic ducts (13 cases) served as controls. Controls stained appropriately, and slides were reviewed by 2 pathologists.

Results: The majority of ampullary AdCas stained for p-S6rp (77.5%, 1+ in 13 cases, 2+ in 18 cases). Many cases demonstrated loss of PTEN (77.5% of cases), while p-Akt was expressed in 50% of cases. PTEN and p-Akt were both uniformly positive in normal controls. p-S6rp immunoreactivity was only noted in 1 normal control (8.3%). Results are summarized in the table.

mTOR Pathway Protein Expression

	Ampullary AdCa	Normal Pancreatic Ducts
p-S6rp	0: 9 (22.5%)	0: 11 (91.7%)
	1+: 13 (32.5%)	1+: 1 (8.3%)
	2+: 18 (45%)	2+: 0 (0%)
PTEN	Negative: 31 (77.5%)	Negative: 0 (0%)
	Positive: 9 (22.5%)	Positive: 10 (100%)
p-Akt	Negative: 20 (50%)	Negative: 0 (0%)
	Positive: 20 (50%)	Positive: 13 (100%)

Data refers to number (and percentage) of cases

Conclusions: mTOR pathway activation, as evidenced by p-S6rp immunoreactivity and decreased PTEN staining, is frequent in ampullary AdCa. In most cases this appears to be independent of p-Akt status. Given evidence of pathway activation and the existence of specific anti-mTOR therapeutics, mTOR may represent a logical target for directed biologic therapy in ampullary AdCa.

1569 Expression of Phosphorylated ERK in Pancreatic Endocrine Neoplasms as a Predictor of Tumor Behavior

KM Devaraj, H Remotti. Columbia University Medical Center, New York, NY.

Background: Aberrant activation of the RAF/MEK/ERK MAPK pathway has been associated with a number of cancers and is thought to play an important role in tumor angiogenesis, invasion, metastasis, and chemotherapeutic drug response. Little is known about the molecular pathogenesis of pancreatic endocrine neoplasms (PEN) which comprise 8% of pancreatic tumors. PEN are generally indolent, however a subset of PEN show a more aggressive clinical behavior. Currently the most important prognostic factor in determining patient survival is the presence of metastases at the time of diagnoses. In the absence of metastases, other prognostic criteria include tumor size, vascular invasion, and mitotic rate. We investigate the immunohistochemical expression of activated (phosphorylated) ERK1/2 (pERK) in PEN to see if the MEK/ERK pathway is activated in these tumors and to determine if expression of pERK correlates with tumor behavior.

Design: Fifty-two cases of PEN resected during the interval 1998 to 2006 were retrieved from the tissue archives. Patient and tumor characteristics were recorded. Six tissue microarrays were created from paraffin-embedded blocks of PEN, sampling five 2mm cores of tumor and one 2mm core of normal pancreas for each case. Immunohistochemistry for pERK1/2 (Cell Signaling Technology, Inc) was performed on 5 micron sections of the PEN TMAs. Cytoplasmic staining intensity was graded on a scale of 1+ to 3+ and percentage of positive staining tumor cell nuclei recorded (<5% of nuclear staining considered negative).

Results: Expression of pERK was seen in 25% (13/52) PEN cases. Nuclear staining was patchy and often noted in tumors showing diffuse cytoplasmic staining. Between pERK positive and pERK negative groups there was no significant differences in patient sex, median age (61 vs. 62 yrs), or tumor size (2.5 vs. 2.0 cm). Vascular invasion was present in 85% (11/13) of pERK+ cases, compared to 46% (18/39) of pERK- cases (p=0.016). Similarly, 85% of pERK+ cases were locally invasive vs. 44% of pERK- cases (p=0.010). Lymph node metastases were noted in 46% (6/13) of pERK+ cases compared to 18% (7/39) of pERK- cases (p=0.042).

Conclusions: Expression of pERK in pancreatic endocrine neoplasms strongly correlates with markers of tumor aggressiveness and poor prognosis. These findings suggest that the MEK/ERK pathway may be important in PEN progression and metastases. Furthermore a subset of aggressive PEN with expression of pERK may benefit from treatment with multikinase inhibitors.

1570 Isoniazid-Associated Hepatotoxicity: A Clinicopathologic Study of 8 Cases

JS Do, MM Yeh. University of Washington, Seattle.

Background: Tuberculosis (TB) remains an ongoing major health problem in the developed and developing world. Isoniazid (INH) has been one of the advances in treating TB; however, it has known hepatotoxicity, ranging from asymptomatic elevations of liver function tests, to acute hepatitis, or fulminant liver failure. A limited number of published data precludes chronic liver diseases as established risk factors for INH hepatotoxicity during TB therapy. We examined the pathologic features and clinical outcome of INH associated hepatotoxicity.

Design: 8 cases of documented (including 4 definite and 4 suspicious) INH-associated hepatotoxicity with available surgical pathology specimens were identified from our file. H&E and available special stained slides, clinical records, and laboratory data were reviewed.

Results: The 8 patients ranged from 23-69 years of age (mean: 44; M:F= 4:4). Time from initiation of INH therapy to development of symptoms/elevated LFT ranged from 1 to 6 months. AST ranged from 41 to 2451 (mean: 608); ALT ranged from 26 to 1591 (mean 500); alkaline phosphatase ranged from 99 to 530 (mean 213); total bilirubin ranged from 1.1 to 17.8 (mean 7.2). 3 definite and 1 suspicious cases for INH hepatotoxicity had no underlying liver disease. Histologically, 5 cases showed cholestasis, bridging necrosis and marked bile ductular reaction, whereas the remaining 3 cases showed mild lobular and focal portal inflammation. Acidophil bodies were common. In the 4 cases suspicious for INH hepatotoxicity, 3 had known underlying liver disease (1 had HCV/HIV and 2 were post liver transplant for HCV and/or HBV). 2 showed hepatitis and 2 showed extensive bridging necrosis and cholestasis on histology. Clinically, 2 definite cases for INH hepatotoxicity completely recovered after INH withdraw, whereas the other 2 definite cases for INH hepatotoxicity required liver transplant (1 died 1 day after transplant due to downhill hepatotoxicity, who also had concomitant non-alcoholic steatohepatitis and the other had no known adverse outcome after transplant).

Conclusions: While there is a spectrum of histology of INH-associated hepatotoxicity including cholestasis in addition to hepatitis and extensive liver necrosis, these observations may be obscured by concomitant liver disease. The common findings of marked bile ductular reaction is typically associated with extensive necrosis, suggesting activation of the regeneration compartment. As the outcome may be severe, caution should be exercised when prescribing INH, especially in patients with underlying liver disease.

1571 The Role of High Fat Diet in Non Alcoholic Fatty Liver Disease (NAFLD)

A Don-Wauchope, H El-Zimaity, A Holloway. McMaster University, Hamilton, ON, Canada; Hamilton Regional Laboratory Medicine Program, Hamilton, ON.

Background: Fatty Liver is an increasing health problem contributing to cirrhosis. The increased incidence is associated with the rise of obesity. To understand its early development we examined the development of fatty liver from high fat diet in Wistar Rats.

Design: We introduced high fat feed and normal diet to weaning pups. The high fat diet was selected to simulate the typical western high fat diet (RD Western Diet, Opensource Diets ™). One third of the animals were selected for necropsy at 7 weeks of age after 4 weeks of a high fat diet. The animals were weighed twice a week and at necropsy. The intra-abdominal fat pads were weighed at necropsy. Blood was collected in serum tubes and the liver was sampled for histology and proteomics. At 7 week necropsy a portion of the liver samples were collected after perfusion with 0.9% saline solution.

Results: Thirty-one animals were selected at random for necropsy. Twelve pairs (5 female and 7 male) and 7 individual (6 female and 1 male) animals were processed. The weights of the animals were not significantly different between the high fat and the low fat diet. However, the abdominal fat pads were significantly different ($p<0.0003$). When analyzed by gender the females showed significant weight gain ($p< 0.002$) and increase in abdominal fat weight ($p<0.001$). In contrast, the males only showed a significant increase in abdominal fat ($p<0.001$). On histology 6 out of 8 of the females on the high fat diet developed fatty liver whereas only 3 of 8 males developed fatty liver ($p=0.14$). The distribution of fatty change was different to that usually reported with steatosis in zone 1 rather than the zone 3. The findings on histology are shown in table 1.

Table 1. Histology Findings at 7 week necropsy

Diet	Gender	N	Fat present	Fat Type
Low Fat	Female	8	0	none
High Fat	Female	8	6 (p=0.03)	Macrovesicular 6 (p= 0.03)
Low Fat	Male	7	0	none
High Fat	Male	8	3 (p=0.08)	Macrovesicular 3 (p= 0.08)

Conclusions: The early introduction of a high fat diet has resulted in histological changes consistent with fatty liver or NAFLD without fibrosis after 4 weeks. In addition to gender differences, the distribution of fatty change was different from that commonly seen in NAFLD. Abnormal fat deposition in zone 1 has been previously described with nitric oxide synthase knock-out mice (Biochimica et Biophysica Acta 1782 (2008) 180–187).

1572 Immunohistochemical Expression of Progesterone Receptor in Neuroendocrine Tumors: Expression Is Present Predominately in Low-Grade Pancreatic Endocrine Neoplasms

JS Estrella, H Wang, MW Taggart, SC Abraham, A Rashid. MD Anderson Cancer Center, Houston, TX.

Background: Previous studies have reported immunohistochemical expression of progesterone receptor (PR) in neuroendocrine tumors of different sites. However, the prognostic significance of PR expression in neuroendocrine tumors has not been studied.

Design: We investigated the immunohistochemical expression of PR in 133 neuroendocrine tumors, including 71 pancreatic endocrine neoplasms (PENs), and 45 gastrointestinal and 17 lung carcinoid tumors using tissue microarray. Statistical analyses were done using Fisher's exact test, T-test and overall survival by log-rank method.

Results: Thirty-eight of 71 (51%) PENs showed positive PR immunohistochemical staining compared to 2 of 45 (4%) gastrointestinal and 0 of 17 (0%) lung carcinoids

(p=0.0001). In PENs, PR expression was significantly associated with WHO grade and size of tumors. PR staining was present in 14 of 15 (93%) WHO grade 1A, 7 of 8 (88%) grade 1B, 16 of 44 (36%) grade 2 and 0 of 5 (0%) grade 3 tumors (p=0.0001). PR positive PENs averaged 2.9 ±0.3 cm versus 5.5 ±0.7 cm for PR negative PENs (p=0.001). MEN-1 associated PENs were more frequently PR positive (88%) compared to sporadic tumors (48%), however, the data was not statistically significant (p=0.057). The mean overall survival of patients who had PR positive PENs was 272 ±42 months compared to 116 ±13 months for patients with PR negative PENs, although statistical significance was not met (p=0.08).

Conclusions: In neuroendocrine tumors, PR expression is present predominately in smaller WHO grade 1 PENs, and PENs in syndromic patients. PR positivity may help in differentiating benign from aggressive PENs in a biopsy specimen and may help to ascertain site of origin of metastatic low-grade neuroendocrine carcinomas.

1573 Immunohistochemical Classification of Hepatic Adenomas and Atypical Hepatocellular Neoplasms: Correlation with Clinicopathologic Characteristics and Chromosomal Abnormalities

K Evason, J Grenert, L Ferrell, S Kakar. UCSF, San Francisco, CA.

Background: The distinction of hepatic adenomas(HA)from hepatocellular carcinoma(HCC)is difficult in males,elderly women,or when focal atypical features are present.These tumors can show chromosomal abnormalities(Chr Abn)typical of HCC and can recur or metastasize.Recently,HAs have been classified based on inflammatory features and β-catenin(βC)pathway abnormalities.The latter may have higher risk for progression to HCC.We examine the relationship of SAA expression and βC abnormalities with clinicopathologic features and Chr Abn.

Design: Immunohistochemistry for βC,glutamine synthetase(GS)and serum amyloid associated protein(SAA)was done in 23 HA,36 AHN and 18 well-differentiated HCC. AHN was used for HA-like tumors in men,women ≥50 or ≤15 years and/or with focal atypia(small cell change,pseudoglands,thick plates).Tumors with nuclear βC and/or diffuse GS were regarded as βC abnormal.Chromosomal gains/losses had previously been determined in 39 cases using CGH or FISH.

Results: βC and Chr Abn in AHNs were more common than HA,but were similar to HCC(table1).HAs and AHNs with abnormal βC were associated with atypical morphology(table2).Follow-up data was limited but adverse outcome was observed in 3 tumors with abnormal βC(2 recurrences,1 metastasis);in addition,transition to areas of HCC was observed in 2 cases.Chr Abn were more often seen in tumors with abnormal βC(89%vs12%,p<0.001).

	Inflammation	Telangiectasia	βC abnormal	SAA +	Chr Abn
HA	45	41	6	63	0
AHN	36	33	44	62	53
HCC	-	-	50	29	55
p value	0.17	0.19	0.003,0.21	0.58,0.03	0.007,0.3

Figures reflect percentages;p values are AHN vs HA,AHN vsHCC

	Atypical age/sex	Atypical morphology	Inflammation	Telangiectasia	Chr Abn
βcatenin abn vs normal	43 vs 30	71 vs 20	35 vs 44	35 vs 38	89 vs 12
p value	0.17	<0.001	0.2	0.23	<0.001
SAA positive vs negative	43 vs 22	33 vs 42	48 vs 26	45 vs 21	50 vs 38
p value	0.12	0.37	0.1	0.08	0.47

Conclusions: Most adenoma-like neoplasms with βC abnormalities detectable by immunohistochemistry showed atypical morphological features,and were associated with Chr Abn typical of HCC.Some of these tumors can recur and metastasize.It is likely that these tumors represent extremely well-differentiated HCC.SAA expression shows borderline significant correlation with inflammation and telangiectasia,but not with atypical morphological features or Chr Abn.

1574 Sinusoidal Obstruction Syndrome and Ascites Resulting from Severe Acute Cellular Rejection Post Liver Transplantation

C Fan, MH Sanei, TD Schiano, MI Fiel. Mount Sinai Medical Center, New York, NY; Isfahan Univ, Isfahan, Islamic Republic of Iran.

Background: Ascites formation post liver transplantation (LT) is multifactorial. Sinusoidal obstruction syndrome (SOS) is a rare cause of ascites post-LT and has been rarely reported to occur as a sequela of acute cellular rejction (ACR). We sought to examine the histology of patients developing ascites in the setting of ACR.

Design: Using the Mount Sinai Pathology database, we identified 5 patients with ACR developing ascites and another 5 patients who had severe ACR without ascites (control). Degree of congestion, central venulitis, and hepatocyte necrosis were each scored: 0 = absent; 1 mild; 2 moderate and 3 severe; perivenular fibrosis was scored: 0 absent; 1 mild; 2 fibrous septa present in zone 3; 3 numerous fibrous septa beyond zone 3; and 4, bridging fibrous septa. Rejection activity index (RAI) was based on the Banff criteria. None of the baseline donor liver showed fibrosis.

Results: Note that the patients with ascites had mean perivenular fibrosis = 3.7; all having score of 3 for congestion, central venulitis and hepatocyte necrosis. Serological work up for other causes was negative. All 5 control cases had negligible perivenular fibrosis (mean 0.25), minimal congestion (mean 0.75) and no hepatocyte necrosis.

1

Pts age/gender	Liver Disease	Days post-LT	Perivenular fibrosis	Hepatocyte necrosis	Congestion	Venulitis	RAI
1- 46 F	Alcohol	244	4	2	3	3	3/3/3=9
2- 46 F	AIH**	249	4	2	3	3	2/3/2=7
3- 45 F	Biliary Cirrhosis	191	4	2	3	3	3/3/3=9
4- 58 F	Alcohol	360	4	2	3	3	3/3/3=9
5- 51 F	HCV	420	2	2	3	3	2/3/3/=8
6- 73 M	PSC*	2650	1	1	1	1	2/2/3=8
7- 49 F	AIH**	471	0	2	1	3	3/2/3=8
8- 39 M	Alcohol	152	0	1	1	3	3/2/3=8
9- 46 M	PSC*	43	0	2	1	1	3/3/2=8
10- 60 M	HCV	180	0	1	0	1	3/3/3=9

Cases 1-5, Control 6-10; **autoimmune hepatitis; *primary sclerosing cholangitis

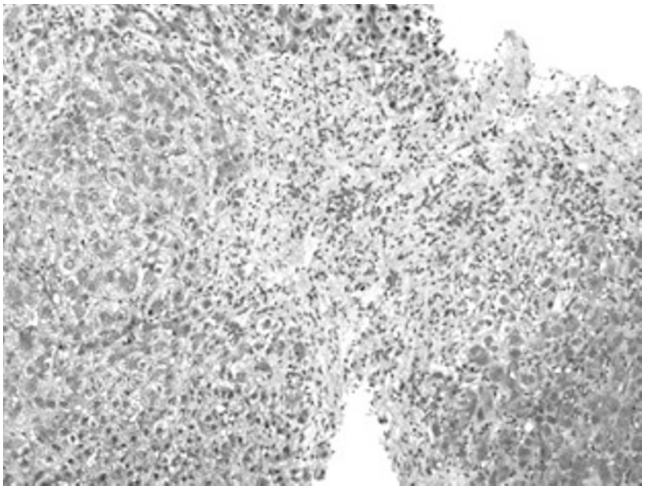

Conclusions: Severe ACR resulting in SOS may be the cause of ascites formation post-LT. The presence of significant perivenular fibrosis, hepatocyte necrosis and congestion in the setting of severe ACR may signify a poor prognosis for recovery.

1575 EGFR Expression and KRAS Mutation in Cholangiocarcinoma: Implication in EGFR-Targeted Therapies

LF Fan, V Datta, A Riley-Portuges, J Lopategui, F Lin, H Xu, HL Wang. Cedars-Sinai Medical Center, Los Angeles, CA; Geisinger Medical Center, Danville, PA; University of Rochester, Rochester, NY.

Background: Cholangiocarcinoma is a highly aggressive malignancy with extremely poor patient survival. It shares many of the histologic and immunophenotypic features with pancreatic ductal adenocarcinoma (PDA) but may differ from it pathogenetically. Mutational activation of the *KRAS* oncogene is a very common event in PDA, reported in over 90% of the cases in some studies, and these patients would not benefit from anti–epidermal growth factor receptor (EGFR) therapies. EGFR expression and *KRAS* mutation have not been well characterized in cholangiocarcinoma, however**.**

Design: A total of 59 cases of surgically resected cholangiocarcinoma (48 intrahepatic and 11 extrahepatic) were immunohistochemically stained for EGFR expression utilizing a monoclonal antibody. A tumor was recorded positive when ≥1% of the tumor cells exhibited any membranous staining above background. Positive cases were further stratified as 1+ (weak), 2+ (moderate) and 3+ (strong), as well as focal (1-50% of tumor cells stained) and diffuse (>50%). EGFR gene amplification was analyzed by FISH using commercially available probes. In each case, 200 nuclei were assessed and EGFR was considered amplified when the ratio of EGFR signals to chromosome 7 centromere was >2. *KRAS* mutational testing was performed employing a 92-bp amplicon containing both codons 12 and 13 in exon 2 followed by high-resolution melting curve analysis using DNA extracted from formalin-fixed paraffin-embedded tumor tissue.

Results: Positive EGFR immunostaining was detected in 43 of 59 (73%) cholangiocarcinomas, among which 26 (60%) exhibited 2+ or 3+ and diffuse immunoreactivity. EGFR amplification was detected in only 1 of 12 (8%) cases that showed 2+ or 3+/diffuse EGFR expression. KRAS mutation was detected in 1 of 49 (2%) cases with amplifiable DNA and interpretable results. This case showed 2+/focal EGFR expression but did not exhibit EGFR amplification.

Conclusions: EGFR is frequently overexpressed in cholangiocarcinoma independent of gene amplification. In contrast to PDA, cholangiocarcinoma infrequently harbors *KRAS* mutations. These observations may have important therapeutic implications since EGFR-targeted therapies have shown promise for malignancies that lack *KRAS* mutations.

1576 Necrotizing Arteritis Presenting as a Pancreatic Mass: A New Addition to the Immune-Related Tumoral Pancreatitides

AB Farris, I Coban, DS Klimstra, G Kim, V Deshpande, N Ohike, N Adsay. Emory U, Atlanta; Memorial-Sloan Kettering Cancer Center, New York; UCSF, San Francisco; Massachusetts General Hospital, Boston.

Background: Autoimmune pancreatitis (AIP) has thus far been categorized in two distinct subtypes: 1) IgG4-related lymphoplasmacytic-sclerosing (LPSP), often associated with exocrine organ disease such as Sjögren, and 2) granulocytic-epithelial lesion(GEL)-forming (idiopathic duct-centric), often associated with ulcerative colitis and related conditions. Here we present 4 examples of a distinct subset characterized by arteritis and lacking the stigmata of the other 2 types.

Design: Clinicopathologic features of these 4 cases were analyzed. Reviewed separately were pancreatic sections from 41 resected ordinary AIPs and 28 collagen vascular disease (CVD) autopsies.
Results: Study group patients (2 male, 2 female) underwent resection with a clinical suspicion of adenocarcinoma (3 pancreatoduodenectomies, 1 distal pancreatectomy). They had mean age of 60 and presented with abdominal pain (n = 2) and jaundice (n = 1). Microscopically, all had arteritis with focal fibrinoid necrosis in pancreatic parenchymal large and medium-sized arteries. No GEL formation was noted. None had classical stigmata of LPSP such as storiform fibrosis. Three cases had relatively mild inflammation. Acinar lobules were well-preserved. There were no (n = 2) or only focal (n = 2) plasmacytic infiltrates including a systemic lupus erythematosus (SLE) case in which inflammation spared the ducts. SLE and psoriasis were present in 2 cases and 1 case, respectively, and a 4th case was lost to follow up. In CVD autopsy cases, 6/28 showed focal pancreatic vasculitis but no associated pancreatic injury. Among 41 ordinary AIP cases, 3 had focal arterial involvement amidst abundant periarterial inflammation [regarded as 2°, not 1° vasculitis].
Conclusions: This rare but distinct sub-type of AIP is characterized by arteritis and a lack of the classical stigmata of LPSP and GEL-forming AIP categories. This arteritic-type AIP appears to be associated with CVDs such as SLE. Further studies are warranted to clarify this sub-type's nature and its association with other variants.

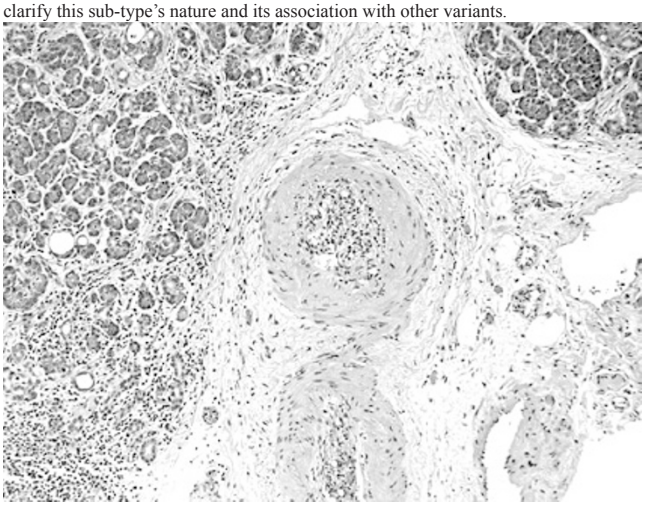

1577 Glutamine Synthetase (GS) Expression in Cirrhosis, Veno-Occlusive Disease (VOD), Congested Liver Adjacent to Mass Lesions, and Focal Nodular Hyperplasia (FNH)

KE Fleming, IR Wanless. Dalhousie University, Halifax, NS, Canada.

Background: In normal liver, GS is expressed in a narrow rim of perivenous hepatocytes. In cirrhotic human liver GS expression was undetectable in one study (Racine-Samson 1996). In another study GS expression was present in a perivenous pattern within cirrhotic nodules or at the periportal interface when hepatic veins (HVs) were adherent to a septum (DiTommaso 2007, Rebouissou 2008). We have noted many hepatic veins in cirrhotic nodules do not have perivenous GS expression. The purpose of this study is to clarify the patterns and mechanisms of GS expression, including the loss of GS staining in some perivenous regions in cirrhosis and other liver conditions.
Design: Surgically resected specimens of liver with a variety of conditions were studied after staining serial sections for connective tissue (trichrome), GS, and CD34. Specimens included cirrhosis removed at transplantation (alcohol 6, NASH 1, HCV 5, biliary cirrhosis 5), congenital hepatic fibrosis (1), tissue adjacent to mass lesions (4), VOD (2), chronic cholestasis without cirrhosis (1), and FNH (4).
Results: We confirmed the perivenous GS pattern in cirrhosis as described by DiTommaso et al. and the map-like increase in perivenous expression in FNH reported by Bioulac-Sage et al. 2009. In addition, we noted GS positive hepatocytes within nascent cirrhotic nodules within septa (buds). GS was absent adjacent to approximately one third to half of HVs within cirrhotic nodules, most of which were also CD34 negative. GS negative HVs were especially prominent in highly regressed cirrhosis. GS staining was also lost in areas of congestive injury, especially in congested cirrhotic nodules and in non-cirrhotic liver adjacent to mass lesions, in VOD, and in congested regions of FNH.
Conclusions: GS staining is lost during the acute phase of congestive zone 3 injury. HVs in highly regressed cirrhosis are often GS negative and CD34 negative. We interpret these HVs as recruited veins remodeled from sinusoidal structures, supporting the suggestion that cirrhosis regresses as new HV outflow capacity is generated. Buds arising from paraductal tissue are GS positive and appear to give rise to small GS positive nodules in advanced micronodular cirrhosis.

1578 Mismatch Repair Status in Seventy Biliary Tract Carcinomas

WL Frankel, JJ Liu, H Hampel, AM Bellizzi. The Ohio State University Medical Center, Columbus, OH; Brigham and Women's Hospital, Boston, MA.

Background: Lynch Syndrome (LS) is a cancer predisposition syndrome due to germline mutations in DNA mismatch repair (MMR) genes. Deficient MMR function results in microsatellite unstable tumors. In addition to colon cancer, there is increased risk of cancer at a defined subset of extracolonic sites, including the biliary tract. Population-based LS screening by MMR immunohistochemistry (IHC) is effective in colon cancer, and LS-colon cancers are associated with certain histologic features. We studied the MMR status of a group of biliary tract carcinomas unselected for age or personal cancer history.
Design: Tissue microarrays were constructed from 47 cholangiocarcinomas (CC) and 23 gallbladder adenocarcinomas (GB). MMR IHC for MLH1, PMS2, MSH2, and MSH6 was performed. The proteins were scored as present or absent (no definite nuclear staining in the setting of intact staining in internal control). Clinical data (age, sex, personal history of cancer) was collected and histologic features (grade, presence of tumor infiltrating lymphocytes or mucinous features) assessed in patients with abnormal MMR IHC.
Results: Two of 47 (4.3%) cholangiocarcinomas (2 women, ages 70, 75) and 1 of 23 (4.3%) gallbladder adenocarcinomas (woman, 62) demonstrated absent MLH1/PMS2 expression. All were moderately differentiated adenocarcinomas without tumor infiltrating lymphocytes (TIL) or mucinous features. The patient with the GB had concurrent clear cell renal cell carcinoma; the 2 patients with CC had no known history of malignancy.
Conclusions: Biliary tumors demonstrate a low rate of deficient MMR function (4.3%). Patterns of abnormal IHC especially suggestive of LS (i.e., absent MSH2/MSH6 expression, isolated loss of PMS2 or MSH6) were not observed. The 3 abnormal cases lacked features of microsatellite unstable tumors as seen in the colon (i.e., poor differentiation, TIL, mucinous features). Absent MLH1/PMS2 expression in rare tumors may reflect *MLH1* promoter hypermethylation. Population-based screening of CC and GB does not appear warranted. Instead, testing of select cases (e.g. those with compelling histologic features; instances in which one represents the only tumor tissue available in a family with suggestive family history) is recommended.

1579 Characterization of CD34 Expression in Nonalcoholic Steatohepatitis

RM Gill, NM Bass, LD Ferrell. Univ Calif, San Francisco; Univ Calif, SF.

Background: Non-alcoholic steatoheptitis (NASH) is increasing in incidence and is among the most prevalent liver diseases in the developed world. Correct classification of NASH liver biopsies is of critical importance and relies on correct orientation to microscopic liver architecture. Centrizonal arteries in NASH cases represent a potential source of diagnostic error and so, to better characterize this previously reported finding, we evaluated CD34 expression in NASH liver biopsies.
Design: 100 biopsies, with NASH fibrosis stage >1a, from NASH Clinical Research Network participants (2/05 - 8/06) were randomly selected, H&E stained slides were reviewed, and adjacent unstained sections were immunostained for CD34. Prevalence of CD34+ centrizonal microvessels was graded as 0 (none in central zones), 1 (1-2 central zones with microvessels), 2 (<50% of central zones with microvessels), or 3 (>50% of central zones with microvessels). Pericentral sinusoid CD34 immunostaining was also graded (0, 1, and 2) and lobular microvessels (MV) were quantified.
Results: Microvessels were present in portal tracts and lobular parenchyma in all cases and in central zones in 73/100 biopsies (in comparison, centrizonal arteries were identified in 40% of cases on H&E stained sections). Higher stage lesions demonstrated more prevalent central zone involvement by CD34+ microvessels (grades 2+3) [stage 1: 5/19 (26%); stage 2: 8/34 (24%); stage 3: 24/36 (67%); stage 4: 9/11 (82%)], with increasing prevalence correlating directly with more advanced disease ($p < 0.001$). Evaluation of pericentral sinusoid CD34 immunostaining (grades 1+2) revealed a similar significant association with higher stage lesions [stage 1: 13/19 (68%); stage 2: 26/34 (77%); stage 3: 32/36 (89%); stage 4: 10/11 (91%)] ($p<0.001$). Microvessel density in lobular parenchyma (stage 1: 1.5 +/- 0.23 MV/mm2; stage 2: 1.2 +/- 0.12 MV/mm2; stage 3: 2.2 +/- 0.2 MV/mm2; stage 4: 3.3 +/- 0.51 MV/mm2) was also significantly increased in advanced disease ($p < 0.001$).
Conclusions: Centrizonal arteries/microvessels are common in NASH and, along with sinusoidal capillarization, are notably increased in patients with higher NASH fibrosis stage. Pathologists should be aware of the possible finding of CD34+ centrizonal arteries/microvessels in higher stage cases and not fail to diagnose NASH. The finding of increased centrizonal arteries and sinusoidal capillarization in advanced stage NASH support an etiologic role for angiogenesis and/or vascular remodeling in NASH progression to cirrhosis.

1580 The Role of K-ras Mutations in Pancreatic Neuroendocrine Tumors

K Gilliland, HJ Dong, S Hochwald, C Liu. University of Florida, Gainesville, Fl.

Background: Mutations in K-ras appear to be early events in the progression of tumors in colorectal, pancreatic, and lung primary sites. K-ras mutations are important in the signaling pathway, downstream from the epidermal growth factor receptor (EGFR), and are usually due to a single base pair substitution. Mutations in codons 12 and 13 of the K-ras gene have been demonstrated in pancreatic and colonic adenocarcinomas with a reported incidence varying between 35-88%. However, K-ras mutations have not been studied extensively in pancreatic neuroendocrine tumors, particularly in a large cohort of cases, due to their relative rarity. The goal of this study is to determine the K-ras status in pancreatic neuroendocrine tumors.
Design: We examined 52 cases of pancreatic neuroendocrine tumors from the pathology files of our institution for the presence of K-ras mutations. Based on WHO criteria, the tumors were classified into 33 cases of well differentiated tumors, of which 12 were benign and 21 were uncertain behavior categories, and 19 cases of well differentiated endocrine carcinoma. DNA was extracted from formalin-fixed paraffin-embedded tissue, followed by PCR amplification of the K-ras gene. Sequencing of the K-ras gene product was performed using pyrosequencing at codons 12 and 13.
Results: No mutations were detected in codons 12 and 13 in all of the 52 cases of pancreatic neuroendocrine tumors. No sequence alterations were detected in well-differentiated (benign) pancreatic tumors, as well as uncertain metastatic potential and (malignant) pancreatic neuroendocrine carcinomas.

Conclusions: This study is the first to examine the role of K-ras mutations in pancreatic neuroendocrine tumors in a large cohort with pyrosequencing methods. Our findings suggest that mutations in codons 12 and 13 of the K-ras gene are not involved in the pathogenesis of pancreatic neuroendocrine tumors. This study indicates that the K-ras pathway may not be involved in pancreatic neuroendocrine tumors. Considering that the majority of pancreatic adenocarcinomas have K-ras mutations, K-ras sequencing analysis is valuable for differentiation of adenocarcinomas from neuroendocrine carcinomas in some cases.

1581 Histomorphologic Analysis of Preoperative Intensity Modulated Radiotherapy (IMRT) and Chemoembolization for Hepatocellular Carcinoma in Liver Explants

C Gimenez, HK Islam, M Facciuto, US Katta. New York Medical College at Westchester Medical Center, Valhalla, NY.

Background: Preoperative adjuvant therapies are documented to improve the overall survival of liver transplant recipients with concurrent hepatocellular carcinoma (HCC) and various therapeutic modalities are described including recently used IMRT (Intensity Modulated RadioTherapy). In this study, we analyzed the histomorphologic effects of IMRT on HCC as well as in the adjacent parenchyma; and compared them with those of chemoembolization.

Design: Thirty cases of ESLD (end stage liver disease) with concurrent HCC who underwent preoperative adjuvant therapy (15, IMRT; 15, chemoembolization) prior to liver transplant with documented histologic findings of therapy effects were included in this study. The histologic slides were retrieved from our archives and reviewed by 2 different pathologists and consensus findings were graded for final interpretation. Extent of therapy induced tumor necrosis was graded as, 0, 0-5% necrosis, grade 1, 6-50% necrosis, and grade 2-≥50% necrosis. Congestion and hemorrhage were interpreted as undesirable side effects.

Results: In IMRT group, tumor necrosis was observed in 53% (8/15) cases; 13% with grade 1 and 40% with grade 2 necrosis while 47% cases showed no tumor necrosis (grade 0). Undesirable side effects were noted in 67% (10/15) cases, however, all of them were confined within 5 mm area around the targeted tumor nodules, except in one case, where the targeted tumor was missed. In contrast, in the chemoembolization group, tumor necrosis was achieved in 87% (13/15) cases; 20% with grade 1 and 67% with grade 2 while only 13% cases showed no therapy induced tumor necrosis (grade 0). Side effects in the latter group are more haphazard and not limited to immediate surrounding areas.

Conclusions: IMRT, a relatively less invasive procedure, is recently described as a modality of adjuvant therapy for HCC in ESLD, who subsequently requires liver transplantation. Our preliminary data suggests that it may have lesser overall effects in inducing tumor necrosis but it can target the lesions more precisely and the side effects are essentially confined to immediate surrounding areas as compared to other modalities, namely chemoembolization. IMRT, thus, may have the potential of minimal functional damage as compared to others, especially in the setting of ESLD with already compromised liver functions.

1582 Clinicopathologic and Molecular Characterization of Hepatocellular Adenomas (HCA) and Focal Nodular Hyperplasias (FNH)

A Gru, RK Pai, EM Brunt. Washington University in St. Louis, Saint Louis, MO.

Background: HCA are benign neoplasms that occur in women exposed to exogenous estrogen. FNH are non-clonal proliferations that result from a dysregulation of angiopoietins. Inflammatory adenomas (IA), previously known as telangiectatic FNHs, can present a diagnostic difficulty between both FNH and HCA; they have recently been shown to have a characteristic mutation in gp130. Serum amyloid A (SAA) is overexpressed in IA. We aim to identify clinicopathologic features and molecular characteristics in HCA and FNH in a large American population.

Design: 42 cases of FNH, and 41 cases of HCA were retrieved from our files (1999-present). Clinicopathologic data included: age, gender, medications, body mass index (BMI), ethnicity, (BMI), liver tests, symptoms, tumor size, number, location, and all accompanying features (eg hemorrhage, rupture, etc). All cases were reviewed. Immunohistochemistry was performed in 25 cases for: Serum amyloid A (SAA), LFABP, b-catenin (BC), and Glutamine synthetase (GS). New potential molecular targets were also performed: VEGF, p16, CD68, and pSTAT3.

Results: The clinical follow-up available was similar for both groups (22 and 26 mos respectively); there were no adverse outcomes. Table 1 summarizes the clinical information and patterns of IHC. 3 LFABP mutated adenomas, 9 IAs, and 13 FNHs were tested with IHC. No activated BC adenomas were found. 4 unusual features were identified: 1) SAA+ was found in 2/13 FNHs, (2) GS, present in all FNH, was also diffusely present in 2/9 IA; 3) senescence (as determined by p16) was negative in all;; 4) BMI was not a discriminant feature of adenoma subtype.

Conclusions: This is the largest series of HCA with IHC reported in America. All HCA are found in obese patients; steatosis is present in nearly one-third in background liver. IHC may be a useful tool to distinguish FNH and IA, but lacks specificity. Senescence does not appear to play a role in ductular reaction in FNH or IA. In-Situ PCR is being evaluated.

	HCA (%)	FNH (%)	Statistics	
Female	83	88	NS	
BMI	32.5 (mean)	27.8 (mean)	0.009	
Abnormal LFT	29	7	0.065	
Oral Contraceptives	55	22	0.002	
Multiplicity	32	58	NS	
Rupture / Hemorrhage	24 / 12	0 / 0	<0.05	
NT Liver: Steatosis / SH	29 / 7.5	11 / 4	<0.05	
IHC	LFABP Adenoma	ßCatenin	IA	FNH
GS	0/3	0	2/9	13/13
SAA	0/3	0	9/9	2/13
LFABP	0/3	0	8/9	13/13
p16	0	0	0	0
CD68	3/3	0	9/9	13/13
VEGF	3/3	0	9/9	13/13
pSTAT3	0	0	0	0

1583 Epithelial to Mesenchymal Transition in Peripheral Cholangiocarcinoma

N Guedj, PE Rautou, F David, B Jacques, B Pierre, F Olivier, P Valerie. Beaujon Hospital, Clichy, France.

Background: Epithelial to mesenchymal transition (EMT), defined by the loss of epithelial characteristics and the acquisition of mesenchymal phenotype, has been shown to play a major role in tumoral invasion. Several morphological features of peripheral CC, such as the presence of an abundant desmoplastic stroma, frequent neural invasion and satellite nodules, suggest that EMT could be activated in these tumors. Therefore, we aimed to study expression of relevant markers consistent with the acquisition of an EMT phenotype and to evaluate the implication of this process in the aggressiveness of peripheral CC.

Design: Clinicopathological data were retrospectively collected from 57 peripheral CC surgically treated. We evaluated the expression of several EMT markers, including different types of cytokeratins (CK), vimentin and adhesion cell molecules (Ep-CAM, E-cadherin) using immunohistochemistry in tissue microarray. EMT phenotype was considered present when tumors acquired vimentin expression (>10% of tumor cells), and displayed a decreased expression in at least one CK (<20%). We also noted if an aberant E-Cadherin cytoplasmic staining was present. Main histoprognostic criteria of CC were correlated with expression of each EMT tissue marker.

Results: Mean age was 59.3±10.9 years [33-82] with 32 females and 25 males. Mean tumor size was 7.9±4.3cm [0.5-22]. Tumors corresponded to well-differentiated (n=36) or moderatly/poorly-differentiated adenocarcinomas (n=22). We observed that 24 CC (42%) expressed vimentin. We noted a decreased in CK8 expression and an aberrant E-cadherin cytoplasmic staining respectively in 19% and in 58% of tumors. According to our criteria, 16% (n=9) of peripheral CC displayed an EMT phenotype. CC with EMT phenotype did not differ from CC without EMT phenotype regarding tumor size, differentiation grade, presence of satellite nodules, perineural and node invasion. However, decreased expression of CK8 and CK19 was respectively associated with vascular invasion (63% vs 80%, p=0.06) and lymph node metastasis (86% vs 98%, p<0.0001). Decreased expression of Ep-CAM was also associated with lymph node involvement (23% vs 4%, p=0.043).

Conclusions: Our results showed that a small proportion of peripheral CC switch from epithelial to a mesenchymal phenotype but no evidence clinical relevance was observed. Nevertheless, we found that the progressive acquisition of an EMT process is implied in the invasiveness of peripheral cholangiocarcinoma.

1584 Is Autoimmune Pancreatitis Associated with an Increased Risk of Malignancy? A Retrospective and Comparative Study

RK Gupta, M Genevay, NB Johnson, GY Lauwers, V Deshpande. Massachusetts General Hospital, Boston; University of Geneva, Geneva, Switzerland; Beth Israel Deconess Hospital, Boston.

Background: Autoimmune pancreatitis (AIP) is a recently recognized form of chronic pancreatitis. Chronic pancreatitis-not otherwise specified (CP-NOS) is a well recognized risk factor for pancreatic carcinoma (PCA). Thus, theoretically, AIP may represent a risk factor for PCA. Furthermore, PCAs in patients with AIP have been reported. However, there has been no systematic study to explore this link. In this study we used PanINs as a surrogate marker for PCA, and compared the number, grade, and mutation profile of PanIN lesions in pancreatectomy specimens from well characterized cases with AIP, CP-NOS and serous cystadenoma (SCA).

Design: Pancreatic resection specimens with histological diagnoses of AIP, CP-NOS and SCA were reviewed. We chose 32 cases each from the cohorts of AIP, CP-NOS and SCA . We counted the number of PanIN lesions, and graded these lesions in all the three patient groups. A tissue microarray composed of high grade PanIN lesions was constructed and these arrays were stained for p16, p53, SMAD4 and Ki-67.

Results: Patients with AIP were older than those with CP-NOS (AIP 54 yr, CP-NOS 48 yr, SCA - 64yr) (p=NS). The AIP and CP-NOS cases showed both PanIN1 and 2 lesions, while individuals with SCA showed only PanIN1 lesions. On follow-up one patient each in the AIP and CP-NOS cohort developed PCA in the unresected pancreas. There were no PanIN3 lesions identified. Patients with AIP (mean =1.19) showed significantly more PanIN2 lesions than patients with CP-NOS (mean = 0.22) and serous cystadenomas (mean =0.12) (p = 0.04 and 0.03, respectively). Significantly, there were no statistically significant differences in the number of slides examined between the 3 groups. On immunohistochemistry, the majority of PanIN2 lesions in the AIP cohort (7 of the 8) and all 3 CP associated PanIN2 lesions showed loss of p16 protein expression . Two of the 7 PanIN 2 lesions in AIP expressed p53, while none of the 3 CP associated PanIN 2 lesions expressed this protein. AIP associated PanIN2 lesions showed a higher Ki67 labeling index (mean 4.92%) than similar grade lesions in CP-NOS (mean 0.52) (p=0.06).

Conclusions: The risk of PCA in AIP is at least similar to that posed by CP-NOS. A prospective longitudinal study is required to more definitively estimate the risk of malignancy in PCA. In the interim, long-term follow-up of cases with AIP may be required.

1585 Impact on Cell Proliferation of Proteins of the AKT/mTOR and MAPK Pathways in Human Pancreatic Adenocarcinoma

A Handra-Luca, P Hammel, V Rebours, A Sauvanet, A Martin, R Fagard, JF Flejou, J Belghiti, P Bedossa, P Ruszniewski, A Couvelard. APHP Univ Paris 13, Bondy, France; APHP Univ Paris 7, Clichy, France; APHP Univ Paris 13, Bobigny, France; APHP Universite Paris 13, Bobigny, France; APHP Univ Paris 6, Paris, France.

Background: The mitogen activated protein kinase (MAPK) and AKT pathways are main signaling pathways involved in cell proliferation, survival and chemoresistance in pancreatic ductal adenocarcinoma (PDAC) carcinogenesis.

Design: We aimed to analyze the expression of the main proteins of the MAPK (ERK1/2, P38, MKK4) and AKT (AKT, mTOR) pathways with respect to cell proliferation in PDAC. The expression of phosphorylated mTOR (p-mTOR), p-AKT, p-ERK1/2, p-P38; of AKT2, MKK4 and of Ki67 was determined by immunohistochemistry in 99 PDAC. Medians of the protein expression score (based on intensity and percentage of stained tumor cells) and of the percentage of Ki67 stained nuclei, were used to classify tumors. Statistical analysis used the Fisher's and Kendall's rank correlation tests.

Results: The expression of the 3 MAPK was coordinated.

	Kendall's Tau	p value	95% Confidence Interval
p-ERK1/2vs.MKK4	0.195	0.0053	-0.0024-0.360
p-ERK1/2vs.p-P38	0.462	<0.0001	0.270-0.6210
MKK4vs.p-P38	0.200	0.0047	-0.0051-0.3900

High expression of the 3 MAPK proteins was related to high p-mTOR [MKK4 (39/60vs.15/45, p<0.0001); p-P38 (23/50vs.8/44, p=0.0047); p-ERK1/2 (28/51vs.15/45, p=0.0411)]. A high cell proliferation Ki67 index was correlated to a high MKK4 (43/57vs.10/37, p<0.0001) and high p-mTOR (41/58vs.10/37, p<0.001), but not to AKT, ERK1/2 or P38.

Conclusions: Our results suggest that in human PDAC: 1) the expression of the 3 MAPK proteins was coordinated and correlated to p-mTOR expression, and that 2) a high cell proliferation was related to high p-mTOR and to MKK4 expression, suggesting a crosstalk between the two signaling pathways, with impact on cell proliferation at p-mTOR level. These data warrant further studies on the framework of these signaling pathways, which could impact on the choice of PDAC treatment.

1586 Clonal Origin of Multifocal Hepatocellular Carcinoma

KB Hodges, OW Cummings, R Saxena, M Wang, S Zhang, A Lopez-Beltran, R Montironi, H Nour, L Cheng. Indiana University School of Medicine, Indianapolis, IN; Cordoba University, Cordoba, Spain; Polytechnic University of the Marche Region (Ancona), United Hospitals, Ancona, Italy.

Background: Hepatocellular carcinoma (HCC) is the most common primary tumor of the liver. Patients frequently have multiple histologically similar, but anatomically separate tumors. The clonal origin of multiple hepatocellular carcinomas is uncertain.

Design: We analyzed 31 tumors from 12 different patients (11 female, 1 male), who had multiple hepatocellular carcinomas involving one or both lobes. Genomic DNA was extracted from formalin-fixed, paraffin-embedded tissue using laser capture microdissection. DNA was analyzed for: loss of heterozygosity (LOH) using four highly polymorphic microsatellite loci including 9p21 (D9S161), 11q13 (D11S970), 9p21 (IFNA, D9S171), and 17p13.1 (TP53); X-chromosome inactivation status; and, TP53 gene mutations in exons 5, 7 and 8.

Results: All patients had synchronous tumors. Chronic liver disease was present in 10/12 (83%) patients, and 6 (60%) of these patients had cirrhosis. HCV infection was the main cause of chronic liver disease. All of the separate tumors from an individual patient had similar histology and grade. Ten of the 12 (83%) cases had vascular invasion. Pathologic stages were as follows: pT2 in 2 cases (16%), pT3 in 5 cases (42%), and pT4 in 5 (42%) cases. Ten of the 11 (91%) informative cases showed LOH at one or more of the analyzed microsatellite markers. Eight of the 10 (80%) cases demonstrated identical allelic loss patterns indicating common clonal origin. The remaining two (20%) informative cases had discordant patterns indicating independent clonal origin. Nine of the 10 (90%) informative female patients demonstrated a concordant pattern of non-random X-chromosome inactivation. The remaining case demonstrated a discordant non-random pattern of X-chromosome inactivation suggesting independent clonal origin. TP53 mutations were identified in 8 of 12 (67%) patients. Tumors in 7 of these 8 (88%) patients showed different point mutations. Normal tissue did not harbor any TP53 mutations in these exons.

Conclusions: In summary, our findings suggest that the majority of patients with multifocal hepatocellular carcinomas have common clonal origin. A better understanding of the genetic relationships between multiple tumors may be clinically important in assessing prognosis, and selecting therapeutic options in these patients.

1587 Clonality and TP53 Mutation Analysis of Focal Nodular Hyperplasia of the Liver

KB Hodges, S Zheng, OW Cummings, R Saxena, S Zhang, M Wang, L Cheng. Indiana University School of Medicine, Indianapolis, IN; North China Coal Medical College, Tangshan, China.

Background: Focal nodular hyperplasia (FNH) is considered a benign tumor of the liver. The pathogenesis and biologic nature of FNH is not clear. It has been proposed that FNH might be a benign reactive lesion related to hyperperfusion of blood caused by local arterial malformation. However, the clonality status of FNH is not well established. We sought to determine the clonality and TP53 mutation status of FNH to better characterize the nature of FNH in these patients.

Design: We analyzed 15 cases of FNH from female patients who underwent surgical resection of their lesions. All cases of FNH were diagnosed according to published criteria; all cases showed classic FNH features. Laser-capture microdissection of tumor and normal tissue from each patient was performed on sections with a PixCell II Laser Capture Microdissection system. Cell clusters were microdissected from multiple separate locations within a nodule of FNH to avoid the artifact of a monoclonal patch. Approximately 600-1000 cells of each FNH were microdissected from 5 micron histological sections. Normal tissue microdissected from the same patient was used as a control. The dissected tissue was incubated overnight in digestion buffer and proteinase K at 37°C. Genomic DNA was extracted and analyzed for X-chromosome inactivation status and TP53 mutations in exons 5, 7 and 8 by direct DNA sequencing. Correlations between clonality and different clinical variables were analyzed using chi-square test. A p-value of 0.05 was considered significant.

Results: The patients' age ranged from 16 to 54 (mean, 36 years). The sizes of the lesions ranged from 2 to 11.7 cm (mean, 5.1 cm). None had history of hepatitis viral infection or cirrhosis. Thirteen out of 15 cases (87%) were informative in our X-chromosome inactivation analyses. A nonrandom X-chromosome inactivation pattern was observed in 4 of the 13 (31%) informative cases. A random pattern of X-chromosome inactivation was observed in 9 of 13 (69%) informative cases. The clonality status was not associated with any of the clinical-pathological parameters including age and nodule size. No TP53 mutations were detected in any of the cases.

Conclusions: Our data indicate that a significant proportion of FNH have a monoclonal origin, suggesting that these lesions are neoplastic in nature rather than reactive. The lack of mutation in the TP53 gene supports the notion that FNH is a benign entity.

1588 Low Expression of Ribonucleotide Reductase M1 (*RRM1*) Determined by Quantitative Reverse Transcription-PCR (QRT-PCR) Is Predictive of Adjuvant Gemcitabine Treatment Benefit in Patients with Resectable Pancreatic Adenocarcinoma: A Pilot Study

W Jiang, A Tan, J Jiang, Y Wang, R Kim, JF Palma, Y Zhang, X Liu. Cleveland Clinic Foundation, Cleveland, OH; Johnson & Johnson Company, San Diego, CA.

Background: Gemcitabine (2', 2'-difluorodeoxycytidine) has been a cornerstone of current chemotherapy for pancreatic cancer. Recent studies showed low expression of *RRM1*, the regulatory subunit of ribonucleotide reductase, determined by immunohistochemistry, was predictive of treatment benefit of gemcitabine in patients with resectable pancreatic adenocarcinoma in a palliative setting. However, whether or not the expression of *RRM1* is predictive of treatment benefit of gemcitabine in an adjuvant setting in patients with resectable pancreatic adenocarcinoma has not been reported. This study aims to determine if *RRM1* expression level is a predictive marker for treatment benefit of gemcitabine used as an adjuvant treatment for pancreatic adenocarcinoma.

Design: 179 consecutive patients underwent pancreatoduodenectomy at our institution for resectable pancreatic adenocarcinoma from 10/1999 to 12/2006. Total RNA was isolated from micro-dissected paraffin-embedded tumors in 84 patients. 18 of them received adjuvant gemcitabine treatment prior to disease recurrence/metastases. The expression of *RRM1* in tumors was determined by QRT-PCR and the expression levels were normalized to two endogenous reference genes. The correlation of *RRM1* expression levels and overall survival (OS) was determined using the Kaplan-Meier method. Cox's proportion hazards multivariate model was employed to examine the association of *RRM1* expression with OS and Progression Free Survival (PFS).

Results: *RRM1* expression did not have prognostic value in the entire group of patients regarding OS. However, in the subgroup of 18 patients who received gemcitabine treatment as an adjuvant treatment, patients with low *RRM1* expression had significantly better overall survival (median survival 40 months vs. 23 months, p=0.022; hazard ratio 0.55, p=0.038).

Conclusions: Low *RRM1* expression determined by QRT-PCR on paraffin-embedded pancreatic carcinoma tissue in patients who received gemcitabine as an adjuvant treatment predicts an overall survival benefit. Further large prospective studies are warranted to confirm the current finding and to provide guidance for individualized chemotherapy regimen.

1589 Insulin-Like Growth Factor 1 Receptor Beta (IGF-1R Beta) Expression in Hepatocellular Carcinoma (HCC)

W Jiang, X Liu, F Aucejo, R Kim, LM Yerian. Cleveland Clinic, Cleveland, OH.

Background: The IGF signaling axis, including IGF-I and IGF-II and their receptor IGF-1R, has been implicated in development and progression of HCC. Constitutive activation of IGF-1R is frequently observed in HCC cell lines and is crucial for oncogenic transformation and tumor cell survival. However, IGF-1R expression by immunohistochemistry and its significance in human HCC have not been reported.

Design: 126 patients with HCC underwent liver transplant from 06/2002 to 08/2006. 72 paired HCC and corresponding adjacent cirrhotic liver samples were studied. Immunohistochemical staining for IGF-1R beta was performed on formalin-fixed, paraffin-embedded sections. IGF-1R beta immunoreactivity was scored using a four-tier grading system (0 to 3+). Correlation of IGF-1R beta staining and clinicopathologic features of HCC including tumor grade, being beyond Milan criteria, vascular invasion, and underlying liver disease was determined.

Results: 58.3% (42/72) of HCC expressed IGF-1R beta, whereas only 5.6% (4/72) of non-tumorous livers showed IGF-1R beta expression in (p<0.0001). Please see tables 1 and 2 for the correlation of IGF-1R with various clinicopathologic features.

Table 1. IGF-1R beta correlation with tumor variables

IGF-1R beta in tumor	Vascular invasion	Beyond Milan Criteria	Poor tumor grade	Recurrence
Positive (0.5-3) (n=42)	13 (31.0%)	25 (40.7%)	12 (28.6%)	3 (7.1%)
Negative (0) (n=30)	5 (20%)	25 (16.5%)	1 (3.3%)	1 (3.3%)
P value	0.269	0.030	0.010	0.635

Table 2. IGF-1R beta correlation with etiology

IGF-1R beta in tumor	HCV	HBV	Alcohol	NASH
Positive (0.5 - 3) (n=42)	29 (69.0%)	2 (4.8%)	10 (23.8%)	1 (2.4%)
Negative (0) (n=30)	17 (56.7%)	3 (10.0%)	5 (16.7%)	6 (20.0%)
P value	0.325	0.643	0.562	0.018

Conclusions: Our results show that HCC have a higher expression of IGF-1R beta than adjacent non-tumorous cirrhotic liver. IGF-1R beta expression is associated with poor tumor differentiation and tumors beyond Milan criteria. Interestingly, IGF-1R expression is less frequent in non-alcoholic steatohepatitis (NASH)-associated HCC than in other causes of cirrhosis. Our findings support a role for IGF-1R signaling in HCC tumorigenesis and strongly suggest an intrinsic difference in IGF-1R signaling in HCC occurring in NASH versus other liver diseases.

1590 Impact of *Glutathione S- Transferase P 1 GSTP1*) Polymorphism on Survival of Patients with Unresectable Pancreas Cancer Receiving Multimodal Therapies

YF Jin, T Ioka, M Song, M Tomoeda, S Nagata, M Kitamura, M Yuki, H Yoshizawa, C Kubo, Y Nishizawa, Y Tomita. Osaka Medical Center for Cancer and Cardiovascular Diseases, Osaka City, Osaka Prefecture, Japan.

Background: Pancreatic ductal adenocarcinoma (PDAC) is still one of the most fatal cancers, although its prognosis has improved recently with the introduction of multimodal therapy. Most patients with IVa or IVb stage pancreatic cancer receive chemo- or chemoradiotherapy, however correlation between response to treatment and host genotyping of genes involved in detoxification of cytotoxic drugs has not been well-examined.

Design: Our retrospective analysis included 247 patients, who were diagnosed as having primary PDAC (WHO classification: stage IVa and IVb). Treatment regimens during the entire disease process were collapsed into 3 groups: TS1-based therapy, GEM-based therapy, and TS1/GEM-based therapy.Ile^{105}Val polymorphism of the *GSTP1* gene was analyzed using the PCR-RFLP technique from peripheral blood samples.

Results: Patients receiving TS1-based therapy showed a more favorable prognosis compared to those with other therapy in patients with GSTP1 Ile/Val or Val/Val, but not in patients with GSTP1 Ile/Ile. Patients receiving TS1/GEM-based therapy showed a more favorable prognosis compared to those with other therapy in patients with GSTP1 Ile/Ile, but not in patients with Ile/Val or Val/Val.

TABLE 1 Treatment Modality and Overall Survival by GSTP1105 Polymorphisms patients With Pancreatic cancer

Treatment Modality		Ile/Ile			Ile/Val ande Val/Val		
		No.of patient/ deaths	MS, Months	P	No.of patient/ deaths	MS, Months	P
TS1-base	1:received	51/39	12.62	0.49	15/10	15.54	0.03
	2:No received	130	113	10.89	41/36	9.38	
GEM-base	1:received	150/124	10.98	0.3	38/29	10.36	0.66
	2:No received	41/28	12.95		18/17	10.85	
TS1/GEM-base	1:received	65/48	16.43	<.0001	25/23	12.82	0.67
	2:No received	126/104	9.21		31/23	9.44	

MS: medial survival

Conclusions: Favorable prognosis of patients with *GSTP1*^{105}Val variant receiving TS1-based therapy was demonstrated. For those with 105Ile/Ile, TS1/GEM-based therapy proved as the most efficient treatment modality. Further in-depth study is necessary to clarify the molecular regulatory mechanism of chemotherapeutic reagents against cancers in each genetic variation.

1591 PSMA Expression in Pancreatic Endocrine Neoplasms: A Potential Diagnostic Pitfall

K Jockovic, L Schultz, R Sharma, A Maitra, PB Illei, RH Hruban, GJ Netto. Johns Hopkins Medical Institution, Baltimore, MD.

Background: Prostate specific membrane antigen (PSMA) is a transmembrane glycoprotein with glutamate carboxypeptidase activity, which is expressed by prostatic epithelium. PSMA expression has been occasionally described in non-prostatic neoplastic (and non-neoplastic) tissues emphasizing the need for cautious interpretation of this marker. Furthermore, given that prostate cancer recurrence may be detected clinically by radioimmunoscintigraphy using a radio-labeled antibody against PSMA, PSMA expression by non-prostatic neoplasms may also lead to misinterpretation of PSMA radio-immunoscintigraphy. We recently noted PSMA expression in a case of pancreatic endocrine neoplasm/islet cell tumor (PEN). Here, we further evaluate PSMA expression in a group of primary and metastatic PENs.

Design: We investigated the immunoexpression of PSMA in PENs using a set of tissue microarrays (TMAs) constructed from archival tissues of 37 primary PENs and 19 related PEN lymph node and hepatic metastases. In each tumor, extent (percentage) of staining was categorized as focal (<25%), multifocal (25-75%), or diffuse (>75%). Staining intensity was scored on a scale of 0 to 3+.

Results: PSMA expression was observed in 35% (13/37) of primary and 42% (8/19) of metastatic PENs. The staining pattern was cytoplasmic and granular, while cell membranous staining pattern was not demonstrated by any of the PSMA positive PEN cases. Of the PEN cases that expressed PSMA, the majority exhibited multifocal extent of staining both in primary (9/13) and metastatic (8/8) postive PENs.

Conclusions: We found PSMA, a marker expressed by both benign and malignant prostatic epithelial cells, to be expressed by a significant number of pancreatic endocrine neoplasms. The staining pattern in PENs was cytoplasmic and granular in contrast to the usual membranous staining pattern encountered in prostatic adenocarcinoma. Nevertheless, in light of our current findings, when addressing the differential diagnosis of metastatic PEN vs. prostatic adenocarcinoma we recommend the use of additional immunohistochemical markers including other prostate lineage markers (eg. p501s and PSA) as well as neuroendocrine lineage markers (eg. synaptophysin and chromogranin). We are in the process of assessing PSMA expression in other non-pancreatic neuroendocrine neoplasms.

1592 PAX8 Expression in Pancreatic Endocrine Neoplasms: Diagnostic Pitfall and Potential Prognostic Role

K Jockovic, RH Hruban, L Schultz, R Sharma, A Maitra, PB Illei, GJ Netto. Johns Hopkins University, Baltimore.

Background: PAX8, a lineage-specific transcription factor, is expressed in the majority of renal cell carcinomas (RCC). We noted PAX8 expression in a rare case of pancreatic endocrine neoplasm/islet cell tumor (PEN). Occasional PEN may enter the differential diagnosis of metastatic RCC especially when exhibiting clear cell change. We here evaluated PAX8 and CD10 (a marker with known positivity in RCC) expression in primary and metastatic PEN. We also explored potential prognostic significance of PAX8 expression in PEN.

Design: Immunohistochemical evaluation of PAX8 and CD10 was performed using a set of tissue microarrays (TMA) constructed from 37 primary PEN and 18 related lymph node and hepatic PEN metastases. For PAX8, the extent (percentage) of nuclear staining was categorized as focal (<25%), multifocal (25-75%) or diffuse (>75%). An intensity score of (0-3+) was also assigned for each tumor. An H score of immunoreactivity was calculated as the product of intensity x extent (percentage) of tumor cell staining and was used for outcome analysis.

Results: PAX8 expression was observed in 51% (19/37) of primary and 44% (8/18) of metastatic PEN. Of the cases with PAX8 expression, 18/19 exhibited multifocal or diffuse extent of staining and 11/19 exhibited moderate or strong intensity. CD10 was expressed in 40% (14/35) of primary and 37% (7/19) of metastatic PEN. Co-expression of both PAX8 and CD10 was detected in 22% (8/37) of primary and 22% (4/18) of metastatic PEN. PAX8 and CD10 co-expression was also noted in non-neoplastic pancreatic islets. Median follow up in our cohort was 51.5 months (range 2-179). Disease specific survival (DSS) rate was 71%. On univariate analysis, positive PAX8 expression in primary PEN demonstrated statistically significant correlation with DSS (p=0.02). PAX8 positivity was encountered in 6/18 (33%) PEN tumors in patients that remained without evidence of disease while only 1/19 (5.2%) PEN tumor was PAX8 positive in the group of patients who died of their disease.

Conclusions: RCC markers PAX8 and CD10 are frequently expressed in PEN with a subset of cases co-expressing both markers. Therefore, when addressing the differential diagnosis of PEN vs. metastatic RCC, additional immunohistochemical markers (e.g. neuroendocrine lineage markers) should be used. Given PAX genes known role in modulating cell migration and differentiation in solid neoplasms, our finding of a potential prognostic role of PAX8 expression in PEN warrants further investigation.

1593 The Role of Oval Cell Activation and Periportal Ductular Reaction Presence in Two Different Models of Experimental Cirrhosis

C Kalogeropoulou, I Tsota, P Zabakis, D Kardamakis, T Petsas, AC Tsamandas. University of Patras, Patras, Greece.

Background: Oval cells (OC) are liver stem cells involved in the progress of liver disease and hepatocellular carcinoma development. This study investigates the potential correlation of OC activation and the resultant periportal ductular reaction (PDR), and impaired liver cell replication, in experimental liver fibrosis.

Design: The study comprised 102 male Wistar rats divided in 3 groups: A (n=6) controls, B (n=48):CCl4 injection (intraperitoneally 2ml/kg/BW-1:1 vol in corn oil twice weekly), C (n=48): thioacetamide administration in drinking water (300 mg TAA/L) for 3 months. In group B, rats were sacrificed at 4, 8, 12 weeks and in group C, at 1, 2 and 3 months. At all times, liver tissues were obtained and were stained with antibodies to CK19, LCA, CD34, and p21. Cells with features of OC that were CK19+/LCA(-)/CD34(-) were scored. PDR was defined according to standard reference (Roskams T, Hepatology 39:1739, 2004). The presence of OC was also determined by quantification of AFPmRNA (RT-PCR method). PDR was quantified as % of biopsy area.

Results: The table lists the results. Statistical analysis revealed significant correlation between **a)** OC with fibrosis (group B: p=0.0021, group C: p=0.0032), **b)** PDR and fibrosis (group B: p=0.0012, group C: p=0.0019). Impaired hepatocyte replication (%p21+ cells) was independently associated with **a)** %OC (group B: p=0.0028, group C: p=0.0041) and **b)** PDR (group B: p =0.0057, group C: p =0.0075). Multivariate analysis showed that PDR is independent factor for the prediction of fibrosis.

Table: OC expression and PDR presence in the different groups

Groups	CK19	AFPmRNA	PDR
A	2.7±0.4	2.5±0.7	1.6±0.09
B1	15.6±4.8^{c}	16.8±6.4^{d}	14.3±5.7^{e}
B2	36.1±7.2^{c}	37.5±8.3^{d}	35.7±7.4^{e}
B3	54.8±7.7^{c}	56.4±8.9^{d}	49.6±6.4^{e}
C1	14.2±5.6^{h}	17.3±5.2^{i}	16.4±5.8^{j}
C2	36.9±8.5^{h}	37.8±7.4^{i}	35.9±8.1^{j}
C3	59.5±9.4^{h}	58.3±6.8^{i}	54.3±8.5^{j}

$^{a, c, d, e, f, h, i, j}$: p<0.001 and $^{b, g}$: p<0.05 when compared to controls.

Conclusions: This study demonstrates that in experimental liver fibrosis (irrespective of the model used for cirrhosis induction), OC activation and PDR degree, strongly correlates with the progress of liver fibrosis. The fact that these factors are associated with impaired hepatocyte replication implies the presence of an alternative pathogenetic pathway during liver regeneration that leads to PDR and progressive liver fibrosis, with consequent liver failure.

1594 Choledochal Cysts: A Clinicopathologic Study of 36 Cases with Emphasis on the Morphologic and the Immunohistochemical Features of Premalignant and Malignant Alterations

N Katabi, V Pilarisetty, M D'Angelica, DS Klimstra. Memorial Sloan-Kettering Cancer Center, NY, NY.

Background: Choledochal cysts (CDCs) are rare congenital dilatations of the biliary tree. Metaplasia, dysplasia, and carcinoma may develop in CDCs with significant frequency. Therefore, the aim of this study was to focus on neoplastic changes in CDCs and to characterize their morpholologic and immunohistochemical features.

Design: 36 CDCs were identified in the files of MSKCC from 1990 - 2008. Cases were subjected to clinical, histopathologic, and immunohistochemical analyses.

Results: The mean age of pts was 36 (11-67) yrs; there was a female predominance (30/6). The mean size of cysts was 4.37 (0.9-11.5) cm. The cysts were classified based on the Todani classification: type I, 71%; type II, 8.5%; type IV, 14%, and type V, 5.7%. Metaplasia was found in 14/35 cases (40%), of which 9 were also had dysplasia. Of the 14 cases with metaplasia, 13 showed pyloric gland (PG) metaplasia, 5 intestinal (INT) and 2 squamous metaplasia. Dysplasia was found in 10/35 cases (28.5%), 6 low grade, 2 moderade and 2 high grade. Carcinoma was identified in 5/35 cases (14.3%). The histologic type was poorly differentiated adenocarcinoma in 3 cases, papillary in one and tubular in 2. Three carcinomas were associated with metaplasia and dysplasia. Only 1/18 cases without metaplasia had dysplasia and none had carcinoma (p=00008). There was a trend towards more dysplasia and carcinoma with INT metaplasia (5/6) than PG metaplasia (7/12). There was a trend toward increasing p53 and Ki 67 immunoexpression from metaplasia to dysplasia to carcinoma. Additional imunohistochemical features are listed below.

[table1]

	Normal (n=3)	PG (n=12)	INT(n=6)	Dysplasia (n=8)	Carcinoma (n=5)
Smad4	3	12	6	8	5
CK7	3	12	6	8	4
CK20	1	5	5	6	2
CDX2	0	0	4	1	0
MUC1	0	0	0	0	3
MUC2	0	3	6	5	3
MUC6	2	12	5	8	0
MUc5AC	0	3	0	4	3
CEA-M	0	0	0	1	5
B72.3	0	0	0	0	2
CA125	0	0	0	0	0
Mesothelin	2	4	4	4	4
COX2	3	12	6	8	3

FU was available on 35 pts (median 26 mos). 4/5 pts with carcinoma were DOD and one was AWD 25 mos after diagnosis. All others were NED except one who developed new cystic lesions.

Conclusions: CDCs are associated with a high rate of dysplasia (28.5%) and carcinoma (14.3%). CDCs show a sequence of tumor progression from metaplasia to dysplasia and carcinoma. This highlights a characteristic feature of biliary carcinogenesis.

1595 Acute Cellular Rejection Occurring in Allograft Livers after Combined Small Bowel/Liver Transplantion and Multivisceral Transplantation

S Kerkoutian, SH Ra, GR Cortina, D Farmer, CR Lassman. University of California Los Angeles, Los Angeles, CA.

Background: Patients undergoing combined small bowel/liver transplantation (SBLTx) or multivisceral transplantation (MVTx) typically undergo a more aggressive immunosuppression (IS) regimen than patients with orthotopic liver transplantation alone. Due to the IS regimen, acute cellular rejection (ACR) in allograft liver biopsies after SBLTx or MVTx is an uncommon occurrence, especially with small bowel biopsies that are negative for ACR.

Design: We reviewed 58 allograft liver biopsies and their concurrent small bowel biopsies from 33 SBLTx and MVTx patients performed between the years 1995 to 2009.

Results: The 58 liver biopsies with concurrent small biopsies revealed: no ACR in 36 cases (62%), ACR of the small bowel alone in 13 cases (22%), ACR of the liver alone in 8 cases (14%), and ACR of both the liver and small bowel in 1 case (2%). The nine allograft liver biopsies with ACR were from five patients, four female and one male, ranging in age from 2 to 29 yrs. (median: 4 yrs.). Four of the allograft liver ACRs were from one case and two ACRs from another. SBLTxs and MVTxs were initially performed for gastroschisis in four patients and abdominal trauma in one patient. All five patients were cirrhotic from TPN toxicity. One patient underwent a redo SBLTx due to severe exfoliative small bowel rejection. All five patients had elevated liver function tests at the time of biopsy. The biopsies were performed 22 to 3192 days from SBLTx or MVTx (median: 207 days). The allograft liver biopsies revealed mild ACR in seven cases and moderate ACR in two cases. Classic features of ACR including mixed portal inflammatory infiltrates, bile duct infiltration, and portal and central vein endothelitis were seen in 7 cases. Two of the biopsies demonstrated perivenular inflammation with hepatocyte dropout and a mild hepatitis consistent with late acute rejection. Four patients were successfully treated with intravenous steroids and one patient was treated with an increase in immunosuppression.

Conclusions: The diagnosis of ACR in allograft liver biopsies after SBLTx and MVTx is not an uncommon occurrence and can occur in the presence of a normal small bowel biopsy. Although the majority of cases show classical mild acute ACR, moderate ACR and late ACR can be seen in this setting. Also, multiple episodes of allograft liver ACR can be seen despite heavy IS.

1596 Epidermal Growth Factor Receptor and Glypican-3 in Hepatocellular Nodules: A Clinicopathologic Study

LE Kernochan, J Alexander, PE Swanson, MM Yeh. Univ. of Washington, Seattle.

Background: Epidermal growth factor receptor (EGFR) is overexpressed in hepatocellular carcinoma (HCC) and is a potential therapeutic target, but correlation between EGFR and clinicopathologic attributes of HCC including clinical outcome is controversial and correlation between EGFR and the novel HCC selective marker Glypican-3 (GP3) is lacking. We herein examined the expression of these markers in HCC and other diagnostically challenging, mimicking lesions including high grade dysplastic nodule (HGDN) and hepatocytic adenoma (HCA), and the correlation between GP3 and EGFR in HCC with correlation to survival.

Design: Formalin-fixed sections of 59 HCC, 8 HGDN, and 17 HCA were stained with antibodies to EGFR and GP3. The results were scored for intensity (none, weak, moderate, strong) and distribution (none, <10%, 10-33%, 34-66%, 67-100%) in lesional and non-lesional cells. The results were compared with differentiation (well, moderate or poor), Edmonson-Steiner (ES) nuclear grade (1-4) and survival in HCC.

Results: GP3 and EGFR were very sensitive for HCC, but GP3 was more specific in separating HCC from cirrhotic liver, HGDN, and HCA:

Sensitivity/Specificity of GP3 and EGFR in distinguishing HCC from cirrhotic liver, HGDN, and HCA

	cirrhotic liver	HGDN	HCA
GP3	85.7/100	85.7/50	85.7/100
EGFR	82.5/54.2	82.5/16.7	n/a

Neither EGFR nor GP3 staining correlated with survival. Poorer differentiation of HCC was associated with greater GP3 intensity (p=0.01) and distribution (p=0.0007). Higher ES grade also correlated with higher GP3 intensity (p<0.0001) and distribution (p=0.0007). Although there was significant correlation between EGFR and GP3 in both intensity (p=0.01) and distribution (p=0.005), EGFR intensity and distribution alone did not correlate with HCC differentiation or ES grade.

Conclusions: To our knowledge, this is the first study investigating both the expression of EGFR and GP3 in HCC and their correlation, and to correlate with clinical outcome. GP3 is a sensitive and specific marker for HCC that readily distinguishes HCC from cirrhotic liver and HCA. Intensity and distribution of GP3 staining correlate with poorer differentiation and higher ES grade. Our results of significant correlation between EGFR and GP3 staining in HCC, but no correlation in survival based on staining characteristics further support the recent phase 2 trial results that there has not been a survival difference based on EGFR status. The role for GP3 in the EGFR hepatocarcinogenesis pathway awaits further investigation.

1597 Prognostic Relevance of Subgroup Classification of Minimally Invasive Intraductal Papillary-Mucinous Carcinoma of the Pancreas

JY Kim, HJ Park, KT Jang. Samsung Medical Center, Seoul, Korea.

Background: Intraductal papillary-mucinous neoplasm (IPMN) is a distinct entity of pancreas, which shows a good prognosis than conventional ductal adenocarcinoma. When IPMN accompanied invasive cancer, it is known that IPMN follows similar clinical course with ductal adenocarcinoma. However, the postoperative outcomes of invasive intraductal papillary-mucinous carcinoma (I-IPMC) showed various results. Recently non-aggresive subgroup classification of IPMC, as minimally invasive IPMC (MI-IPMC) was introduced.

Design: We reviewed surgically resected IPMN cases during 1996~2008. We selected IPMC, and investigated the clinicopathological characteristics of fifty patients of IPMC. The cases were classified into 5 noninvasive IPMC and 45 I-IPMC on the basis of WHO classification. I-IPMC were divided further into 18 MI-IPMC and 27 invasive carcinomas originating in IPMC (IC-IPMCs) according to recently proposed subgroup classification criteria.

Results: When analyzed according to histologic subtype, 23 were intestinal type, 26 were pancreatobiliary type, and one was oncocytic type, respectively. Increased preoperative CA19-9 level was more frequently identified in IC-IPMCs (63%, 17/27) than in MI-IPMCs (16.7%, 3/18). Lymph node metastasis was noted in 9 patients, and all of them were IC-IPMC. The group of IC-IPMC showed more frequent recurrences such as lymph node or distant metastasis (72%) than MI-IPMC (0%) during follow up duration. There was no tumor recurrence or metastasis in patients of MI-IPMC, however 17 patients (62.9%) of IC-IPMC showed tumor recurrence and/or distant metastasis during follow.

Conclusions: The current results demonstrated the prognostic relevance of newly proposed subgroup classification of MI-IPMC, which should be differentiated from IC-IPMC. Thus, the recent subgroup classification of MI-IPMC seems to be a valid tool for prognostic analysis. If preoperative differentiation of MI-IPMC from IC-IPMC may be possible, it can be beneficial for avoiding unnecessary radical resection and additional LN dissection.

1598 Pathologic Factors Affecting the Recurrence and Survival of Pancreatic Intraductal Papillary Mucinous Neoplasm

SA Kim, E Yu, SC Kim, JH Kim. University of Ulsan College of Medicine, Asan Medical Center, Seoul, Korea.

Background: Intraductal papillary mucinous neoplasm (IPMN) of the pancreas constitutes a heterogeneous group with several subtypes. The frequency of each subtype has not been fully examined yet in Korean population. In addition, the benefit of clearing resection margin is still controversal.

Design: We reviewed surgically resected 281 cases of IPMN for 13 years in a single institute. Dividing all cases into either noninvasive IPMN or invasive carcinoma group, the recurrence of each group was compared according to the histologic grade (benign or borderline IPMN, carcinoma in situ, invasive carcinoma) and size (PanIN; lesions involving small ducts less than 0.5cm in diameter and IPMN; more than 0.5cm-sized lesions) of the residual lesions in the resection margin.

Results: Sixty cases (21.4%) were invasive carcinoma, and 221 (78.6%) non-invasive cases included 87 cases (31.0%) of benign, 107 (38.1%) cases of borderline and 11 (3.9%) cases of carcinoma in situ. Main duct was involved in 154 (54.8%) cases. According to the type of epithelium, gastric foveolar, intestinal and pancreatobiliary type were 230 (81.9%) cases, 27 (9.6%) cases and 24 (8.5%) cases, respectively. Invasiveness, main duct involvement and large tumor size were associated with decreased patient survival (P<0.001, =0.009, and <0.001) and disease-free survival (P=0.001, 0.011, and <0.001). In noninvasive IPMN, increased recurrence in patients with five or more years of follow-up was related to the involvement of resection margin by carcinoma in situ, but not by PanIN, benign or borderline IPMN. In addition, the recurrence rate of invasive carcinoma was significantly high (27.3%) even when the resection margin was clear, and was not related to the grade or size of residual tumors in resection margin.
Conclusions: The proportion of gastric foveloar type was higher in our series than previously reported. Invasiveness is the strong risk factor for recurrence in IPMN regardless of the status of resection margin. However, in noninvasive IPMN, the histologic grading is more important than the size of residual lesion in the evaluation of pancreatic resection margin.

1599 Up-Regulation of Prion Protein Associated with K-Ras Mutation in Pancreatic Ductal Adenocarcinoma

C Kletecka, Q Li, W Xin, L Zhou. University Hospitals Case Medical Center, Cleveland, OH.

Background: Mutations of the K-Ras oncogene are the most common genetic alteration in human pancreatic cancer. However, the mechanism by which the activation of the Ras signaling promotes tumor growth and metastasis remains to be fully elucidated. A recent study shows that prion protein (PrP) is over-expressed in a subgroup (41%) of human pancreatic ductal adenocarcinomas (PDAC), and its expression confers a poor prognosis. It also shows that PrP confers a growth advantage and contributes to the invasiveness of PDAC by binding with filamin A (FLNa), a cellular integrator of mechanics and signaling. In this study, we investigated the relationship between PrP and k-RAS mutation in PDAC.
Design: K-Ras mutation analysis was performed on paraffin embedded tissue blocks including 8 normal human pancreatic tissues and 28 human PDAC specimens, using TrimGen's K-Ras Mutector Detection Kit. K-Ras mutation signals were enriched by the Shifted Termination Assay technology and analyzed by fragment analysis on the ABI 3130 Genetic Analyzer. Immunohistochemistry was performed using monoclonal antibody specific for PrP.
Results: K-Ras mutation was identified in one normal human pancreatic specimen. Among 28 PDAC specimens, K-Ras mutation was identified in 19 cases (67.9%). No K-Ras mutation was identified in the resected normal peripheral pancreatic tissue of the corresponding PDAC specimen. Fifteen PDAC specimens have up-regulation of PrP by immunohistochemistry, showing focal or diffuse strong (3+) positive staining of infiltrative PDAC cells. PrP up-regulation is present in 13 of K-Ras mutation-positive PDAC specimens (68.4%). In comparison, PrP up-regulation is only found in 2 K-Ras mutation-negative specimens (22.2%) ($p < 0.05$).

PrP Expression Status and K-Ras Mutation in PDAC

	K-Ras (+)	K-Ras (-)	Total
PrP (+)	13	2	15
PrP (-)	6	7	13
Total	19	9	28
% of PrP (+)	68.4%	22.2%	53.6%

Conclusions: Our studies have identified a strong association between K-Ras mutation and PrP up-regulation in human PDAC. Because K-Ras mutation is an earlier event in the progression of the pancreatic cancer than PrP up-regulation, these findings suggest that K-Ras mutation may promote pancreatic cancer growth by up-regulation of PrP. Further understanding the mechanism of PrP in conferring pancreatic cancer aggressiveness will lead to novel therapeutic options for treatment of this deadly disease.

1600 Capillarization of Hepatic Sinusoids after Neoadjuvant Therapy

PW Klonowski, B Tan, DC Linehan, MR Porembka, EM Brunt. Washington University School of Medicine, St. Louis, MO.

Background: Oxaliplatin-based neoadjuvant therapy for hepatic colorectal metastasis (HCM) has been associated with hepatic injury including sinusoidal ectasia, peliosis and nodular regenerative hyperplasia. Currently, there exists no method to grade the injury. **Aim:** To further characterize the sinusoidal lesions and create a vascular injury scoring system.
Design: Forty patients who underwent neoadjuvant treatment and resection for HCM were retrospectively selected by an oncologist; 26 received oxaliplatin-based therapy (ox+), 14 did not (ox-). Samples of non-tumor liver were blindly evaluated by H&E, trichrome, and anti-CD34 immunostain (CD34).
Results: The injury patterns noted were hepatocellular anisonucleosis, varying degrees of sinusoidal disruption and cord atrophy, peliosis and steatosis. Steatosis, present in 16/40 (40%) total cases, did not correlate with neoadjuvant treatment. Thirteen of 40 (33%) cases showed injury; 10 were ox+. Hepatocyte anisonucleosis, peliosis and hemorrhage were only seen in ox+ cases. CD34 (score 0-2, based on low power extent) showed a trend of aberrant expression, focally in areas of damage as well as sinusoids not visibly injured in 22/25 (88%) ox+ vs 9/13 (69%) ox- cases; ≥2+ CD34 (multifocal, extensive) was present in 8 (32%) ox+ and 2 (15%) ox- cases. One ox+ patient died of liver failure 10 months post-op. Table 1 lists the proposed vascular injury score based on H&E and trichrome findings.
Conclusions: By blinded analysis, the majority of cases (62% ox+, 79% ox-) had no vascular findings. However, anisonucleosis and severe microvascular injury occurred in ox+ treated livers. Aberrant CD34 expression suggests more extensive injury than is observed by routine stains; altered endothelium in the parenchyma could result from unopposed arterial pressure in the damaged sinusoids. Anisonucleosis in ox+ cases warrants further study.

Table 1. Vascular Injury Score

Vascular Injury Score	H&E	Trichrome
0	None ± anisonucleosis	Negative
1	Anisonucleosis	Delicate PSF; suggestive sinusoidal ectasia
2	Extensive anisonucleosis	As above + clusters of deep basophilic hepatocytes
3a	Sinusoidal prominence + RBCs in sinusoids	As above + PSF outlines affected sinusoids
3b	z3 sinusoidal ectasia + cord atrophy	z3 PSF
3c	As above + early peliosis	Trichrome negative in peliosis
4a	Definite peliosis, extensive	As above
4b	Sinusoidal disruption + cord atrophy, hemorrhage, multifocal	PSF + intrasinusoidal debris
4c	As above + outflow vein obliteration	As above + terminal hepatic venule fibrosis

PSF=perisinusoidal fibrosis; z3=zone 3

1601 Prognostic Value of *hENT-1* in Patients with Resected Pancreatic Adenocarcinoma

KK Lai, A Tan, RD Kim, J Jiang, Y Wang, LA Rybicki, X Liu. Cleveland Clinic, Cleveland, OH; Veridex LLC, San Diego.

Background: Pancreatic adenocarcinoma is a malignancy with dismal prognosis. Gemcitabine, a nucleoside analog, is an agent often used to treat pancreatic cancer. Previous studies suggested that human equilibrative nucleoside transporter 1 (*hENT-1*) as determined by immunohistochemistry or quantitative reverse transcription-PCR (QRT-PCR) on laser microdissected frozen pancreatic cancer tissue was associated with gemcitabine sensitivity in pancreatic cancer. It remains unknown if *hENT-1* has a general prognostic value in patients with resected pancreatic adenocarcinoma.
Design: 84 patients underwent pancreaticoduodectomy from 2000 to 2005 were included in this study. Patients were followed a median of 60 months (range 44-110). No patients received preoperative chemoradiation. Total RNA was isolated from microdissected paraffin-embedded tumors. *hENT-1* expression levels in tumors were evaluated by QRT-PCR, normalized to two reference genes, and expressed as ΔCt (low ΔCt means high expression). Cutoff levels were generated by recursive partitioning analysis. Univariable and multivariable prognostic factors for overall survival (OS) and progression-free survival (PFS) were identified via Cox proportional hazards analysis.
Results: Univariable analysis identified *hENT-1*, stage, angiolymphatic invasion, perineural invasion, and adjuvant therapy as prognostic factors for both PFS and OS, and number of positive nodes as an additional prognostic factor for OS. Multivariate analysis confirmed *hENT-1* as a prognostic factor for OS (HR 1.75, p=0.034) and PFS (HR 2.80, p=0.003). High expression of *hENT-1* (low ΔCt) was associated with better OS (figure 1) and PFS.

Figure 1: *hENT-1* expression and OS

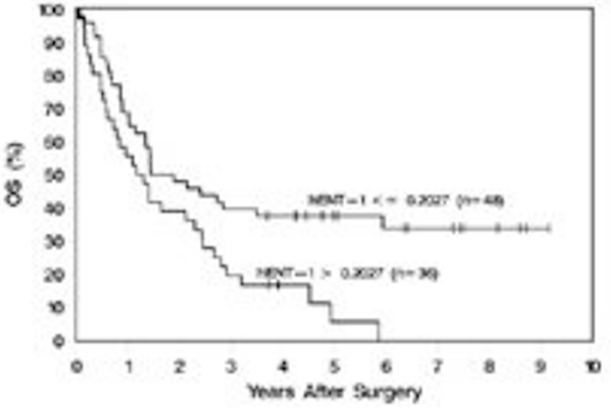

Conclusions: High expression of *hENT-1* as determined by QRT-PCR on paraffin-embedded pancreatic cancer tissue is associated with better OS and PFS in patients with resected pancreatic adenocarcinoma. Further studies are needed to confirm the general prognostic value of *hENT-1* in resectable pancreatic adenocarcinoma.

1602 Identification of Reference Genes for Gene Expression Analysis by Real Time Quantitative PCR (RTQ-PCR) in Pancreatic Adenocarcinoma

KK Lai, X Liu. Cleveland Clinic, Cleveland, OH.

Background: Pancreatic adenocarcinoma is a disease with dismal prognosis. Recent studies utilizing RTQ-PCR in patients with this cancer have identified gene expression patterns with prognostic implication. As the clinical utility of RTQ-PCR has increased, traditionally used internal reference genes have been shown to exhibit differential levels of expression in different tissues, leading to the drive to identify tissue-specific reference genes. Identification of reference genes for normalization of RTQ-PCR data from paraffin-embedded tissue samples of human pancreatic adenocarcinoma have not yet been reported.
Design: Eight eight pancreatic adenocarcinomas resected from 2000 to 2005 were included in this study. Tumor samples were either formalin fixed (n=67) or Hollandes-

fixed (n=21). Total RNA was isolated from micro-dissected paraffin-embedded tumors. One-step multiplex RTQ-PCR was performed to examine expression levels of the three housekeeper genes β-actin (*ACTB*), hydroxymethylbilane synthase (*HMBS*) and ribosomal protein L13 A (*RPL13A*). NormFinder (v19) and geNorm (v3.5) software programs were used for stability comparisons of these 3 housekeeper genes. The programs evaluate expression stability via independent algorithms.

Results: NormFinder identified *HMBS* as the most stably expressed (lowest stability value, table 1), followed by *RPL13A* and *ACTB*. Fixative type did not alter the order of stability. Analysis using geNorm yielded the same order of stability, again regardless of fixative (table 2).

Table 1: NormFinder analysis results of reference gene expression stability

Formalin (n=67)			
Rank	Gene	Stability value	Tumor Intragroup variation (n=67)
1	HMBS	0.013	0.001
2	RPL13A	0.018	0.000
3	ACTB	0.029	0.002
Hollandes (n=21)			
Rank	Gene	Stability value	Tumor Intragroup variation (n=21)
1	HMBS	0.022	0.001
2	RPL13A	0.025	0.000
3	ACTB	0.037	0.001

Table 2: geNorm analysis results of reference gene expression stability

Formalin (n=67)		
Rank	Gene	M value
1	HMBS	0.070
2	RPL13A	0.072
3	ACTB	0.088
Hollandes (n=21)		
Rank	Gene	M value
1	HMBS	0.067
2	RPL13A	0.069
3	ACTB	0.081

Conclusions: The results of this tudy indicate that *HMBS* is a good internal reference gene for use in normalization of QRT-PCR data for paraffin-embedded human pancreatic cancer tissue.

1603 Chronic Hepatitis Feature and Liver Mass in Idiopathic Hypereosinophilic Syndrome – Analysis of Twelve Cases

HJ Lee, SY Choi, YB Kim, MK Yeo, DY Kang. Chungnam National University School of Medicine, Daejeon, Korea.

Background: The hypereosinophilic syndrome is a disease characterized by a persistently elevated eosinophil count (≥ 1500 eosinophils/mm^3) in the peripheral blood for more than six months without evidence for any known causes of eosinophilia and with multisystem organ involvement. Most reported cases of the syndrome were predominant among men and showed chronic hepatitis with the multiple liver masses in radiology.

Design: We analyzed twelve cases of the hypereosinophilic syndrome with chronic hepatitis features in a liver biopsy and a liver mass from 2000 to 2009 at Chungnam National University Hospital.

Results: The cases were ten men and two women, ranging in age from 27 to 66 years (mean, 49.2 years). The clinical presentations of the patients were incidental findings of liver masses (seven cases), fevers (three cases), and abdominal pain or soreness (two cases). The radiologic evaluation showed eight cases with multiple and variable sized lesions, but, in four cases, a single liver mass mimicking malignancy was shown. Most of the cases revealed hypereosinophilia initially, but only one case showed the normal range of eosinophil count initially and was followed by hypereosinophilia.

Conclusions: Our results showed four cases of the idiopathic hypersosinophilic syndrome, which represented a single mass in the liver and a case of normal eosinophil count in initial laboratory tests. All cases showed chronic hepatitis features.

1604 Epithelial-Mesenchymal Transition (EMT) of K19 Structures within the Stromal Compartment of HCV Cirrhosis Parallels Hepatocarcinogenesis

JK Lennerz, WC Chapman, EM Brunt. Washington University, St.Louis; Massachusetts General Hospital, Boston.

Background: The stromal compartment of cirrhosis harbors vascular channels, inflammatory and fibrogenic cells, and K19 positive epithelial structures. We documented progressive loss of K19 ductular structures in progression from cirrhotic (CN) to dysplastic (DN) to hepatocellular carcinoma (HCC) [LabInv 2009; 89:314A]. The aim is to assess possible EMT.

Design: Sections from 36 HCV cirrhotic explants with HCC were studied for features diagnostic of EMT: a) co-expression of S100A4 or SNAIL with loss of membranous ECadh, or b) nuclear pSMAD concurrent with cytoplasmic SMAD2/3 and TGFß1R. Marker quantification of K19 profiles was performed in randomly chosen perinodular sectors that covered at least 25% of the stromal circumference.

Results: Quantification of K19 structures shows significant differences (*P<0.001; Mann-Whitney U test) between CN and DN (Table). Co-localized EMT markers were found within single cells of most K19 structures surrounding CN. EMT markers decreased in conjunction with both loss of stromal K19 structures as well as malignant progression of the nodule itself. Correlating with the fewer K19 cells in stroma around DN several marker proportions are reversed (ECadh>Smad2/3>S100A4>pSmad>Snail >TGFßR1) compared to CN (ECadh>Smad2/3>TGFßR1>Snail>pSmad>S100A4).

Conclusions: Perinodular stromal K19 loss is associated with alterations of TGFß1R, Smad2/3 and other markers of EMT. K19 loss parallels the progression of intranodular hepatocyte transformation from cirrhosis to DN to HCC. Together, these findings strongly suggest altered paracrine signaling at the interface of hepatocellular nodules and surrounding stroma.

K19 Compartment and EMT Markers

	CN (n=71)	DN (n=45)	HCC (n=54)
Ductules H&E	numerous	present	(-)
K19 profiles (s)	408.9±23.7* (36)	106.3±14.6* (27)	1.52±0.2 (30)
K19 cells (in n sectors)	2088±262* (27)	300±44* (30)	2.4±0.3 (27)
Ecadh+ (%;s)	51±4 (~80%;54)	7±0.6 (~78%;54)	(-) (-;20)
S100A4+ (%;s)	5.2±0.4 (~10%;27)	3.9±0.3 (~65%;27)	(-) (-;20)
Snail+ (%;s)	25.8±2.3 (~34%;27)	5.9±0.6 (~52%;27)	(-) (-;20)
TGFβR1+ (%;s)	40.6±3.6 (~48%;27)	1.4±0.2 (~15%;27)	(-) (-;20)
Smad2/3+ (%;s)	58.3±5 (~68%;27)	6.8±0.5 (~74%;27)	(-) (-;20)
pSmad+ (%;s)	22.9±2 (~27%;27)	9.2±0.8 (~60%;27)	(-) (-;20)

(-):absent; s:sectors; ±SEM; +:positive cells; %:of nuclei in profiles

1605 Comparing Visual, Morphometric and Biochemical Methods for Estimating Liver Fat Content

M Li, J Song, S Mirkov, MJ Ratain, W Liu, J Hart. Univ of Chicago, Chicago, IL.

Background: The degree of macrovesicular steatosis of liver is usually assessed by visual estimation of fat content on histology. It is known that visual estimation is subject to intra- and inter-observer variations. More objective methods, such as morphometric and biochemical methods, have also been described. We conducted the first study to evaluate the relationship among these three methods.

Design: We obtained 26 fresh frozen liver specimens from the Pharmacogenetics of Anti-cancer Agent Research Group at University of Chicago. Each specimen was divided into four 50 mg aliquots. Three were homogenized and treated by organic solvents to extract fat, and fat content was measured as the average weight percentage. The other was formalin fixed for H&E histology. Two pathologists independently reviewed the slides and estimated fat content. The slides were then scanned at 100x, and the percentage of area occupied by fat was measured by morphometry using ImagePro Plus 6.0. For morphometry, distinct fat droplets were used as references for image segmentation, and artifacts were minimized by appropriate thresholds for object size, shape and roundness.

Results: The fat content measured by the 3 methods showed different ranges: visual, 0-80%; morphometry, 0-19.6%; biochemical, 2.2-15%. Very strong correlation was seen between any two methods (correlation coefficients 0.83-0.95, all p values < 0.01). Linear regression equations and correlation coefficients are shown in Figure 1.

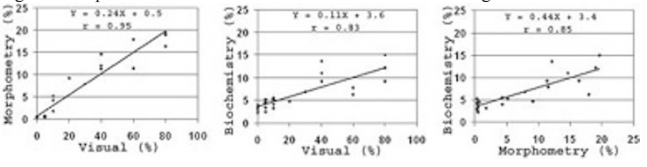

Conclusions: Visual, morphometric and biochemical methods all showed very strong correlation, suggesting that all three are accurate and reliable for estimating fat content. The morphometric and biochemical methods provide results as a continuous variable and may be more useful in research settings. In the clinical setting, visual estimation has been proven to be reliable and correlate well with the severity of steatosis; therefore, morphometric and biochemical method may not add more value. The consistently higher percentage given by the visual method reflects the fact that in this method the percentage of cells with fat is counted, rather than the area occupied by fat droplets (morphometric method) or the total fat content (biochemical method).

1606 Significance of S100A4 in Angiogenesis of Hepatocellular Carcinoma

W Li, D Tan, P Zhang. University of Texas Medical School at Houston, Houston, TX; University of Texas M.D. Anderson Cancer Canter, Houston, Houston, TX.

Background: Angiogenesis is an essential process for progression of hepatocellular carcinoma (HCC), and antiangiogenic therapy may represent one of the most promising modalities for HCC treatment. S100A4, a member of the S100 family of calcium-binding proteins, has been recognized for its role in regulating neoangiogenesis. The role of S100A4 in HCC progression has been little analyzed.

Design: Formalin-fixed paraffin-embedded tissue sections of 62 HCC, 15 hepatocellular adenoma (HA), 59 cirrotic nodules (CN) and 24 normal liver tissues (NLT) were selected. Expression levels S100A4 were evaluated by immunohistochemistry using standard avidin-biotin techniques. Endothelial marker, CD31 was used as positive control stain for endothelial cells. The number of immunoreactive endothelial cells of above reactants in sinusoidal endothelial cells was scored as follows: 0 (no immunoreactive cells), 1 (<10%), 2 (10–50%), and 3 (>50%). Staining intensity was graded as 0 (negative), 1+ (weak), 2+ (moderate), or 3+ (strong). The expression of immunoreaction was further assessed using a numerical scoring system ranging from 0 to 6.

Results: The number of S100A4 positive sinusoidal endothelial cells and the intensity of immunostaining were significantly increased in HCC compared with HA, CN and NLT (P < 0.01). There was a significant positive correlation between S100A4 and a venous and capsular invasion of HCC. There was no significant correlation between the expression of S100A4 protein and the grade and stage of HCC. No significant difference of S100A4 expression was observed between HA and CN, and between HA and NLT.

Conclusions: Increased expression of S100A4 in sinusoidal endothelial cells in HCC suggests that S100A4 may be involved in promoting tumor angiogenesis and metastasis. The findings may have significant implications in the development and application of targeted therapy. The molecular mechanism(s) of S100A4 in HCC progression are currently under study.

1607 Expression of Ezrin in Neoplastic and Nonneoplastic Liver Lesions

W Li, D Tan, P Zhang. 1The University of Texas Medical School at Houston, Houston, TX; University of Texas M.D.Anderson Cancer Canter, Houston, TX; University of Texas M.D. Anderson Cancer Canter, Houston, TX.

Background: Ezrin is a cytoskeleton-associated protein involved in involved in cell adhesion to the extracellular matrix, cell–cell communication, signal transduction, and apoptosis. Ezrin has been implicated in cancer metastasis and progression in a variety of neoplasms. This study aims to evaluate immunohistochemical expression of the Ezrin in neoplastic and nonneoplastic liver lesions, and assess its value in the diagnosis of liver tumors.

Design: Formalin-fixed paraffin-embedded tissue sections of 73 hepatocellular carcinoma (HCC) (17 well, 37 moderately and 19 poorly differentiated), 15 hepatocellular adenoma, 63 cirrhotic nodules and 19 normal liver tissues were immunostained for Ezrin using standard avidin-biotin techniques. The level of Ezrin expression was categorized into four grades: 0 (negative), 1+ (weak), 2+ (moderate), or 3+ (strong) based on intensity of staining. The expression of Ezrin was further assessed using two scales: high expression (2+ or 3+) and low expression (0 or 1+).

Results: Expression of Ezrin is significantly enhanced in HCC tissue compared with non-HCC tissue. High expression of Ezrin was found in 86 % of HCC tissue including 89 % of well-differentiated HCC. In contrast, only 10 % of hepatocellular adenoma, 17 % of cirrhotic nodules and 5 % of normal liver tissues showed high expression for Ezrin. The differences in Ezrin expression between well-differentiated HCC and hepatocellular adenoma or cirrhotic nodules was significant ($P < 0.001$). No significant correlation was found between Ezrin expression and HCC grade.

Conclusions: The expression of Ezrin is highly enhanced in HCC. Ezrin staining may serve as a useful marker for the differential diagnosis of well-differentiated HCC from hepatocellular adenoma. Increased Ezrin expression suggests that Ezrin may play a role in HCC development and progression. The molecular studies of Ezrin in HCC are currently under investigation.

1608 The Epigenetic Effect of Histone Demethylase LSD1 on Hepatic Steatosis of ApoE Deficient Mice

C Lian, B Lian, M Lisovsky, Y Liu, K Dresser, L Pang, V Ricchiuti, G Williams, G Adler, B Woda, Y Shi. University of Massachusetts, Worcester, MA; Dartmouth Medical School, Lebanon, NH; Brigham & Women's Hospital, Harvard Medical School, Boston, MA.

Background: Non-alcoholic fatty liver disease is the most frequent cause of abnormal liver function with a prevalence of 18% in US. The pathogenesis of the condition is poorly understood. Even though the epigenetic mechanism has been increasingly recognized, their role in the pathogenesis of hepatic steatosis is not well defined. Here, we study the effect of histone Lysine Specific Demethylase (LSD1) on diet-induced hepatic steastosis in apoE deficient mice.

Design: All ApoE-deficient mice were fed with a high cholesterol diet containing 42% fat and 1.5% cholesterol from 8 weeks. The control group (n=6) was treated with control GFP-AAV, while the LSD1 knockdown group (n=6) was treated with LSD1 siRNA -AAV. All mice were injected intravenously with the AAV ($x10^{12}$) at 18 weeks. Blood and liver tissue were collected when the mice were sacrificed at 30 weeks.

Results: Histologically, the liver injury of steatosis with mild inflammation was induced by the diet in the control apoE deficient mice. The liver of siRNA-based LSD1 knockdown mice showed significantly reduced steatosis in comparison to the control mice ($p<0.05$).

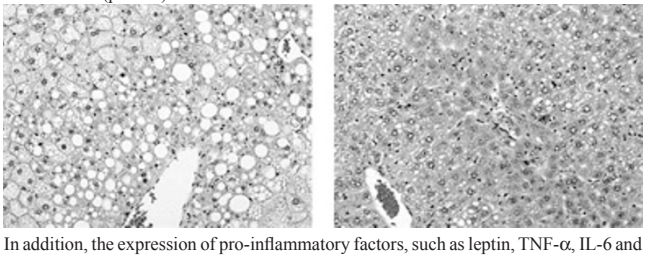

In addition, the expression of pro-inflammatory factors, such as leptin, TNF-α, IL-6 and MCP-1 was significantly decreased in the liver of LSD1 knockdown mice as compared to control ($p<0.05$). Furthermore, adiponectin expression was markedly increased in LSD1 knockdown mice versus the control mice. These changes of gene expression are correlated with the decrease of steatosis assessed morphologically.

Conclusions: Our data demonstrate that LSD1, a key enzyme of histone regulation, play an important role in hepatic steatosis. By inhibition of LSD1, gene expression of pro-inflammatory factors was reduced and anti-inflammatory adiponectin was increased significantly. These findings are correlated with the reversal of steatosis morphologically in the apoE deficient mice.

1609 High Levels of Expression of Activating Transcription Factor-2 (ATF2) Are Associated with Worse Prognosis in Patients with Pancreatic Ductal Adenocarcinoma

JJ Liang, H Wang, R Bruggeman, DB Evans, H Wang. Penn State Milton S Hershey Medical Center, Hershey, PA; The University of Texas M. D. Anderson Cancer Center, Houston, TX.

Background: Activating transcription factor-2 (ATF2, or CREB2), is a sequence-specific DNA-binding protein that belongs to the bZIP family, a key factor in p38/C-Jun N-terminal kinase signaling passway. ATF2 overexpression has been detected in various tumors, including melanoma, ovary and breast caners. The expression and significance of ATF-2 in human pancreatic ductal adenocarcinoma (PDA) have not been studied in detail.

Design: We prepared a tissue microarray consisting of 1.0-mm cores of tumor (two cores per tumor) and paired non-neoplastic pancreatic tissues from 77 pancreaticoduodenectomy specimens of PDA. Nuclear expression of ATF-2 was evaluated by immunohistochemistry with rabbit anti-human ATF-2 (N-96) polyclonal antibodies (1:150, Santa Cruz Biotechnology Inc**).** The staining results were categorized as ATF-2-high (H) (strong nuclear staining of 20% of tumor cells) or ATF-2-low (L) (no staining or weak staining of <20% of tumor cells). Statistical analyses were performed using SPSS software and survival was evaluated by Kaplan-Meier log-rank test.

Results: 33/77 (43%) PDAs demonstrated high levels of ATF-2 expression . The median overall survival rates for patients with ATF-2-H PDAs were 22.4 months,, compared to 38.9 months for patients with ATF-2-L tumors (log-rank test, p=0.0494). High ATF-2 expression was not correlated with patient's age, gender, tumor size, tumor differentiation and lymph node metastasis

Conclusions: High levels of ATF-2 expression are associated with poor overall survival in patients with PDA. ATF-2 may serve as a useful prognostic marker for PDA.

1610 High Levels of Expression of Activating Transcription Factor-2 (ATF2) Are Associated with High-Grade Pancreatic Intraepithelial Neoplasia and Pancreatic Ductal Adenocarcinoma

JJ Liang, S Zhu, W Li, R Bruggeman, B Han. Penn State Milton S Hershey Medical Center, Hershey, PA; University of Texas Health Science Center at Houston, Houston, TX.

Background: Activating transcription factor-2 (ATF2, or CREB2) is a sequence-specific DNA-binding protein that belongs to the bZIP family, a key factor in p38/C-Jun N-terminal kinase signaling passway. ATF2 overexpression has been detected in various tumors, including melanoma, ovary and breast caners. The expression and significance of ATF2 in human pancreatic intraepithelial neoplasia (PanIN) and pancreatic ductal adenocarcinoma (PDA) have not been studied in detail. In this study, we examined expression of ATF-2 in human PanIN lesions and PDA.

Design: We prepared a tissue microarray consisting of duplicated 2.0-mm cores of PDAs (n=38), PanIN I (n=16), PanIN II (n=8) and PanIN III (n=6) lesions and non-neoplastic pancreatic tissues (n=22). Nuclear expression of ATF-2 was evaluated by immunohistochemistry with rabbit anti-human ATF-2 (N-96**)** polyclonal antibodies (1:500, Santa Cruz Biotechnology Inc). Immunoreactivity was scored based on the sum of staining intensity (0 = none, 1 = mild, 2 =moderate, 3 = marked) and percentage of cells staining (0 = <1%, 1 = 2~10%, 2 =11~40%, 3 = >40%) (Potential range of 0 to 6). Statistics was performed by Student's t test.

Results: There was significantly higher expression of ATF-2 in PDAs (mean 4.2±0.8) and PanIN III (mean 3.8 ±0.7), compared to PanIN II (mean 2.4 ±0.5), PanIN I (mean 2.1 ±0.4), and normal bile ductal epithelium (mean 1.8 ±0.5) ($p<0.01$). However, there is no significant difference in ATF-2 expression between normal bile ductal epithelium and either PanIN I or PanIN II lesions ($p>0.05$).

Conclusions: High levels of expression of ATF-2 are associated with high-grade PanIN lesion and PDAs. Our results suggest that activation of ATF-2 gene involve the progression of later stage PanIN to PDAs.

1611 Diagnostic Utility of C4d Immunohistochemical Staining in Pancreas Allograft Biopsies and Correlation with HLA Donor Specific Antibodies

JJ Liang, RE Domen, T Uemura, A Khan, K Kugler, R Bruggeman, FM Ruggiero, AB Abt, Z Kadry, CS Abendroth. Penn State Milton S Hershey Medical Center, Hershey, PA.

Background: The major causes of transplant failure are post-transplant acute cellular and/or antibody-mediated rejection (AMR). AMR of pancreas allografts is poorly understood. C4d is a complement split product generated during antibody-mediated immune response. The C4d staining has been routinely performed in kidney, heart and lung transplant biopsies to aid in diagnosis of AMR; however, its diagnostic utility in AMR of pancreas allografts has not been well defined.

Design: This study includes a total of 28 pancreas allograft biopsies from 12 patients over a two year period. Formalin-fixed, paraffin-embedded sections were immunostained with rabbit polyclonal antibody to C4d (ab36075) (dilution 1:200). C4d staining was graded as positive when strong staining involved more than 50% of interacinar capillaries and as negative when no or focal, weak staining was observed. Positive DSA presence was determined to be ≥1000 Mean Fluoresence Intensity (MFI); negative presence of antibody was <1000 MFI. Each biopsy was correlated with the grade of acute rejection, levels of serum amylase, lipase, presence of HLA DSA, and clinical treatment.

Results: Three of 12 patients (25%) (patients A, B and C;) had HLA DSA during the biopsy period. C4d staining was negative in the biopsy from patient A, who had a moderately high level of HLA anti-A11 DSA (MFI: 3435) and increased amylase and lipase. C4d staining was negative in 5 biopsies from patient B, who had a moderately high level of HLA anti-DQ5 DSA (MFI: range 2257 to 8447) and increased amylase and lipase. By contrast, C4d staining was strongly positive in two of four biopsies from patient C, who had a negative to marginally positive HLA anti-A2 DSA and mildly increased amylase and lipase. All three patients had grade II acute cellular rejection. The remainder of our study patients had no HLA DSA identified and C4d staining was negative. All three allografts are functioning well after a mean followup of 31 months.

Conclusions: 1) Positivity of C4d staining did not appear to be correlated with either HLA DSA or serum amylase/lipase level. 2) C4d IHC staining may not be a sensitive method to detect antibody-mediated rejection in pancreas allograft biopsies and should always be performed in conjunction with HLA antibody screening.

1612 Diagnostic Utility of von Hipple-Lindau Gene Product (pVHL), Maspin, KOC, and S100P in Adenocarcinoma of the Gallbladder

F Lin, J Shi, HL Wang, H Liu. Geisinger Medical Center, Danville, PA; Cedars-Sinai Medical Center, Los Angeles, CA.

Background: Our recent study demonstrated the upregulation of S100P and downregulation of pVHL in pancreatic intraepithelial neoplasia and ductal adenocarcinoma of the pancreas (Lin et al. AJSP 2008;32:78-91). Additional unpublished studies showed maspin and KOC were also useful markers in differentiating adenocarcinoma of the pancreas from benign/reactive pancreatic ducts. Distinction of adenocarcinoma of the gallbladder from benign/reactive glandular epithelium can be challenging if based on H&E-stained sections alone. This study investigates the utility of these four markers in the diagnosis of adenocarcinoma of the gallbladder.

Design: Immunohistochemical stains for maspin, KOC, S100P and pVHL were performed on 43 gallbladder specimens, including adenocarcinoma (N=23) and normal/reactive gallbladder (N=20). The staining intensity was graded as weak or strong. The distribution was recorded as negative (<5% of the cells of interest stained), 1+ (5-25%), 2+ (26-50%), 3+ (51-75%), or 4+ (more than 75%).

Results: The results demonstrated a nuclear and cytoplasmic staining pattern of maspin and S100P in 23 of 23 (100%) and 17 of 23 (74%) of adenocarcinoma cases, respectively, and cytoplasmic staining for KOC in 18 of 23 (78%) adenocarcinoma cases. In contrast, none of the 20 reactive/normal gallbladder cases was positive for S100P and KOC. Four cases of normal gallbladder were weakly positive for maspin. Glandular epithelium in all normal/reactive cases was diffusely (3+ and 4+) positive for pVHL with membranous/cytoplasmic staining. In contrast, all adenocarcinoma cases were negative for pVHL, whereas the adjacent normal ductal/glandular epithelia were positive for pVHL. The staining results are summarized in Table 1.

Table 1. Summary of the Immunostaining Results for pVHL, S100P, Maspin and KOC

Markers	Adenocarcinoma Cases (N=23)	Normal/Reactive Cases (N=20)
pVHL	0/23	20/20 (100%)
Maspin	23/23 (100%)	4/20 (20%)
KOC	18/23 (78%)	0/20
S100P	17/20 (74%)	0/20
Positive for 3 markers	14/23 (61%)	0/20
Positive for 2 markers	20/23 (87%)	0/20

Conclusions: Our data suggest that the expression patterns of pVHL, maspin, KOC and S100P can be used as a panel of diagnostic markers to confirm the diagnosis of adenocarcinoma of the gallbladder.

1613 Reevaluation and Identification of the Best Immunohistochemical Panel for Adenocarcinoma of the Pancreas

F Lin, J Shi, HL Wang, H Liu. Geisinger Medical Center, Danville, PA; Cedard-Sinai Medical Center, Los Angeles, CA.

Background: Differentiation of adenocarcinoma of the pancreas from non-neoplastic pancreatic tissues can be challenging, especially in small core biopsies, pancreatic surgical margins and fine needle aspiration specimens on cell blocks. Many tumor-associated markers have been reported in this regard; however, the reproducibility of these markers has not been tested and confirmed in one system. This study investigates the utility of 26 different immunohistochemical markers in the diagnosis of adenocarcinoma of the pancreas.

Design: We immunohistochemically evaluated the expression of 1) epithelial markers (CAM5.2, CK7, CK20, CK17, CK19), 2) mucin gene products (MUC1, MUC2, MUC4, MUC5AC, MUC6), 3) tumor suppressor genes and transcription factors (p53, Dpc4/SMAD4, CDX2, pVHL), and 4) tumor-associated proteins (S100P, KOC, maspin, mesothelin, claudin 4, claudin 18, annexin 8A, fascin, PSCA, MOC31, CEA, CA19-9), on 70 cases of pancreatic adenocarcinoma (20 conventional tissue sections and 50 tissue microarray sections). Non-neoplastic pancreatic tissue was present in 40 cases. The staining intensity was graded as weak or strong. The distribution was recorded as negative (<5% of tumor cells stained), 1+ (5-25%), 2+ (26-50%), 3+ (51-75%), or 4+ (>75%).

Results: The results demonstrated 1) over 90% of cases are positive for maspin, S100P and KOC; 2) all cases show loss of expression of pVHL in adenocarcinoma, whereas non-neoplastic ducts and acini are strongly positive for pVHL in all cases; 3) normal/reactive pancreatic ducts are frequently positive for CAM 5.2, CK7, CK19, MUC1, MUC6, CEA, MOC31, PSCA, mesothelin, annexin 8A, and claudin 4, claudin 18; 4) normal pancreatic ducts are usually negative for KOC, maspin, S100P, MUC2, MUC4, and MUC5AC; 5) 60% of cases show loss of expression of Dpc4/SMAD4; and 6) a strong staining background is frequently seen in fascin, PSCA, and annexin 8A.

Conclusions: Our data demonstrate that pVHL, maspin, S100P and KOC are the best diagnostic panel of markers for confirming the diagnosis of adenocarcinoma of the pancreas.

1614 Loss of BRG1/SMARCA4 Expression in Pancreatic Ductal Adenocarcinoma

M Lin, F Scrimieri, T Nguyen, CL Wolfgang, C Iacobuzio-Donahue, A Maitra, M Goggins, J Eshleman, K Olino, SE Kern, RH Hruban. Johns Hopkins University School of Medicine, Baltimore, MD.

Background: Pancreatic ductal adenocarcinoma is an almost universally fatal disease, with a 5 year survival rate of approximately 5%. The coding genome of 24 human pancreatic cancers was recently sequenced (S. Jones et al., Science 2008) and the *BRG1* (also known as *SMARCA4*) gene was found to be bi-allelically inactivated in one of the 24 cancers suggesting that *BRG1* may function as a tumor suppressor gene in pancreatic cancer. An additional cancer with monoalleic inactivation was identified in the validation phase of the sequencing study. The prevalence of *BRG1* gene inactivation in a larger series of pancreatic cancers has not been defined.

Design: Formalin-fixed, paraffin-embedded tissues from the 2 patients with mutations of the gene were immunohistochemical labeled with a monoclonal antibody to BRG1 (amino acids 209-296; Santa Cruz Biotechnology, Santa Cruz, CA) using standard methods. Subsequently, tissue micro-arrays from 397 patients with invasive pancreatic ductal adenocarcinoma and 44 patients with pancreatic intraepithelial neoplasia were immunolabeled using the anti-BRG1 antibody. Each tissue micro-arrays included two cores of normal tissue and two of tumor.

Results: As expected, the primary and metastases from the patient with biallelic inactivation had a complete loss of BRG1 protein expression, while BRG1 expression was retained in the neoplastic cells of the patient with monoalleic inactivation. Loss of BRG1 expression was identified in only two (0.5%) of the 397 cases with invasive pancreatic ductal adenocarcinoma and none of the 44 cases of pancreatic intraepithelial neoplasia.

Conclusions: These data indicate that loss of BRG1 protein expression is uncommon in pancreatic ductal adenocarcinoma, and suggest that *BRG1* gene inactivation is a relatively rare event in pancreatic cancer. Further studies are needed to elucidate the possible pathogenesis of *BRG1* mutations in rare pancreatic ductal adenocarcinomas.

1615 Differentiation of Pancreatic Intraepithelial Neoplasia-3 (PanIN-3) and Ductal Adenocarcinoma of the Pancreas from Lower Grade PanINs Utilizing Immunohistochemistry for Cell Polarity Protein *Lethal Giant Larva 2* (lgl2)

M Lisovsky, K Dresser, B Woda, M Mino-Kenudson. Massachusetts General Hospital, Boston; UMassMemorial Medical Center, Worcester.

Background: Pancreatic intraepithelial neoplasia (PanIN) is a precursor of ductal adenocarcinoma of the pancreas (PDAC). PanIN-3 has the highest potential to progress to PDAC and its distinction from lower grade PanINs, such as PanIN-1 and PanIN-2, is important for clinical management. However, morphologic grading of PanIN suffers from significant interobserver variability and may be difficult. A product of cell polarity gene *lgl2* is a marker of gastric foveolar epithelium, which is expressed in a basolateral fashion, and is lost or mislocalized in gastric epithelial dysplasia and adenocarcinoma. Since PanIN shows gastric differentiation phenotype, we investigated the utility of Lgl2 expression for differentiating PanIN-3 from lower-grade PanINs.

Design: The immunohistochemical patterns of Lgl2 expression were examined in normal pancreatic ducts, 48 PanIN lesions of all histologic grades, and 91 PDACs on a tissue microarray or conventional sections. The expression pattern was recorded as basolateral, cytoplasmic, negative, or combinations of any of them.

Results: While normal duct epithelia showed negative Lgl2 immunoreactivity, all but one of 33 lesions of low-grade PanIN showed basolateral Lgl2 staining. Conversely, all 14 lesions of PanIN-3 and all 91 PDACs showed loss of Lgl2 staining or its abnormal cytoplasmic localization. Interestingly, a basolateral expression was focally seen in 4 PDACs with a foamy gland pattern, and was always admixed with negatively stained areas.

Conclusions: Our results show that low-grade PanINs express Lgl2 in a basolateral fashion recapitulating expression in benign gastric epithelium. Loss or abnormal Lgl2 expression is seen in PanIN-3 and PDAC and could be useful in separating them from lower-grade PanINs.

1616 K-ras Mutations in Hepatocellular Carcinomas

C Liu, D Cardona, HJ Dong. University of Florida, Gainesville, FL.

Background: K-ras mutations are detected in many types of human cancers. Mutation status of this gene plays a critical role in guiding clinical therapy for colon cancer. K-ras mutations have been detected in hepatocellular carcinomas (HCC) induced in animal models, but the characteristics of K-ras mutations and their clinical significance in human HCCs have not been well studied. The objective of our study is to examine and characterize K-ras mutations in HCC.

Design: Fifty-two cases of HCC and forty cases of colorectal carcinomas (CRC) were selected for K-ras mutation analysis. Total DNA was extracted from formalin-fixed tissue using Waxfree DNA extraction kit according to the manufacturer's instructions. K-ras gene region was amplified by PCR using a pair of gene-specific primers with the forward primer labeled with biotin. Three sequence-specific primers that are designed for detecting mutations at codon 12 or 13 were then used for pyrosequencing analysis. The mutant group and the wild type group were compared regarding clinical parameters and histological features. Student's t test was used for statistical analysis.

Results: K-ras mutations were detected in 11 out of total 52 cases (21%) of HCCs, while K-ras mutations were detected in 15 out of total 40 cases (38%) of CRCs. In contrast to CRCs that have both codon 12 and 13 mutations, the K-ras mutations in HCC are exclusively in codon 12. Among the 11 cases of HCCs with K-ras codon 12 mutations, 8 cases have hepatitis C viral (HCV) infection (72%); Among the K-ras wild type cases, 18 out of 45 have HCV infection (40%). The difference is statistically significant (p value is 0.006). Compared with the K-ras mutant and K-ras wild type groups, the average age in the K-ras mutant group is 54.8 year-old and the average age in the K-ras wild type group is 58.2 year-old. There is no significant difference in tumor differentiation, vascular invasion, or tumor stage between the two groups.

Conclusions: From this study, we conclude that: 1. K-ras mutations can be detected in 21% of human HCCs; 2. K-ras mutation in HCC occurs exclusively at codon 12; 3. K-ras mutation appears to be associated with higher incidence in HCCs with underlying HCV chronic infection.

1617 PAX8 Expression in Pancreatic Endocrine Tumors: Correlation with Pathologic Features and Behavior

KB Long, A Srivastava, MS Hirsch, JL Hornick. Brigham and Women's Hospital, Harvard Medical School, Boston, MA; Dartmouth-Hitchcock Medical Center, Lebanon, NH.

Background: PAX (paired box) genes encode a family of transcription factors that regulate organogenesis and cell-lineage specification in multiple organ systems. In

the pancreas, PAX proteins play a critical role in islet cell differentiation. We recently observed that islet cells show strong, diffuse staining for PAX8. However, PAX8 expression has not been examined in pancreatic endocrine tumors (PETs). The purpose of this study was to evaluate PAX8 in PETs, and to correlate expression with clinical and pathologic features and behavior. PAX8 expression in other well-differentiated neuroendocrine tumors (WDNET) was also studied.

Design: In total, 149 tumors were evaluated: 63 PET and 28 ileal, 5 duodenal, 5 gastric, 19 appendiceal, 13 rectal, and 16 pulmonary carcinoid tumors. Immunohistochemistry was performed after pressure cooker antigen retrieval using a rabbit anti-PAX8 polyclonal antibody (Proteintech; 1:800). Nuclear staining in >5% of tumor cells was considered a positive result. Statistical analysis was performed using the Fisher exact or chi square test; all reported p values are two-tailed.

Results: In the normal pancreas, PAX8 expression was restricted to islet cells, with absence of staining in acinar and ductal epithelium. PAX8 was positive in 40/63 (63%) PET. Expression of PAX8 was significantly associated with WHO category 1.1 vs category 1.2 or 2 (positive in 94%, 58%, and 48%, respectively; $p<0.05$) and inversely correlated with the development of liver metastases (positive in 71% of localized tumors vs 41% with liver metastases; $p<0.05$). PAX8 expression was not associated with functional status or other pathologic features. PAX8 was detected in 1/5 (20%) gastric, 5/5 (100%) duodenal, 0/28 (0%) ileal, 4/19 (21%) appendiceal, 11/13 (85%) rectal, and 0/16 (0%) pulmonary carcinoid tumors.

Conclusions: PAX8 is expressed in normal pancreatic islet cells as well as in a high proportion of PETs. In the GI tract, PAX8 is positive in the majority of duodenal and rectal carcinoid tumors, and in a minor subset of appendiceal and gastric carcinoids. PAX8 expression is absent in ileal and pulmonary carcinoid tumors. These findings suggest that PAX8 may be helpful in determining primary site for a WDNET metastatic to the liver, since ileal (PAX8 negative) and pancreatic (PAX8 positive) tumors most often present as a metastasis from an occult primary. PAX8 may be a prognostic marker in PETs, since loss of expression is associated with malignant behavior.

1618 Microsteatosis More Significant Than Macrosteatosis in Predicting Early Post-Transplant Hepatic Non-Function

I Lytvak, TJ Prihoda, KV Speeg, WK Washburn, GA Halff, FE Sharkey. University of Texas Health Science Center, San Antonio, TX.

Background: The extent of macrovesicular steatosis may be used to exclude potential donor livers from transplantation, since those with >50% are believed to have a greater risk of primary non-function. However, favorable clinical experience with steatotic donor livers has led us to re-examine this guideline.

Design: The H&E slides of post-perfusion donor liver biopsies from 161 transplants were examined. The type of steatosis (macrovesicular [Mac] vs. microvesicular [Mic]) was determined, and the extent of macrosteatosis (% of lobule involved) was semiquantitated into three grades (none, ≤50%, and >50%). These were analyzed along with the MELD score and both the patient's and the donor's age against post-operative outcome variables, including three different quantitative serial measures of serum lactate (days to normalize, days to reach 1/2 peak, and late rise), as well as days in ICU, days in hospital, and death <3 months post-transplant.

Results: Mac was present in 91 cases (57%), 29 at the >50% level. Mic was present in 18 cases (11%), 17 of them in association with Mac, and 15 at the ≤25% level). By chi-square analysis, there was no significant association between the extent of Mac and any of the outcome variables. In contrast, the presence of Mic was significantly associated with all three measures of elevated serum lactate post-op (p=~.01 each). Logistic regression analysis failed to reveal any significant additive effect of Mac, MELD score or patient/donor age to the effect seen with Mic.

Frequency of patients with each outcome variable.

Type of Steatosis	≥1 day to nl. SerLact	≥1 day to 1/2 peak SerLact	Late Rise in SerLact	>2 ICU days	>5 Hospital Days	Death <3 mos.
Mac	14%	13%	3%	63%	88%	8%
Mic	28%	33%	17%	88%	89%	6%

SerLac - Serum Lactate; all dates are post-transplant.

Conclusions: The relationship between macrosteatosis and early liver non-function post-transplant appears to be a result of the associated microsteatosis, when present. Histologic evaluation of hepatic steatosis in advance of transplantation needs to take microsteatosis into account.

1619 Fatty Acid Synthase: A Potential Serum Marker for Non-Alcoholic Steatohepatitis (NASH)

Z Maleki, M Torbenson, S Medghalchi, WF Han, FP Kuhajda. Johns Hopkins University School of Medicine, Baltimore, MD; FASgen Inc, Baltimore, MD.

Background: Non-alcoholic fatty liver disease (NAFLD) is a clinically silent condition most commonly occurring in obese individuals. Left undiagnosed and untreated, a subset of individuals with NAFLD will develop steatohepatitis (NASH) with an increased risk of cirrhosis. Since elevated expression of fatty acid synthase (FAS), the enzyme responsible for de novo fatty acid synthesis, has been reported in the liver of patients with NAFLD, we hypothesized that serum FAS levels are increased in the blood of patients with NASH and may be a useful serum marker to identify individuals at greater risk for NASH.

Design: FAS was measured in presurgical serum from 101 bariatric surgery patients using a human anti-FAS monoclonal sandwich ELISA assay (FASgen Inc, Baltimore, MD). Intraoperative liver biopsy was performed on 77 patients and semiquantitatively scored with a NASH activity score (0-2 steatosis, 3-5 mild NASH, 6-7 marked NASH). Age, gender, body mass index (BMI), serum ALT, AST and alkaline phosphatase values were collected. Hepatic FAS expression was assessed with immunohistochemistry. Serum FAS was also measured in 119 healthy controls.

Results: Of the 77 patients with both serum FAS and liver biopsy, FAS ranged from 1-88 ng/mL (avg 15.2). Biopsy results showed: 43 steatosis, 28 mild NASH, and 6 marked NASH. BMI ranged from 34-88 (avg 50). Increased serum FAS levels were associated with NASH by linear regression (p=0.007) or 1-way ANOVA (p=0.025). The table shows the data when FAS levels were categorized.

Serum FAS and NAFLD

Serum FAS ng/mL	0-4	5-10	>10
Steatosis (%)	19/25 (76)	10/18 (56)	14/34 (41)
Mild NASH (%)	6/25 (24)	7/18 (39)	15/34 (44)
Marked NASH (%)	0	1 (5)	5/34 (15)

p=0.0027 (regression)

Increasing FAS levels were associated with the severity of liver disease (p=0.0027, regression). FAS levels > 10 ng/mL identified 5/6 patients with marked NASH. Neither liver function tests nor clinical data were significantly associated with NASH. Serum FAS in the 119 healthy controls averaged 0.97 ng/mL (0.18 std. error). Immunoreactive FAS was identified in the liver of patients with either steatosis or NASH.

Conclusions: Serum FAS levels are elevated in morbidly obese subjects compared to healthy controls. Among bariatric surgery patients, FAS levels were significantly associated with NASH. FAS may prove to be a useful marker for detection of NAFLD in obese subjects.

1620 Accuracy of Determining Hepatocellular Carcinoma (HCC) Tumor Grade on Core Needle Biopsy (CNB)

A Manuyakorn, AC Lowe, S Sabounchi, D Lu, CR Lassman. UCLA, Los Angeles; Siriraj Hospital, Bangkok, Thailand.

Background: Low grade and well differentiated HCC have been demonstrated to have better prognosis than high grade/poorly differentiated HCC after resection. Accordingly, it has been suggested that results of CNB be taken into account when considering transplantation of patients with HCC who exceed Milan criteria. This study aims to assess the validity of tumor grade assessment by CNB.

Design: After IRB approval, 344 patients with histology proven HCC were identified at a single institution. CNB and resection material (hepatectomy or resection) was available for review in 40 patients. Two pathologists determined tumor differentiation with agreement by double-headed scope. Well differentiated (WD) was defined as AFIP nuclear grade 1 or grade 2 with a trabecular or acinar pattern, moderately differentiated (MD) as nuclear grade 3 or grade 2 with solid or schirrous pattern, and poorly differentiated as nuclear grade 4.

Results: The 40 patients included 31 men and 9 women, with a mean age of 57 years (range 33-74). Interval time between CNB and resection was <6 months in 24 patients and >6 months in 16. Fifteen cases had a single lesion and 25 had multiple lesions. Thirty patients received preoperative treatment; 10 did not. Concordance of tumor differentiation between CNB and resection was poor (Table 1) with Kappa of - 0.009 (p 0.5384), with CNB underestimating tumor differentiation in resection material in 19 cases, demonstrating the same differentiation in 17, and overestimating in 4. When only nuclear grade was considered, CNB underestimated the resection material in 23 cases, showed the same grade in 14, and overestimated in 3. Concordance was also poor when interval time, number of lesions, and preoperative treatment were considered.

Comparison of tumor differentiation on CNB vs. Resection/Hepatectomy

		Resection/Hepatectomy			
		Well	Moderate	Poor	Total
	Well	4	**19**	0	23
CNB	Moderate	**3**	13	0	16
	Poor	0	**1**	0	1
	Total	7	33	0	40

Conclusions: This study demonstrates that a diagnosis of WD HCC by CNB is likely to be inaccurate; however, a diagnosis of MD HCC by CNB is more likely to be accurate. The inherent limitations of sampling by CNB are the most likely explanation. One may question whether a diagnosis of WD HCC by CNB should be used as a positive criterion when determining transplant eligibility in a patient who has exceeded Milan criteria.

1621 Problematic Cavernous Hemangioma Variants and Other Benign Mimics

AN Mattis, S Fischer, H Makhlouf, W Tsui, S Cho, L Ferrell. UCSF, San Francisco; Univ Toronto, Toronto, Canada; AFIP, Washington, DC; Caritas Medical Centre, HK, Hong Kong.

Background: Cavernous hemangioma (CH), the most common hepatic vascular tumor, typically consists of a single mass composed of large dilated spaces with a single endothelial lining covering septa with fibroblasts and scant smooth muscle cells. CH is usually not a diagnostic problem but we describe unusual CH variants and mimics, many that have previously not been well-described, but may cause diagnostic problems, including those that may be confused with malignancy.

Design: Ten cases of hepatic resections with unusual hemangioma-like lesions were reviewed. When possible, CD31, CD34, SMA, MIB-1, and EVG stains were used to assist in classifying the lesion.

Results: We classified our cases into two broad categories, unusual variants of CH (Type 1, 7 cases) and mixed or unclassified mimics of hemangiomas (Type 2, 3 cases). The CH variants (Type 1) included two subcategories. Type 1A were confined to the interior of the CH, and were problematic due to significant degrees of scarring and/or organizing thrombosis, resulting in increased cellularity and thickening of septa or lesions similar to the intravascular papillary endothelial lesion of Masson. Type 1B had CH-like vessels (CHLVs) not organized into the typical single CH, but composed of numerous clusters of CHLVs admixed with large zones of liver parenchyma within the body of a distinct mass lesion, or CHLVs present in predominatly periportal locations outside of a typical CH and dispersed diffusely in right and left lobes, suggesting a diagnosis of metastatic vascular tumor. Type 2 lesions were composed of capillary, venous, or small muscular vessels. One lesion had dilated sinusoids and hepatic vein-like vessels, typical of a localized venous malformation but that grossly mimicked CH. Two other lesions were more similar to capillary hemangiomas, one associated with similar lesions

in the spleen and lymph nodes, and one similar to a multilobular hemangioma with spindle cell component. These lesions had a sinusoidal pattern of growth that resulted in a residual layer of hepatocytes in the intervening septa, histologic features that could mimic those of epithelioid hemangioendothelioma or angiosarcoma.
Conclusions: We describe unusual variants of CH and other types of hemangioma-like lesions, including rare unclassified types. Defining this expanded spectrum of hemangioma-like lesions may aid in their diagnosis and in understanding their development, progression, and outcome.

1622 Comparison of PAX-2 and PAX-8 in Distinguishing Hepatocellular Carcinomas with Clear-Cell Morphology from Renal Cell Carcinomas

AN Mattis, LW Browne, S Kakar, YY Chen, GE Kim, L Ferrell. UCSF, San Francisco, CA; Kaiser Permanente, Walnut Creek, CA.
Background: Immunohistochemistry (IPOX) for PAX-2 and PAX-8, transcription factors important to renal development, are positive in the majority of clear-cell renal cell carcinomas (RCC). The IPOX profile of PAX-2 and PAX-8 in hepatocellular carcinomas (HCC) have not been compared. In adults, the differential diagnosis for hepatic neoplasms with clear-cell morphology includes metastatic RCC. The distinction between HCC with clear-cell morphology and metastatic RCC can be especially challenging on small tissue samples.
Design: We constructed tissue microarrays (TMAs) to investigate the IPOX patterns of PAX-2 and PAX-8 in HCC. The HCC TMAs contained 1.5-mm cores of 82 HCC tumors with a wide range of differentiation and morphologic subtypes including clear cell morphology. We also constructed a TMA containing 1.5-mm cores of 84 primary RCCs which included clear-cell, chromophobe, and papillary variants. We performed IPOX for PAX-2, PAX-8, as well as EMA and RCC antibodies to evaluate renal differentiation, and HepPar1 and glypican-3 to evaluate hepatocellular differentiation. Negative controls were performed. Neoplasms were interpreted as positive for PAX-2 or PAX-8 if they showed nuclear staining.
Results: Only 4(5%) of HCCs showed any PAX-2 focal or weak nuclear staining while none showed strong staining, and 2(3%) of HCCs (not the same cases which were positive for PAX-2) showed focal intermediate to strong positive nuclear staining for PAX-8. Additionally some scattered lymphocytes within HCCs showed strong PAX-8 staining which could be mistaken for positive nuclear staining. 98% of HCCs were negative for EMA and all were negative for RCC antibody. IPOX staining for HepPar1 and/or glypican-3 was seen in 94% of HCCs. Cytoplasmic or background staining was seen in 23% and 13% of HCCs for PAX-2 and PAX-8 respectively. Nuclear staining for PAX-2 was present in 83% and PAX-8 was present in 92% of RCCs.
Conclusions: PAX-2 and PAX-8 nuclear staining is absent in HCC over a wide range of morphologic subtypes but nuclear staining is present in a vast majority of RCC subtypes. PAX-2 and PAX-8 are both very useful in distinguishing between HCC and RCC, including HCC variants with clear cell morphology, comparable to other markers for RCC, including RCC antibody and EMA, and are helpful, particularly in combination with other markers such as HepPar 1 and GLy-3, in distinguishing HCC from RCC.

1623 Relationship between Number of Portal Tract Macrophages and the Modified Hepatic Activity Index in Chronic Hepatitis C Infection

MK McElroy, MR Peterson. University of California, San Diego, La Jolla, CA.
Background: The Ishak modified hepatic activity index (mHAI) is widely used to score disease activity in chronic hepatitis C. However, the scoring of the mHAI components is subjective and prone to interobserver variation. Liver injury results in increased numbers of portal tract macrophages, which are easily identified via PASD stain. We hypothesize that the number of portal tract macrophages is related to the mHAI in chronic hepatitis C infection, and that this score may provide a quantitative and more reproducible measure of disease activity.
Design: 30 consecutive needle core liver biopsies performed on patients with chronic hepatitis C infection were retrieved, including H&E, PASD, and trichrome stained slides. These biopsies were independently reviewed by two pathologists and scored using the mHAI. The number of portal tract PASD positive macrophages was counted, expressed as the number of macrophages per CM of biopsy length. The macrophage counts were then sorted into the following categories: none, minimal (0-2/CM), mild (2-5/CM), moderate (5-8/CM), and severe (>8/CM). This data was then compared to components of the mHAI.
Results: The number of portal tract PASD positive macrophages was found to be significantly associated with the level of portal inflammation (p=0.039) and total summed mHAI score (p=0.029). The number of portal tract PASD macrophages appeared to be related to the level of interface activity and focal lobular necroinflammatory activity, but these failed to meet significance (p=0.073 and 0.079) in this small study. There was no relationship between portal tract PASD macrophage counts and the level of fibrosis. There was better interobserver agreement for portal tract PASD macrophage counts than any component of the mHAI. Specifically, the kappa coefficient for portal tract PASD macrophage count categories was 0.85, while the kappa coefficient for mHAI components was as follows: portal inflammation 0.55, focal lobular necroinflammatory activity 0.45, and interface activity 0.70.
Conclusions: We conclude that there is a statistically significant relationship between the number of portal tract macrophages and the level of portal inflammation and the total summed mHAI score. In addition, we find better interobserver agreement for portal tract macrophage counts than for any of the mHAI components. This technique may provide a reproducible and useful scoring method as an adjunct to the modified hepatic activity index for assessing the level of disease activity in chronic hepatitis C.

1624 Histologically but Not Clinically Defined Fibrosing Cholestatic Hepatitis C Is Predictive of Poor Patient Outcomes in the Liver Transplant Population

Z Meriden, R Wells, G Makar, R Reddy, EE Furth. University of Pennsylvania, Philadelphia, PA.
Background: Fibrosing cholestatic hepatitis (FCH) is a specific form of liver disease with poor patient outcome following transplantation for hepatitis C. There is no standard definition of FCH, and both clinical and/or histologic ones are used. The goal of our study was to compare patient and liver allograft outcomes of clinically and histologically, prospectively defined FCH.
Design: FCH was diagnosed prospectively by histology (HFCH: pericellular fibrosis, cholestatic injury, minimal inflammation) and clinically (CFCH: total bilirubin >4 for >30 days with other etiologies excluded and high viral load (>6 log normal) from a total cohort of 314 liver transplants performed for hepatitis C (2003-2007). Portal and pericellular fibrosis in post- transplant biopsies were scored by METAVIR (0-4) and a tiered system (absent=0, mild=1, moderate=2, severe=3), respectively. Fibrosis progression and survival among the cohorts and subsets therein were compared by the Kaplan-Meier method.
Results: The total FCH (TFCH) cohort (n=28:13 HFCH, 17 CFCH, 2 had both) had a mean patient and donor age of 50 and 44 years, respectively, with no statistically significant demographic differences between HCFH and CFCH. *Cirrhosis* progression in TFCH approximated that of the total patient cohort (P=0.1316), with a median time to cirrhosis of 4.7 years. Progression to cirrhosis between HFCH and CFCH groups was not different (P=0.5438). However, in TFCH, the rate of severe *pericellular fibrosis* development exceeded that of the total cohort by a factor of 4 (P=0.0076, HR 4.444, 95% CI 1.487-13.28), with 36% of TFCH having severe pericellular fibrosis by the end of year 1 post-transplant. While cirrhosis progression between HFCH and CFCH was similar, the rate of severe pericellular fibrosis development was 10-fold greater in HFCH (P=0.0002; HR=10.41; 95% CI = 3.059-35.43). Patients with HFCH had poorer survival than CFCH, with a nearly 5-fold greater rate of deaths (P=0.0226; HR 4.819; 95% CI 1.247-18.62) and median survival of 1.9 years.
Conclusions: The development of *cirrhosis* in TFCH patients only mirrors that of the general transplanted population, with no difference in those with HCFH vs. FCFH. However, patients with TFCH develop *pericellular fibrosis* more rapidly than the general population, with the effect being more dramatic in the HFCH subtype. In contrast to patients with CFCH, those with HFCH experience not only greater pericellular fibrosis progression, but also poorer patient outcomes.

1625 Lymphocyte-Rich Primary Carcinomas: Rare Tumors of the Liver

Z Meriden, HR Makhlouf, H Daniel, TT Wu, MM Yeh, MS Torbenson. Johns Hopkins Hospital, Baltimore, MD; AFIP, Washington, DC; Mayo Clinic, Rochester, MN; Univ. of Washington, Seattle, WA.
Background: Lymphocyte-rich primary carcinomas of the liver are rare entities with a variety of morphologies, from hepatocellular carcinoma (HCC) to cholangiocarcinoma to lymphoepithelial-like carcinoma (LELC). LELC's in the head and neck are commonly associated with either Epstein-Barr virus (EBV) or human papilloma virus (HPV). To better understand the clinicopathologic spectrum of lymphocyte-rich primary carcinomas of the liver, cases were collected from 4 institutions and characterized at the clinical, histological, and molecular levels.
Design: A total of 9 cases were collected and reviewed. Eight cases had tissue available for molecular testing. Immunohistochemistry for p53, β-catenin, and p16 was performed on cases with available tissue (6/9). In-situ hybridization for EBV (EBER) was performed, as well as PCR on microdissected paraffin-embedded tissues for EBV and HPV. Exon 3 of *CTNNB1* (encoding β-catenin) and exon 7 of *TP53* (encoding p53) were also sequenced.
Results: The average age was 57 years at resection, 60% of individuals were women, and the average tumor size was 6 cm. Four of 7 cases (57.1%) arose in a background of hepatitis C. Two cases had a classic LELC morphology, 5 had an HCC morphology with marked lymphocytosis, and 2 were cholangiocarcinomas. Immunohistochemistry for β-catenin nuclear accumulation was negative in all cases, and tested cases were negative for exon 3 *CTNNB1* mutations. In 4/5 cases, sparse p53 nuclear accumulation was seen, but sequencing for mutations in exon 7 of *TP53* was negative in all tested cases. EBV was detected in 4/9 cases. Two cases were strongly EBV-positive (1 high-copy by real-time PCR, 1 by EBER); and both had a non-HCC morphology, one being a LELC and the other a cholangiocarcinoma. In contrast, the remaining two cases had low-copy EBV positivity by real-time PCR and had HCC morphologies. P16 was positive in 2 cases, with 5-25% of tumor cells showing positivity; however, HPV PCR was negative in all tested cases.
Conclusions: To our knowledge, this is the largest case series and only multi-institutional study of these rare tumors, which demonstrate a spectrum of morphologies. Unlike LELC's of the head and neck**,** lymphocyte-rich primary carcinomas of the liver are not HPV-associated; however, EBV is detectable in 30% of cases. High-copy EBV -positive tumors show non-HCC morphology, while low-copy EBV-positive tumors can have classic HCC features.

1626 Platform of Orthotopic Models Suitable for Preclinical Validation of Therapies in Human Pancreatic Cancer

R Miquel, S Perez-Torras, A Vidal-Pla, V Almendro, L Fernandez-Cruz, S Navarro, J Maurel, N Carbo, P Gascon, A Mazo. Hospital Clinic, IDIBAPS, Barcelona, Spain; School of Biology, UB, Barcelona, Spain.
Background: Pancreatic ductal adenocarcinoma (PDAC) is one of the most lethal cancers due to its high dissemination at early stages together with a bad response to both radio- and chemotherapy. Efforts to find new therapies for human pancreatic ductal adenocarcinoma have not resulted in clear improvements on patient survival. Prognosis is still very poor with a 5 year-median survival of 1-4% and a median survival period

after diagnosis of only 4-6 months. Although a great deal of efforts has been carried out until now, there is still an urgent need to develop new therapies to improve the prognosis of these patients.
Design: This situation has prompted us to generate an in vivo platform of human orthotopic PDAC models by direct implantation of fresh surgical material from human tumor tissue into the pancreas of athymic mice. Tissue microarrays from the primary human tumors and from the xenografted tumors and their consecutive passages were performed. Histological features, immunohistochemical expression of different markers and protein expression and gene status of several tumor supressor genes and EGFR family were compared.
Results: A total of eleven orthotopic xenografts were obtained. Models show stable growth kinetics and representative metastatic behavior. We found a high degree of histological and molecular similarities between patient tumors and the xenografts. Tissue-microarrays studies demonstrate preservation and maintenance of protein expression patterns through passages.
Conclusions: The orthotopic approach we present as a platform established directly from 11 patients offers a good possibility to progress in pancreatic cancer knowledge and treatment. They constitute a useful and worthy preclinical model for further exploring the biological basis of human pancreatic cancer and to draw from them more accurate therapeutic responses with clinical significance.

1627 The Concept of Hepatic Artery-Bile Duct Parallelism in the Diagnosis of Ductopenia in Liver Biopsy Samples

RK Moreira, W Chopp, MK Washington. Columbia University, New York, NY; Vanderbilt University, Nashville, TN.
Background: "Absence of bile ducts (BD) in >50% of portal tracts" is currently the most widely accepted criterion for the diagnosis of ductopenia. The potential use of hepatic artery (HA) branches as landmark structures for a more precise quantitative assessment of interlobular BDs in ductopenic disorders is explored in this study.
Design: In the first part of the study, 500 portal tracts from histologically normal liver resection specimens were studied and a database of morphometric parameters was created. An "unpaired HA" was defined as a) a HA branch of any size within a complete portal tract not accompanied by a BD; b) a HA branch measuring >20 µm in an incomplete portal tract with no BD present within a radius of 10 HA diameters. In the second part, biopsies from patients with hepatitis C, autoimmune hepatitis, steatohepatitis, and post-perfusion liver allograft biopsies (group 1, n=30) were analyzed and the following diagnostic criteria for ductopenia were defined: 1-presence of at least one unpaired HA in ≥10% of all portal tracts; 2-At least 2 unpaired HAs present in different portal tracts in a given sample, regardless of the total number of portal tracts. These criteria were then applied to biopsies from patients with PBC and suspected chronic allograft rejection (group 2, n=32).
Results: HA-BD parallelism was seen in 96.6% of normal portal tracts. The mean HA-BD distance was 4 ± 2.8 HA diameters. BD loss was detected in 59.4% of patients in group 2 by the unpaired HA method compared to 43.7% (P=0.31), 21.9% (P=0.005), and 12.5% (P=0.001) by the traditional method, depending on specific adequacy criteria utilized (no adequacy criteria, >10 portal tracts, or >5 complete portal tracts per biopsy, respectively). The percentage of portal tracts containing BDs was significantly affected by the degree of portal inflammation, fibrosis stage, percentage of complete portal tracts, and biopsy width, while none of these factors influenced the prevalence of unpaired arteries.
Conclusions: The concept of HA-BD parallelism can be used to reliably identify bile duct loss and establish the presence of ductopenia in biopsy samples. The unpaired hepatic artery method described in this study is not influenced by factors that can affect the percentage of portal tracts containing BDs and may be useful in the evaluation of ductopenia, as mild degrees of bile duct loss may be more accurately detected by this method compared to traditional criteria.

1628 Gallbladder Intramural Papillary Mucinous Neoplasm: A New Entity Similar to IPMN of the Pancreas

K Nagata, GY Lauwers, S Murata, M Shimizu. Saitama Medical University, Saitama International Medical Center, Hidaka, Saitama, Japan; Massachusetts General Hospital, Boston, MA.
Background: Intraductal papillary mucinous neoplasms (IPMNs) are classified as one of the pancreatic neoplasms, and recently similar neoplasms have been recognized in the bile duct. These neoplasms show characteristic mucin production, papillary projective growth, and some cyst formation. They have a good prognosis. Pancreatic intraepithelial neoplasia (PanIN) and biliary intraepithelial neoplasia (BilIN) are proposed as a precursor lesion of IPMNs and cholangiocarcinoma, respectively. In the gallbladder, sporadic case reports of these IPMN-like mucin-producing papillary neoplastic lesions are reported, however; no report that examined a series of a preceding lesion, a borderline lesion, or in situ carcinoma has been published. We name these lesions "gallbladder intramural papillary mucinous neoplasm (GB-IPMN)", and examined the mucin expression profiles of the series of hyperplasia/neoplasia, borderline lesion, and carcinoma in situ.
Design: We collected nine suitable cases for this study (three intraepithelial neoplasias, three borderline lesions, and three in situ carcinomas) from the Department of Pathology, Saitama Medical University, Saitama International Medical Center, and Massachusetts General Hospital from 2000 to 2008. The histological classification was made based on the criteria of pancreatic IPMN. One case of intraepithelial neoplasia associated with common tubular adenocarcinoma was also examined. All specimens were fixed in 10% formalin, embedded in paraffin wax, and cut into 4-micrometer-thick serial sections for usual hematoxylin and eosin staining and immunohistochemical staining. Immunohistochemically, MUC1, MUC2, MUC5AC, MUC6, CD10, p53 and MIB-1 were performed.
Results: Characteristically, the series of all intraepithelial neoplasia, borderline lesions, and carcinoma in situ were positive for MUC5AC and MUC6, and were negative for CD10. CD10 was performed by down regulation for the early phase of these neoplastic changes and showed a change which was similar to the PanIN results (Nagata et.al. J Hepatobiliary Pancreat Surg. 2007;14:243-54).
Conclusions: GB-IPMN and its precursor lesions have the same immunohistochemical mucin profiles as PanIN and IPMN of the pancreas. Further study is needed to clarify the significance of these lesions. In addition, a common type of gallbladder cancer derived from GB-IPMN should also be investigated.

1629 Biomarker Profiles Associated with Metastatic Pancreatic Cancer

Y Naito, CA Iacobuzio-Donahue. The Sol Goldman Pancreatic Cancer Research Center, Johns Hopkins Medical Institutions, MD; The Sol Goldman Pancreatic Cancer Research Center, Johns Hopkins Medical Institutions, Baltimore, MD.
Background: We recently reported that pancreatic duct adenocarcinomas are represented by two distinct subtypes, *locally destructive* pancreatic cancer and *widely metastatic* pancreatic cancer, based on their significantly different patterns of failure and metastatic burden encountered at autopsy (Iacobuzio-Donahue et al. JCO 2009). These divergent patterns of failure found at autopsy were unrelated to clinical stage at initial presentation, treatment history, or histopathologic features. Our current goal is to characterize the biomarker profiles characteristic of these two biological subtypes of pancreatic cancer using a high-throughput immunohistochemical approach.
Design: Primary and metastatic cancer tissues from 36 patients who underwent a rapid autopsy in association with the Gastrointestinal Cancer Rapid Medical Donation Program were used to construct a tissue microarray (TMA) containing 208 cores (4 cores per patient). IHC was used to evaluate the expression of 30 biomarkers related to the cytoskeleton, apomucins, tumor antigens, stroma, adhesion, proliferation, cell cycle, Wnt signaling, TGF-beta signaling, Kras signaling, and PTEN signaling. Labeling patterns were correlated to patterns of failure, primary versus metastatic site, and metastatic burden.
Results: At diagnosis, the majority of carcinomas (21/36, 58%) were located in the pancreatic head and the average tumor diameter was 5.6±2.8cm. The overall survival for all patients was 7.5±23.2 months. At autopsy, 13 patients had locally destructive pancreatic cancer and 23 had widely metastatic pancreatic cancer. There were no significant differences in labeling for any marker between matched primary and metastatic samples. However, distinct differences in labeling patterns were noted in association with increasing metastatic burden, in that labeling for vimentin, mesothelin, phospho-MAPK and nuclear beta-catenin was more pronounced in widely metastatic pancreatic cancers, whereas, labeling for DPC4 and cyclin D1 were lost in these same cancers relative to locally destructive pancreatic cancers.
Conclusions: A limited panel of biomarkers may have value in classifying pancreatic cancers based on their most likely pattern of disease progression. These markers also highlight avenues for investigation into the fundamental features associated with metastatic spread.

1630 HCV 3 Trial: Recurrent Hepatitis Histologic Grade on Day 90 Biopsy Predicts Subsequent HCV Stage at One and Two Years Post Transplantation

GJ Netto, GB Klintmalm, CG Fasola, L Jennings, The HCV 3 Group. Johns Hopkins, Baltimore; Baylor University Med Ctr, Dallas.
Background: HCV induced cirrhosis is a main indication for liver transplantation (OLT) in the U.S. Graft survival in HCV patients has not improved in the past decade due to progressive disease recurrence . Better immunosuppressive (IS) regimens could delay progression of recurrent HCV and improve outcome.
Design: The HCV3 randomized prospective multicenter trial compared safety and efficacy of 3 IS regimens in 312 HCV-positive OLT recipients. Arm 1 received tacrolimus (Tac) plus corticosteroids (n=60); arm 2, mycophenolate mofetil (MMF), Tac, and corticosteroids (n=79); and arm 3, MMF, Tac, and daclizumab(n=153). Pts were followed for 2 years. Per protocol, liver biopsies were performed at days 90, 365 and 730. ACR was graded according to Banff schema and HCV recurrence according to Batts and Ludwig classification. All biopsies were reviewed by a central hepatopathologist. Primary endpoints were ACR (grade =>2 + rejection activity index => 4) and, HCV recurrence (stage => 2 at day 365, stage => 3 at day 730 or grade 3 at anytime).
Results: At 2 years F/U, no significant difference in pts survival, graft survival, serum HCV-RNA, incidence of adverse events or ACR was seen among the three arms. The same was true for overall incidence of HCV recurrence as defined by primary end point criteria. Among pts who remained HCV stage =<2 during first year, statistically significant increase in rate of HCV progression to stage 3 or more was seen in arms 1 & 2 (steroid exposure) compared to steroid free arm 3 pts. In patients with HCV stage =<2 during 1st year, freedom from stage 3 or more HCV recurrence at 2 year was: 75%, 85% and 93% respectively ($p<0.01$). The difference remained significant when grouping Arm 1 + 2 (steroid) vs. 3 (no -steroids): 80% vs. 93% ($p=0.01$) and Arm 1 (no-MMF) vs. 2 + 3 (MMF): 75% vs. 90% ($p<0.01$). Furthermore, grade 2-4 histologic grade of HCV recurrence at day-90 biopsy was a strong and significant predictor of stage 3-4 HCV recurrence both at one year (43% vs 11%; $p<0.0001$) and two year follow up (36% vs 20%; $p<0.005$) biopsies.
Conclusions: The choice of immunosuppression may affect the development of advanced fibrosis resulting from recurrent HCV. Steroid-free IS (arm 3) is safe and effective and showed a significant advantage in freedom from stage 3 or more post OLT HCV recurrence. Presence of grade 2-4 recurrent HCV in day 90 biopsy predicted subsequent higher stage HCV recurrence at 1 and 2 years post OLT.

1631 Proliferation of CD163+ Spindle-Shaped Macrophages in IGG4-Related Sclerosing Disease: Analysis of Lymphoplasmacytic Sclerosing Pancreatitis and Sclerosing Sialadenitis

K Notohara, Y Wani, M Fujisawa. Kurashiki Central Hospital, Kurashiki, Japan; Himeji Red Cross Hospital, Himeji, Japan.

Background: To date, types of lymphocytes and plasma cells have been highlighted as a cause of IgG4-related sclerosing disease, but little has been discussed on the role of macrophages.

Design: Resected specimens from 15 patients with lymphoplasmacytic sclerosing pancreatitis (LPSP) and 9 with IgG4-related sclerosing sialadenitis (ISS) were immunostained for CD163, CD68, α-smooth muscle actin (SMA) and IgG4. For comparison, idiopathic duct-centric chronic pancreatitis (IDCP; 2 patients), pancreatic ductal carcinoma (PDC; 10) and sialolithiasis-associated sialadenitis (SAS; 10) were studied simultaneously.

Results: In LPSP and ISS, numerous CD163+ macrophages were observed throughout the lesion, except for two cases. Most of them were spindle-shaped, and were different from those macrophages with abundant cytoplasm. Thus they morphologically resembled mesenchymal cells. Compared to typical myofibroblasts, however, they were more slender and possessed a smaller nucleus. CD163+ spindle-shaped macrophages tended to be clustered and showed a storiform growth pattern in storiform fibrosis, heavily inflamed lobules and pancreatic periductal inflammation. Lymphocytes and plasma cells, including those with IgG4 expression, were admixed with the CD163+ macrophages. Proliferation of SMA+ myofibroblasts with fibrosis was, on the other hand, confined to areas with scarce inflammatory cells, and were absent in foci with abundant CD163+ macrophages. Typically, the more intense lymphoplasmacytic infiltration was in each case, the more CD163+ cells and the less SMA+ cells were found. In two cases (one each of LPSP and ISS) with scarce CD163+ cells, the inflammation was entirely regressive. Nevertheless, small foci with numerous CD163+ cells were focally identified in these cases. Immunostaining for CD68 labeled only a portion of CD163+ macrophages. In IDCP, PDC and SAS, CD163+ spindle-shaped macrophages were fewer and dispersed mainly around the lobules and in fibrosis. However, in one case of PDC with LPSP-like reaction, the distribution of CD163+ cells was similar to LPSP.

Conclusions: CD163+ spindle-shaped macrophages are one of the major inflammatory components of LPSP and ISS, and contribute to forming the unique histology of ISD, such as storiform fibrosis. The proliferation of CD163+ macrophages seen in ISD is unique, and thus CD163 could be a useful marker for the histological diagnosis of ISD.

1632 Bile Duct Colonization by Metastatic Tumor: A Potential Mimic of Cholangiocarcinoma

ML Othman, SC Abraham. MD Anderson Cancer Center, Houston.

Background: Distinction between primary and metastatic carcinoma in the liver has important therapeutic implications. The presence of an "in situ" intraductal growth pattern is often taken as evidence of primary cholangiocarcinoma (CCA), but metastatic colorectal carcinoma (CRC) can occasionally exhibit colonization of biliary epithelium and thereby mimic CCA. The frequency of this pattern and its occurrence with other metastatic tumors are unknown.

Design: We reviewed diagnostic reports and gross descriptions of all liver resections for metastatic tumor between 1997-2009 to identify cases with any suggestion of bile duct involvement. Histologic sections were scored for the following: extent of intrabiliary growth, colonization of biliary epithelium, size of largest involved duct, and duct obstructive histology in non-neoplastic parenchyma. Radiologic findings and liver chemistries were obtained from the computerized medical records.

Results: There were 1072 hepatic resections for CRC and 425 for other metastases (Table 1). Intrabiliary growth was present in 35 (3.3%) CRCs, and colonized biliary epithelium in an apparent "in situ" growth pattern in 28 (85%) of 33 cases with available histologic sections. Intrabiliary growth was focal in 14 (40%) and prominent in 21 (60%); 3 of the latter had predominant intrabiliary tumor with very little stromal invasion. Four cases radiologically mimicked CCA. In contrast to CRC, only 3 (0.7%) of the other 425 metastatic tumors showed intrabiliary growth (p=0.003) (pancreatic endocrine carcinoma, breast carcinoma, and GIST; both breast and endocrine tumors also colonized biliary epithelium).

Conclusions: At least 3% of metastatic CRCs show intrabiliary growth and some have extensive colonization of biliary epithelium that can mimic CCA. Intrabiliary growth and epithelial colonization can also occur with other metastases, but this is significantly less common (p=0.003) and should not pose a diagnostic dilemma. In patients with a history of CRC, apparent "in situ" intrabiliary growth does not negate a metastatic diagnosis.

Table 1

Metastatic tumor	Intrabiliary growth	Colonization of biliary epithelium	Largest involved duct (mean, range)	Obstructive changes in peripheral liver	Biliary abnormalities by radiology	Alkaline phosphatase elevation
CRC (n=1072)	35 (3.3%)	28 of 33 (85%)	0.4 cm (0.01-2.0)	18 of 32 (56%)	18 of 35 (51%)	16 of 35 (46%)
Other (n=425)*	3 (0.7%)	2 of 3 (67%)	0.8 cm (0.02-1.5)	0 of 2 (0%)	1 of 3 (33%)	1 of 3 (33%)
	p=0.003					

*Carcinoma (312), sarcoma (90), melanoma (23)

1633 Perivenular Biliary Metaplasia of Hepatocytes and Not a Periportal Ductular Reaction Correlates with a Cholestatic Liver Chemistry Profile in Patients with Hepatic Venous Outflow Obstruction

RK Pai, J Hart. Washington University, St. Louis; Univ. of Chicago, Chicago.

Background: Patients with venous outflow obstruction often have an unexpected cholestatic pattern of liver chemistry tests. Elevations in alkalaine phosphatase and bilirubin 2 to 5 times normal is not unusual. Kakar et al recently described portal changes in patients with outflow obstruction (Mod Path 2004 17:874). In this study ~50% of patients had evidence of a bile ductular reaction. However, no patient had evidence of biliary tract disease. They argued that such changes could account for the cholestatic profile. However, it is unclear if a ductular reaction can explain the cholestatic profile in all patients with outflow obstruction.

Design: 22 needle liver biopsies from patients with congestive heart failure were analyzed histologically and immunohistochemically for CK7. Histologic parameters were degree of sinusoidal dilatation, fibrosis, ductular reaction, and portal inflammation. The patient's liver chemistry tests at the time of biopsy was recorded.

Results: We found that 32% of patients (7 of 22) had histologic evidence of mild periportal ductular reaction. A CK7 immunostain demonstrated a subtle periportal ductular reaction in two additional cases. Strikingly, the CK7 immunostain also demonstrated prominent biliary metaplasia of perivenular hepatocytes in the majority of cases (focal zone-3 in 11, diffuse zone-3 in 3, and diffuse zones-3 and -2 in 5 patients). The presence of a periportal ductular reaction did not correlate with a cholestatic liver chemistry profile (Table 1). However, the degree of sinusoidal dilatation as well as perivenular biliary metaplasia was a strong predictor of a cholestatic profile.

Correlation with cholestatic chemistry tests in patients with outflow obstruction

Category	N	Bilirubin	Alkaline Phosphatase	AST	ALT
All patients	22	2.15	169	40	39
Sinusoidal dilatation					
Zone 3	7	1.54	149	64	43
Zones 2-3	8	1.83	175	31	37
Zones 1-3	6	3.33	183	27	37
Biliay metaplasia					
Zone 3 (focal and diffuse)	14	1.90	169	30	40
Diffuse Zones 2-3	5	3.90	193	18	27
Ductular reaction	9	2.10	147	26	39

Conclusions: In patients with outflow obstruction there can be marked biliary metaplasia of hepatocytes in zones 2 and 3. Biliary metaplasia and sinusoidal dilatation predict a cholestatic liver chemistry profile. The etiology of the biliary metaplasia is unclear, but may represent a response to an injury to the canalicular system due to compression of the hepatic plates by impairment of blood flow.

1634 Histologic and Clinical Features of Patients with Chronic Hepatitis C with Autoimmune Features

RK Pai, M Westerhoff, E Jenkins, H Te, J Hart. Washington University, St. Louis; Univ. of Chicago, Chicago.

Background: Detailed histologic features of patients with chronic hepatitis C (HCV) and superimposed autoimmune features (HCV+AIH) have not been described in a large series. Furthermore, no study has analyzed the outcome of these patients following therapy (antiviral or immunosuppression). In this study we compared patients with HCV+AIH with those with pure HCV and pure AIH.

Design: Patients with HCV+AIH based on histology and autoimmune markers (+ANA or +ASMA) from 1999 -2008 were identified from the liver and pathology databases (n=28). HCV alone patients matched for age, gender, and race served as controls (n=49). Of the 22 HCV patients tested for ANA, 9 had low titer positivity. Pure AIH patients (n=38) with pretreatment biopsies were also identified. Clinical and laboratory data were collected. Cases were blindly graded and staged (Batts and Ludwig) by 2 pathologists. Other histologic variables recorded included degree of plasma cell and eosinophil infiltrates, and the presence of lymphoid aggregates, steatosis, and rosetting.

Results: Histologic characteristics of HCV, HCV+AIH and AIH patients are shown in Table 1. Patients with HCV+AIH had advanced fibrosis and extensive interface activity compared with HCV patients. Mean HCV RNA (million IU/ml) in HCV+AIH and HCV patients was 1.5+/-0.2 and 2.5+/-0.4 respectively. Baseline ALT (IU/ml) was higher in HCV+AIH patients compared with HCV controls: 140+/-120 versus 62+/-69. 27 HCV+AIH patients underwent therapy (15 IFN-based, 8 IFN+immunosuppression, and 4 immunosuppresion alone). Of the 23 patients who underwent IFN-based therapy, 6 had complete viral eradication with few immune side effects.

Histologic characteristics of patients with CHC, AIH, and CHC+AIH

	HCV (% of patients)	AIH (% of patients)	HCV+AIH (% of patients)	p-value (HCV vs. HCV+AIH
Grades 3-4	6	78	75	p<0.001
Stages 3-4	2	12	39	p<0.001
Plasma cells (≥2+)	4	72	50	p<0.001
Eosinophils (≥2+)	8	22	29	p=0.02
Rosettes	2	34	11	p=0.13
Lymphoid aggregates	63	31	86	p=0.06

Conclusions: HCV+AIH is a distinct entity with greater necroinflammatory activity, ALT and fibrosis compared to patients with HCV alone. The presence of grade 3-4 necroinflammatory activity and/or a prominent portal infiltrate of plasma cells should prompt the pathologist to report the possibility of HCV+AIH and recommend a serum ANA to confirm the diagnosis. IFN-based therapy leads to viral eradication in 26% of cases with few immune-mediated side-effects.

1635 Selected MicroRNAs May Aid the Preoperative Diagnosis of Pancreatic Adenocarcinoma

NC Panarelli, RK Yantiss, XK Zhou, N Kitabayashi, Y-T Chen. Weill Cornell Medical College, New York, NY.

Background: Pancreatic carcinomas show altered expression of microRNAs (miRNAs). They often overexpress miR-21, -181b, -221, and -196a, but show decreased levels of miR-217. In this study, we investigated the expression of these five miRNAs in cytologic preparations obtained from fine needle aspirations to evaluate their utility in distinguishing adenocarcinoma from benign pancreatic lesions in limited samples.

Design: Cell block specimens from 38 clinically, or surgically, confirmed pancreatic adenocarcinomas and 11 benign pancreatic lesions, including chronic pancreatitis and pseudocysts, were analyzed for miRNA expression and normalized with small RNA U6

endogenous controls using quantitative RT-PCR. Mean miRNA expression levels, both individually and in combinations, were statistically compared between the cytologically malignant and benign groups, and fold differences were calculated. A logistic regression model that best distinguished these two groups was used to classify cases originally interpreted as suspicious for malignancy.
Results: Successful miRNA amplification was achieved in all 11 benign lesions and 35/38 cancers. The preoperative cytologic diagnoses of these 35 cases were carcinoma (26) and suspicious for carcinoma (9). The 26 cases diagnosed as carcinoma showed overexpression of miR-21 ($p<0.001$), -221 ($p<0.01$), and -196a ($p<0.001$) compared to the 11 benign lesions [fold change range: 9.45 (miR-196a) to 3.73 (miR-221)]. Combined evaluation of these three miRNAs significantly discriminated between carcinoma and benign lesions ($p<0.001$) with a 180-fold difference. Expression of miR-181b and -217 was statistically similar among benign and malignant groups. Based on these results, a logistic regression model [miR-221 + 2 x miR-196a] was generated, which would accurately predict 24/26 (92%) carcinomas as malignant and 8/11 (73%) benign cases as non-malignant. When applied to cases suspicious for carcinoma, the model correctly classified 8 of 9 (89%) as malignant.
Conclusions: Most pancreatic aspirates yield sufficient miRNA for analysis. Carcinomas show significant overexpression of miR-21, -221, and -196a compared to benign pancreatic lesions. Our logistical regression model accurately predicts the presence of carcinoma in non-diagnostic samples, suggesting that miRNA analysis may be a useful adjunct to the preoperative evaluation of pancreatic lesions.

1636 MicroRNA Analysis May Help To Identify High-Grade Dysplasia in Intraductal Papillary Mucinous Neoplasms

NC Panarelli, Y-T Chen, XK Zhou, RK Yantiss. Weill Cornell Medical College, New York, NY.
Background: Intraductal papillary mucinous neoplasms (IPMNs) are dysplastic pancreatic cystic lesions that show a spectrum of epithelial cell dysplasia ranging from minimal atypia to carcinoma in situ and, importantly, may precede some invasive pancreatic ductal carcinomas (PDCAs). IPMNs with mild or moderate dysplasia are often clinically followed, whereas those with severe dysplasia are generally resected due to perceived cancer risk. Unfortunately, the preoperative classification of IPMNs may be hampered by limited material and/or superimposed inflammatory changes present in biopsy samples. Therefore, molecular markers that aid the distinction between low- and high-risk IPMNs are needed.
Design: We evaluated microRNA (miRNA) expression in IPMNs and PDCAs using microarrays and subsequent quantitative RT-PCR for validation. RNA was extracted from paraffin-embedded tumor sections (8 IPMNs and 8 PDCAs) and subjected to the Luminex microarray assay to identify differentially expressed miRNAs. The expression of selected miRNAs was then analyzed in low-grade (mild-to-moderate dysplasia, n=14) and high-grade (severe dysplasia, n=9) IPMNs. PDCAs (n=4) were analyzed as a control group. Median miRNA expression levels were recorded for each group and the results were statistically analyzed.
Results: Analysis of microarray data revealed higher expression of miR-21 and -155 among PDCAs compared to IPMNs, and these results were confirmed by qRT-PCR ($p=0.01$ and 0.02, respectively). The Luminex assay also revealed higher expression of miR-375, -494, -542-3p, and -363 in IPMNs relative to PDCAs, but qRT-PCR confirmed higher expression of only miR-375 ($p=0.07$). Pair-wise comparisons between the groups showed higher miR-375 expression in low-grade IPMNs compared to both high-grade IPMNs ($p=0.06$) and PDCAs ($p=0.05$). Although expression of miR-21 and miR-155 was increased in PDCAs compared to IPMNs, low- and high-grade IPMNs showed similar expression of these markers.
Conclusions: Pancreatic ductal carcinomas show significantly higher expression of miR-21 and -155 compared to IPMNs, indicating that these biomarkers may aid detection of early carcinoma in cystic pancreatic lesions. Expression of miR-375, a microRNA normally found in non-neoplastic pancreas, was higher in low-grade IPMNs than high-grade dysplasia and invasive carcinoma, suggesting that miRNA analysis may also aid the preoperative classification of IPMNs.

1637 Histological Analysis of Liver Biopsies in Primary Sclerosing Cholangitis and Comparison to Primary Biliary Cirrhosis: Identification of New Biliary Lesions Useful for Sclerosing Cholangitis Diagnosis and Scoring Proposal

M-T Paoletti, P-Y Boelle, C Corpechot, O Chazouilleres, D Wendum. APHP, Hôpital StAntoine, Paris, France.
Background: The diagnostic bile duct lesion of primary sclerosing cholangitis (PSC) associates periductal fibrosis, atrophy of bile cells and sometimes replacement of the duct by a fibrous scar. However, these lesions are infrequent on biopsies and the distinction between PSC and primary biliary cirrhosis (PBC) on histological appearance may be difficult. We analyzed several lesions in PSC and PBC in order to specify the lesions observed in PSC and to find the most useful criteria for the pathological diagnosis of PSC.
Design: 59 liver PSC and 71 PBC biopsies were studied. Patients with cirrhosis or associated auto-immune hepatitis were excluded. The following lesions were assessed in each portal tract : periductal fibrosis, biliary cell vacuolization, biliary cell atrophy, bile duct stenosis,bile duct irregularity, floating cells in the bile duct lumen, cholangitis. Activity, fibrosis, ductopenia and granulomas were also assessed on each biopsy. A statistical analysis was performed (Student's-t or Fisher's exact test, logistic regression).
Results: The PSC and PBC biopsies were comparable according to the length or fibrosis stage. Compared to PBC, PSC biopsies showed more often periductal fibrosis ($p<0.0001$), biliary cell atrophy ($p<0.0001$), irregular bile duct lumen ($p=0.0005$), floating cells ($p=0.001$), stenosis ($p=0.002$) and biliary cell vacuolization ($p=0.02$). PSC biopsies showed less often ductopenia ($p=0.0003$), activity ($p<0.0001$) and granulomas ($p<0.0001$). Only 21 biopsies showed the typical lesions with both periductal fibrosis and cell atrophy. Moreover, for each bile duct analyzed individually, there was no correlation between the presence of concentric fibrosis and cell atrophy. On the contrary there was an association between concentric fibrosis and an irregular lumen ($p<0.0001$), the presence of floating cells ($p<0.0001$) or cell vacuolization ($p=0.02$). Finally a score was build to discriminate PSC from PBC. ROC curves showed an area under the curve of 0.93, and a specificity of 97% and sensitivity of 77% for PSC diagnosis if the score was >6.
Conclusions: We found some new biliary lesions associated with concentric bile duct fibrosis and with PSC diagnosis. We also build a scoring system that could be useful to discriminate PSC from PBC on a liver biopsy.

1638 Hepatocellular Carcinoma Arising from Hepatocellular Adenomas: A Clinico-Pathological Analysis

V Paradis, N Ferreira, S Dokmak, J Belghiti, P Bedossa, O Farges. Beaujon Hospital, Clichy, France.
Background: Regenerative nodules are the underlying pathological conditions of hepatocellular carcinoma (HCC) in patients with cirrhosis. Hepatocellular adenoma (HA) may also transform into HCC without underlying liver disease. The objective of this study was to describe the main clinico-pathological characteristics of a series of HCC arising on HA in order to identify potential risk factors.
Design: Among 218 patients who had undergone liver resection with a pathological diagnosis of HA, 25 had features of malignant transformation. Macroscopic and microscopic features of the tumor (number, size of the overall tumor and HCC part, differentiation, presence of vascular invasion and hemorrhage / necrosis) and non tumoral liver were noted .
Results: Among the 25 patients, 17 were men (68%) and 8 were women (mean age 48 years). In 4 patients, multiple HA were present, 2 with adenomatosis. Metabolic syndrome was noted in 5 patients, all men. Mean size of the overall tumor was 11 cm (3-19), with 10.7 cm in males and 12.4 cm in females. Malignant transformation appeared as either single macroscopic nodule in 8 cases or as multiple microscopic foci in 17 cases. HCC was well-differentiated in 22 cases. In 3 cases, vascular invasion and/or satellite nodules were observed. Macroscopic foci of hemorrhage were present in 14 tumors (58%), and necrotic changes in 1 case. HA subtyping showed 13 telangiectatic, 7 unclassified, 3 with cell atypias, 1 steatotic and 1 indefinite. 8 tumors (32%) displayed a nuclear beta-catenin immunostaining suggestive of beta-catenin mutations (including 3 with cell atypias, 4 telangiectatic and 1 unclassified). All nuclear beta-catenin positive tumors were observed in males. Whereas size of the lesion was not significantly different between men and women, pattern of malignant transformation was different according to sex with a predominant microscopic multifocal form observed in males (82% vs 37%). Non tumoral liver displayed lesions consistent with NAFLD in 9 cases (36%) with no cases of significant fibrosis.
Conclusions: This series confirms the higher prevalence of malignant transformation in HA in males with telangiectatic subtype as the main risk factor. Malignant transformation occurs via 2 ways of progression, through a multifocal microscopic pattern predominantly observed in men and a macroscopic pattern predominantly observed in women. The relatively low prevalence of beta-catenin mutations indicates its poor predictive value as a malignant marker.

1639 Clinicopathologic Analysis of Cystic Ductal Adenocarcinoma of Pancreas – Neglected Variant of Pancreatic Ductal Adenocarcinoma

HJ Park, JY Kim, KT Jang. Samsung Medical Center, Sungkyunkwan University School of Medicine, Seoul, Korea.
Background: Pancreatic ductal adenocarcinoma usually present as a solid tumor and it is rare that pancreatic ductal adenocarcinoma presents as predominantly cystic tumor. Although there are some case reports of cystic ductal adenocarcinoma (CDA) of pancreas, little is known about the clinicopathologic characteristics of CDA.
Design: We reviewed surgically resected pancreatic ductal adenocarcinoma from 1996 to 2009. We found 8 cases of CDA, presenting as predominantly cystic tumor in preoperative radiological evaluation and pathologic gross examination. The main differential diagnoses of CDA are mucinous cystadenocarcinoma, cancer associated pseudocyst, and retention cyst. Mucinous cystadenocarcinoma was differentiated by absence of ovarian stoma. Retention cyst and pseudocyst were ruled out by identification of cyst lined mucosal carcinoma in CDA.
Results: Of 295 pancreatic ductal carcinomas, 8 (2.7%) showed predominantly cystic tumor in preoperative radiological evaluation and pathologic gross examination. Preoperative impressions were mucinous cystic neoplasm, intraductal papillary mucinous neoplasm, or cancer associated pseudocyst. Six patients were female and 3 were male. Mean age was 68 yrs (39-78). Median size of CDA was 9 cm (3.5-15). The locations of CDA were 6 tail, 2 head, and 1 body, respectively. We found 3 different mechanism of cystic change of CDA; central necrosis, cystic dilatation, and pseudocyst-like change. In the mean follow-up period of 12 months (8-20), 7 patients showed tumor recurrence, including peritoneal carcinomatosis and distant metastasis to liver and brain. All 7 patients showed an increased serum CA 19-9 at recurrence and metastasis. Five patients died of disease.
Conclusions: CDA could be made by either each mechanism of central necrosis, cystic dilatation, pseudocyst-like change or combination of mechanisms. Although it is rare, pancreatic ductal adenocarcinoma may present as predominantly cystic tumor. CDA should be differentiated with mucinous cystadenocarcinoma by careful identification of ovarian stroma. Also CDA could be differentiated with cancer related pseudocyst or retention cyst by careful gross and microscopic examination of cyst lining epithelium. Because CDA is not well known to radiologist, clinicians and pathologist. CDA may be overlooked in preoperative radiologic evaluation and pathologic diagnosis. Pathologist should avoid an erroneous diagnosis of CDA as mucinous cystadenocarcinoma or cancer associated pseudocyst or retention cyst.

1640 Pdx1 Expression in Precursor Lesions and Neoplasms of the Pancreas

JY Park, SM Hong, M Goggins, A Maitra, RH Hruban. Johns Hopkins Hospital, Baltimore, MD.

Background: Pdx1 is a homeobox transcription factor required for the development of both the endocrine and the exocrine pancreas. In both animal models as well as in humans, Pdx1 has previously been shown to become restricted to the islets of Langerhans in adult life. However, Pdx1 has been reported to be expressed in some pancreatic ductal adenocarcinomas. Our goal was to characterize the expression of Pdx1 in intraductal papillary mucinous neoplasms (IPMNs), pancreatic intraepithelial neoplasia (PanIN), acinar cell carcinomas (ACCs), pancreatic endocrine neoplasms (PENs), solid pseudopapillary neoplasms (SPNs), invasive ductal adenocarcinomas (IDAs) and non-dysplastic ductal epithelium.

Design: The anti-hPdx1 (clone 267712) mouse monoclonal antibody to Pdx1 (R&D Systems, Minneapolis, MN) was used to examine 12 tissue microarrays containing 655 tissue cores from 322 patients. Tissue microarrays were created from formalin-fixed paraffin-embedded tissue sections from the surgical pathology archives. The microarrays have cores representing the following tissue types: IPMN (n=88), IDA (n=69), PanIN (n=32), ACC (n=2), PEN (n=44), SPN (n=8), invasive ductal adenocarcinoma (n=70), and non-dysplastic ductal epithelium (n=74). Immunohistochemical labeling for Pdx1 was performed using standard methods, and scored for the intensity of nuclear labeling (0, 1+, 2+) as well as the distribution of positive labeling in each tissue type (0=0%, 1=1-25%, 2=26-50%, 3=51-75%, 4=76-100%). A composite score was created by multiplying the intensity and distribution scores.

Results: Pdx1 expression was seen in non-neoplastic ductal epithelium with a previously undescribed pattern of expression within the putative centroacinar cell compartment. The Pdx1 expression score was significantly higher ($p<0.0001$, ANOVA) in ACC (score, 4.11), non-neoplastic ductal epithelia (2.79), and PanIN (2.44), compared to PEN (1.87), IPMN (1.72), IDA (0.99), and SPN (0.40). By subgroup analysis, IPMN cases with mild dysplasia (1.43) had significantly lower ($p=0.002$, ANOVA) expression than non-neoplastic ducts (2.79).

Conclusions: This is the first study to demonstrate the expression of Pdx1 in non-neoplastic ductal epithelium as well as in pancreatic ductal carcinoma precursor lesions (PanIN and IPMN). The results of the present study imply that the capacity for Pdx1 expression in ductal epithelium is not lost after embryologic development. Taken together these results indicate the possibility of a larger role for Pdx1 in pancreatic tumorigenesis.

1641 Sclerocalcifying Cholecystitis (SclCC) and Associated Carcinomas: Characterization of a Clinicopathologically Distinct and Challenging Entity

S Patel, O Tapia, JC Roa, A Cakir, N Dursun, O Basturk, D Akdemir, S Bandyopadhyay, J Sarmiento, I Coban, NV Adsay. Emory, GA; U de La Frontera, Temuco, Chile; NYU, NY; Ohio Northern, OH; WSU, MI.

Background: There are no systematic analyses in the pathology literature of cholecystitis(CC) with extensive sclerosis & calcifications(calcs). We have seen examples of carcinoma(CA) associated with these patterns, which typically presented as a diagnostic challenge.

Design: 3625 consecutive cholecystectomies were systematically analyzed. Separately, consultation & institutional files were also reviewed for cases designated as sclerotic, calcifying or porcelain.

Results: ***SclCC (n=68):*** Incidence in cases systematically reviewed=1.5%(53/3625). F/M=4/1. Mean age=57(*vs* 47 in ordinary CC; $p<0.001$). Characterized by dense, paucicellular fibrosis transforming GB wall into a relatively thin & uniform band and diffusely replacing most(>80%) of the normal structures such that only minimal/none mucosa or muscularis is identifiable. 75% were associated with calcs. ***CA arising in SclCC (n=38):*** F/M=4.4/1. Mean age=62(*vs* 57 in non-cancerous SclCC; $p=0.04$). Carcinomatous glands were well-masked by hyalinization; widely separated, typically spanning into a very large zone and often circumferentially involving the GB wall without forming any localized thickening(mean wall thickness=2.64 mm in *SclCC-associated CA vs* 3.92 mm in *usual CA*; $p=0.002$). Clear cytoplasm, dyspolarized atypical nuclei, washed-off chromatin & irregular contours distinguished these from benign glands. Surface epithelium was entirely denuded in most areas with rare clinging CIS cells. The epithelium of inv glands was also commonly attenuated/denuded, leaving only the necrotic luminal debris as the sole sign of invasion. In many areas, this debris imperceptibly transformed into the hyalinized stroma, suggesting a regression phenomenon akin to that in melanomas. 3 and 5-yr surv were 15% and 15%, respectively(*vs* 36% and 30% for usual CA; $p<0.05$).

Conclusions: *SclCC* is the name we propose to employ for this distinctive type of CC, which is seen in patients a decade older than ordinary CC patients, suggesting long-standing injury in its pathogenesis. *CAs arising in SclCC* are highly subtle and challenging due to their insidious pattern. They are virtually undetectable grossly; careful sampling is warranted. Conventional staging parameters are difficult to apply due to the effaced layering of the GB wall. Overall prognosis appears to be even worse than that of *usual CA*.

1642 A Novel Histologic Scoring System Accurately Identifies Regressed Cirrhosis in Patients with Chronic Viral Hepatitis Otherwise Understaged by Both Conventional Histological Fibrosis Staging and Serological Markers of Hepatic Fibrosis

V Pattullo, SE Fischer, JJ Feld, DK Wong, M Guindi. University of Toronto, Toronto, ON, Canada.

Background: Cirrhosis may be diagnosed histologically despite fibrosis regression when there is evidence of parenchymal remodelling (PR); hepatoma complicates both overt and regressed cirrhosis. The aim of this study was to evaluate a novel scoring system to identify regressed cirrhosis in the absence of overt advanced fibrosis in liver biopsies of patients with chronic viral hepatitis.

Design: Patients with compensated chronic hepatitis B (CHB) and C (CHC) who had a liver biopsy as well as Fibrotest and APRI were identified from a clinical database. Corresponding clinical measures were recorded (serum albumin, coagulation profile, platelets, serum IgG, splenomegaly, varices and radiological features of portal hypertension). Hepatic fibrosis (Ishak criteria) was scored by 2 blinded pathologists. Cases were categorised as overt cirrhosis (Ishak stage 6, or stage 5 with wide fibrous septa), cirrhosis by parenchymal remodelling (cirrhosis-PR), or no cirrhosis (Ishak stage <5 without PR). Qualitative features of regression were recorded for each case to derive a regression score out of 12. A ROC curve was derived to determine the optimal cut-off regression score which distinguished cirrhotics from non-cirrhotics.

Results: 184 biopsies (79 CHB and 105 CHC) were reviewed (mean biopsy length 2.5+/-0.9cm, mean number portal tracts 21.1+/-7.5). Histological diagnoses of overt cirrhosis (45), cirrhosis-PR (21) and no cirrhosis (118) were made. Fibrotest was significantly higher in overt cirrhosis than no cirrhosis (0.57 vs 0.39, $p<0.01$), numerically higher in overt cirrhosis compared to cirrhosis-PR (0.57 vs 0.48, $p=0.15$), but failed to distinguish cirrhosis-PR from no cirrhosis (0.48 vs 0.39, $p=0.15$). Similarly, APRI, and clinical measures failed to distinguish cirrhosis-PR from no cirrhosis. Mean regression scores in overt cirrhosis (7.82) and cirrhotic-PR (7.52) were higher than that of the non-cirrhotics (2.68, $p<0.0001$). A cut-off regression score of ≥5 yielded the highest accuracy for diagnosis of cirrhosis (accuracy 83.4%, sensitivity 93.3%, specificity 79.7%, AUROC 0.9036).

Conclusions: Cirrhosis may be present without histologic evidence of overt advanced fibrosis or clinical evidence of cirrhosis. The histologic hepatic fibrosis regression score accurately identifies patients with regressed cirrhosis whereas Fibrotest and APRI do not.

1643 Hepatic Fibrosis Regression in the Setting of Persistent Viremia in Chronic Hepatitis C: A Dual Biopsy Study

V Pattullo, EJ Heathcote, M Guindi. University of Toronto, Toronto, ON, Canada.

Background: To identify predictors of hepatic fibrosis regression and determine the relationship between body mass index (BMI) and hepatic fibrosis regression by both quantitative and qualitative measures.

Design: All patients in clinic with chronic hepatitis C (CHC) without contraindications routinely undergo pretreatment liver biopsy. Patients with 2 liver biopsies between Jan 1991 and Dec 2008 were eligible for inclusion in this retrospective study. Factors potentially influencing hepatic fibrosis: body weight, body mass index (BMI) and antiviral treatment history and outcome were recorded. Biopsies were scored in a blinded fashion for necroinflammation, fibrosis (Ishak), steatosis, and for 8 qualitative features of fibrosis regression. Regression was defined as ≥2 stage fall in Ishak stage (Reg-I), or <2 stage fall in Ishak stage associated with a rise in qualitative regression score (Reg-Q). Univariate analysis was performed to determine the factors associated with hepatic fibrosis regression.

Results: 159 patients had complete clinical data and evaluable paired liver biopsies were available (genotype 1 81%, BMI 26.7+/- 5.6 kg/m2, treatment naïve 31%, sustained virological response (SVR) 11%). Mean biopsy lengths and were 1.8+/-0.6cm and 2.2+/-0.8cm, and mean number of portal tracts 15.8+/-6.2 and 17.6+/-7.2 at first and second biopsies respectively. The mean interval between biopsies was 5.4+/-3.1 years; the interval between SVR and second biopsy was similar to the biopsy interval in the persistently viremic (4.42+/-3.0 vs 5.17+/-2.9 years, $p=0.78$). Regression (by either definition) was noted in 38 patients (23.9%); Reg-I was observed in 12 patients (7.5%), and Reg-Q in 26 patients (16.4%). Age, gender and BMI were no different between the groups. Regression was more likely in patients infected with genotype 2 ($p=0.047$); 3 of 7 patients infected with genotype 2 regressed, 2 of whom had achieved SVR. Regression was observed in 9 of 18 patients (50%) who had achieved SVR but also in 29 of 141 (21%) patients despite persistent viremia ($p=0.003$). Amongst this limited cohort of persistently viremic individuals, there were no significant predictors of fibrosis regression.

Conclusions: Hepatic fibrosis regression is more likely in patients infected with genotype 2 CHC and in those who have achieved SVR, however hepatic fibrosis regression may also occur in up to 21% of patients in the presence of persistent viremia; further study is required to identify factors predicting regression in this subgroup.

1644 Perihilar Cholangiocarcinoma: S100P Distinguishes Bile Duct Cancer from Cholangiocarcinoma Involving the Hepatic Hilum

F Pedica, L Bortesi, S Pachera, A Guglielmi, I Cataldo, M Chilosi, F Menestrina, G Martignoni, P Capelli. University of Verona, Verona, Italy; University of Verona, Negrar, Verona, Italy.

Background: Cholangiocarcinomas (CC) are classified into intrahepatic, perihilar and distal CC. Based on the anatomical origin, perihilar CC have been further divided into hilar bile duct cancer (BDC) and intrahepatic cholangiocarcinoma involving the hepatic hilus (CCC). BDC is supposed to originate from the epithelium of the common hepatic, right or left hepatic duct, while CCC originates in the intrahepatic bile duct or bile ductules. BDC and CCC have not been immunophenotipically and biologically characterized until now. Recently S100P immunoexpression has been investigated in pancreatic adenocarcinoma, which is known to have morphological similarities to CC. We analyzed S100P expression in CC, focusing on perihilar CC, in particular on BDC and CCC, comparing also to other categories of CC, like intrahepatic and distal types. As controls we investigated hepatocarcinomas (HCC) and liver benign proliferations, such as focal nodular hyperplasia (FNH), biliary adenomas and biliary hamartomas.

Design: We collected 74 cases of CC. As controls we analyzed 20 HCC, 10 FNH, 3 biliary adenomas and 5 biliary hamartomas. In particular, we analyzed 31 intrahepatic CC, 37 perihilar CC and 6 distal CC. Perihilar CC were subdivided into 27 BDC and 10 CCC. Immunohistochemistry was performed using S100P monoclonal antibody (clone

16, diluition 1:1000 BD Biosciences Pharmingen, San Diego) and it was evaluated semiquantitatively.
Results: In the normal liver tissue, hepatocytes and normal intrahepatic bile ducts were negative for S100P. Perihilar were positive in 68% of cases. Moreover, BDC were strongly positive in 85% (23/27 cases), while CCC in 20% of cases (2/10 cases). Positive immunoreactivity for S100P was identified in 100% distal CC, but only in 6% of intrahepatic CC. S100P was positive only in 1 of 20 HCC, while all benign proliferations did not express S100P.
Conclusions: S100P expression distinguishes BDC from CCC and their different immunophenotype may reflect a different biological origin. Moreover, intrahepatic CC and CCC have a similar expression of S100P, which may reflect possible biological similarities. Distinguishing these categories is important because they have different prognosis and distinct biological behaviour.

1645 Evidence-Based Immunohistochemical Panel for the Distinction of Hepatocellular Carcinoma and Metastatic Carcinoma

R Ramachandran, LW Browne, I Mehdi, Y Chen, S Kakar. UCSF, San Francisco; Kaiser, Walnut Creek.
Background: Commonly used markers for diagnosis of hepatocellular carcinoma(HCC) have several limitations. The sensitivity of Hepatocyte Paraffin 1(HepPar) and polyclonal CEA(pCEA) is ~80%, but is low in poorly differentiated cases. Glypican-3(GPC) helps in identification of poorly differentiated HCC, but its specificity is not well established. Adenocarcinoma(AC) markers like MOC31,CK7 and CK19 can be positive in a subset of HCC. Since limited tissue is available in most cases, it is desirable to determine the combination of markers that will yield the highest sensitivity and specificity.
Design: Immunohistochemistry was performed on tissue microarrays generated from 161 HCC, 23 neuroendocrine tumors(NE) and 386 ACs(65 gastroesophageal,6 pancreaticobiliary,55 lung,205 breast,55 colorectal). Three hepatocellular(HepPar,GPC,pCEA) and 5 AC markers(MOC31,CK7,CK19,BerEP4, B72.3,CD15) were evaluated.
Results: HepPar was the most sensitive hepatocellular marker and along with GPC yielded a sensitivity of >95% for HCC. HepPar and GPC were positive in <5% of AC and NE; their combined expression was not seen in any non-HCC case. MOC31 was the most sensitive marker for NE and AC irrespective of site. Addition of CK7 or CK19 to MOC31 increased the sensitivity to 97% for AC and 100% for NE. CK19 had higher sensitivity than CK7 for AC and NE. The characteristic HepPar+/MOC31- phenotype was seen in 71% of HCC. MOC31 was strongly expressed in 13(10%) HCCs; HepPar was negative in 9 of these cases. In 12 of these, CK19 was negative; GPC was positive in 10 of these cases. The addition of GPC and CK19 correctly identified 12 of 13 cases with aberrant HepPar-/MOC31+ immunophenotype.

	HepPar	GPC	pCEA	MOC31	CK7	CK19	BerEP4/B72.3/CD15
HCC	75	70	54	10	2	2	8/1/-
AC	4	5	60	91	67	87	74/83/54
NE	4	0	0	91	9	48	71/13/26

Figures reflect percentages
Conclusions: HepPar and MOC31 are the most sensitive hepatocellular and AC markers respectively. The high sensitivity for AC and NE makes MOC31 a first-choice marker even though 10% of HCC express MOC31. HCC with the aberrant HepPar-/MOC31+ immunophenotype can be mistaken for AC; the addition of GPC and CK19 helps in establishing the correct diagnoses in these aberrant cases. Hence the use of 2 hepatocellular (HepPar,GPC) and 2 AC markers (MOC31,CK19) is recommended. Other markers should be avoided as first-line stains due to their lower sensitivity and specificity.

1646 Impact of Donor Liver Steatosis/Fibrosis Progression on Allograft Outcome in a Cohort of 203 Post Transplant Recurrent Hepatitis C Patients

M Ramineni, M Moeller, K Brown, V Shah. Henry Ford Hospital, Detroit, MI.
Background: Recurrent hepatitis C after liver transplantation progresses faster than hepatitis C in non-transplant settings. Factors such as steatosis and fibrosis are well established in contributing towards worsening of transplant outcome. The aim of this study was to determine the influence of donor graft steatosis and fibrosis progression (FP) on overall outcome in patients who received orthotopic liver transplant for hepatitis C virus induced cirrhosis.
Design: 268 patients were diagnosed with post transplant recurrent hepatitis C from 1999 - 2006 in our institution. 203 patients did not receive any therapy and constituted the cohort for this study to assess the natural progression of steatosis and fibrosis. Pathology records and biopsy slides were reviewed of the 54 patients who developed steatosis/fibrosis (SF group). Donor steatosis was graded as none=1, 0- 5%= 2, 5- 25%=3, 26- 50%= 4, 51- 75%= 5 and 76- 100%= 6. Fibrosis was graded per Metavir scoring as F0= no fibrosis, F1= Portal Fibrosis (PF) without septa, F2= PF with few septa, F3= bridging fibrosis without cirrhosis, F4= cirrhosis. FP rate was calculated in terms of Fibrosis Units (FU): Change in Metavir fibrosis stage/post transplant duration in years. Data was analyzed for allograft failure and retransplantation.
Results: Of the 54 patients in the S/F group, 16(29%) had bridging fibrosis/cirrhosis, 21(39%) had steatosis, 17 had steatosis and fibrosis (32%). The average FP for most patients at their first biopsy was 2.5 FU/year and the average steatosis was 25%. During their last available biopsy most patients had an average FP of 4.2 FU/year and an average steatosis of 15% . Allograft failed in 24 (44%) patients in the S/F group with re-transplantation in 12(22%) patients. Of the re-transplant patients, 5(42%) died in less than 1 year. 7(58%) are surviving after a followup of 2 yrs. Of the 146 patients who were not in the S/F group, 75% of the patients have recurrent hepatitis C with a mean survival of 5.1 years. 16(10%) needed re-transplantation and 48 (32%) died in 3yrs.
Conclusions: 1. The allograft failure related deaths in the S/F group is 1.3 times higher than the non S/F group. 2. The allograft failure in the re-transplant livers accelerated twice faster in patients in the S/F group compared to patients in the non-S/F group. 3. The average fibrosis progression per year (FU=2.5) in recurrent hepatitis C patients in the S/F group is significantly higher than the chronic hepatitis group published in the literature (FU=0.25).

1647 Expression of the Extracellular Matrix Protein Periostin in Liver Tumours and Bile Duct Carcinomas

MO Riener, FR Fritzsche, A Soltermann, H Moch, GO Kristiansen. University Hospital, Erlangen, Germany; University Hospital, Zurich, Switzerland.
Background: Epithelial-mesenchymal transition (EMT) is a process by which an epithelial cell gains features of a mesenchymal cell. EMT enables the cell to migrate more easily which is an important event during malignant tumor progression and metastasis. The periostin protein has been found to be involved in EMT. In different tumor types its expression was noted in tumor cells and/or stromal cells and correlated with increased tumor aggressiveness and reduced overall-survival. Here, we studied the relevance of Periostin, known to be involved in EMT, in hepatocellular and bile duct cancer.
Design: Immunohistochemical Periostin expression was semiquantitatively analyzed in normal liver tissue (n=20), hepatocellular carcinoma (HCC; n=91), liver-cell adenoma (n=9), focal nodular hyperplasia (n=13) and bile duct carcinomas (BDC; n=116) using tissue microarrays.
Results: Normal bile ducts, gall bladder epithelium and hepatocytes showed weak cytoplasmic Periostin expression. In HCC, there was strong epithelial Periostin expression in 19/91 (20.9%) and strong stromal Periostin expression in 10/91 cases (11%). Epithelial expression in tumour cells was significantly associated with a higher tumour grade ($p<0.05$) and HBV infection ($p=0.007$). Importantly, there was no strong Periostin expression in benign liver tumors. Strong stromal Periostin expression was detected in 78/116 (67.2%) BDC and strong epithelial expression in 39/116 (33.6%) BDC. pT stage, differentiation grade and proliferation rate in primary BDC were independent of Periostin expression. Epithelial Periostin expression was associated with reduced overall-survival in univariate and multivariate analysis.
Conclusions: The EMT protein Periostin is expressed in the stroma and epithelium of a subset of BDC and HCC. Epithelial Periostin expression is a marker for malignant transformation of hepatocytes and a novel prognostic marker in BDC.

1648 Fibrolamellar Carcinomas Are Positive for CD68

HM Ross, MM Yeh, TT Wu, HR Makhlouf, HH Daniel, P Vivekanandan, R Kannangai, M Torbenson. Johns Hopkins Hospital, Baltimore; University of Washington, Seattle; Mayo Clinic, Rochester; Armed Forces Institute of Pathology, Washington, DC.
Background: Fibrolamellar carcinomas are a unique type of liver carcinoma that arise in non-cirrhotic livers of young individuals. Despite their distinctive appearance, recent studies have demonstrated a lack of consistency in how fibrolamellar carcinomas are diagnosed by pathologists. Interestingly, gene expression studies show an increased expression of CD68 in these tumors. The CD68 gene encodes for a transmembrane glycoprotein located within lysozymes and endosomes. Thus, macrophages as well as other cell types rich in lysozomes/endosomes are CD68 positive. In this study, the staining pattern of CD68 was explored in the epithelial cells of both fibrolamellar and typical hepatocellular carcinomas.
Design: Cases were collected from 4 academic centers. To be sure of the appropriate diagnosis, only full sections from completely resected tumors were evaluated. Control groups included hepatocellular carcinomas arising in both non-cirrhotic livers as well as cirrhotic livers. A group of cholangiocarcinomas were also stained. CD68 immunostaining was scored for both intensity and distribution on a scale of 0 to 3+.
Results: 23 primary fibrolamellar carcinomas and 9 metastases (total of 24 individuals) were immunostained and showed a distinctive granular, dot-like or stippled pattern of cytoplasmic staining in nearly all cases (31/32), with a median distribution and intensity score of 3+. In control hepatocellular carcinomas that arose in non-cirrhotic livers, 10/39 showed CD68 staining with a median distribution and intensity score of 2+. In 4 of these 10 cases, there was a stippled dot-like cytoplasmic staining similar to fibrolamellar carcinomas, while 6 cases showed diffuse cytoplasmic positivity. In hepatocellular carcinomas arising in cirrhotic livers, 3/27 cases showed CD68 positivity, all with stippled dot-like cytoplasmic staining similar to that of fibrolamellar carcinomas. All 5 cholangiocarcinomas were negative. Overall, CD68 positivity was strongly associated with fibrolamellar carcinomas, $p<0.001$.
Conclusions: Fibrolamellar carcinomas have a distinctive stippled cytoplasmic staining for CD68, likely reflecting increased numbers of cytoplasmic lysosomes. This staining pattern is not specific and can be seen in a subset of typical hepatocellular carcinomas, but the lack of a stippled cytoplasmic pattern would strongly suggest a tumor is not a fibrolamellar carcinoma.

1649 Expression of Glypican-3 (GPC-3), Heat Shock Protein 70 (HSP70), and Glutamine Synthetase (GS) in Non-Exocrine Tumors of the Pancreas: A Tissue Microarray Analysis

R Sela, F Remotti, H Remotti. Columbia University Medical Center, New York, NY.
Background: A 3-marker panel of Glypican-3 (GPC-3), Heat Shock Protein 70 (HSP70), and Glutamine Synthetase (GS) has been shown to be sensitive and highly specific for diagnosing well differentiated hepatocellular carcinoma (HCC) on biopsy, when at least 2 of 3 markers are positive. Prior studies on the 3-marker panel have focused on differentiating non-neoplastic liver, dysplastic liver nodules, hepatic adenomas, or focal nodular hyperplasia from HCC. To date no study evaluated expression of these markers in tumors that may present as a solitary metastasis to the liver. Certain non-exocrine pancreatic tumors, including pancreatic endocrine neoplasms (PEN), solid pseudopapillary tumors (SPPT), acinar cell carcinomas (ACC) and pancreatoblastomas (PB) may present as a single liver lesion, in the absence of an identified lesion in the

pancreas. In the present study we looked at expression of the 3-marker panel in these pancreatic tumors.
Design: Paraffin-embedded TMAs sampling 59 PEN, 10 SPPT, 2 ACC, and 1 PB were stained for GPC-3 (Santa Cruz Biotechnology, SC-24)), HSP70 (Cell Marque, 261M-96), and GS (Millipore/Chemicon, MAB302). The degree of staining was graded on a scale from 1+ to 3+ and the percentage of positive staining cells was recorded.
Results: Two of three markers were positive in 11 of 59 PEN (19%); all 11 of which co-expressed HSP70 and GS. None of the PEN were positive for all three markers. Seven of 10 (70%) of SPPT were positive for either two (5/10) or three (2/10) markers. Of the five cases positive for two markers, four were positive for HSP70 and GS and one was positive for GPC-3 and GS. Neither the ACC (2 cases) nor the PB (1 case) showed positivity for two or more of the stains.
Conclusions: The immunoprofile of PEN and SPPT of the pancreas, with respect to the 3-marker panel (GPC-3, HSP70, and GS), may overlap with the immunoprofile of hepatocellular carcinomas and may be a diagnostic pitfall if a limited panel of immunohistochemical stains is performed.

1650 Symptomatic Traumatic Neuroma Causing Common Bile Duct Stricture Following Orthotopic Liver Transplantation: A Retrospective Three and a Half Year Review

MJ Shealy, DM Cardona, JL Burchette, TJ Cummings, AD Smith, DN Howell, CD Guy. Duke University Medical Center, Durham, NC.
Background: Traumatic neuromas (TN) result from abnormal regeneration of peripheral nerve fibers following trauma. Symptomatic TNs causing common bile duct (CBD) stricture following orthotopic liver transplant (OLT) are rarely reported. We present 7 cases of clinically significant bile duct TNs following OLT and examine their role in the need for retransplantation.
Design: A retrospective review of our pathology database between 1/1/06 and 7/1/09 identified 17 patients that underwent hepatectomy with repeat transplant (n=16) or bile duct revision (n=1) at least 1 month following OLT. Sections of CBD were examined using H&E and an immunohistochemical stain for S100 protein and were reviewed by a neuropathologist masked to the study.
Results: Within the group, 10 (59%) demonstrated neural abnormalities of the CBD including 7 (41%) TNs and 3 (18%) lesions characterized as neural hyperplasia. All 7 cases of TN had radiographic and histological evidence of CBD stricture/compromise between 1 and 4.5 months (mean=3.4) following OLT, while the time to either revision or retransplant varied from 8 to 35 months (mean=19.6) (table 1). The donor bile duct appeared to be the origin of the TN in 5 cases (71%). There was an association with chronic hepatitis C infection in the TN cases when compared to non-TN cases requiring retransplant.

Table 1. Clinical, pathologic and radiographic findings of the patients with a traumatic neuroma.

Case	Age	Sex	Primary Dx	ERCP Findings	Corresponding Liver Biopsy	Stricture Dx Interval	Retransplant/ Revision Interval
1	56	M	Chronic hepatitis C	anastomotic stricture	mild cholangiolar proliferation with canalicular cholestasis	4.5 months	12 months
2	51	M	Chronic hepatitis C	distal CBD stricture	extensive cholangiolar proliferation and cholestasis	4 months	27 months
3	49	M	Chronic hepatitis C	distal CBD stricture	cholangiolar proliferation and mild cholestasis	1 month	8 months
4	51	M	Chronic hepatitis C	distal CBD stricture	cholangiolar hyperplasia and mild cholestasis	3 months	35 months
5	57	M	Chronic hepatitis C	CBD mass	extensive cholangiolar proliferation and cholestasis	4 months	32 months
6	12	F	Hepatopulmonary Syndrome	distal CBD stricture	cholestasis and bile duct injury	3 months	12 months
7	57	M	Cryptogenic Cirrhosis	mild distal CBD stricture	mild cholangiolar proliferation and telangiectatic vessels	4 months	13 months

Conclusions: In our retrospective review, bile duct TNs were seen in every case of clinically significant CBD stricture leading to bile duct revision or retransplant. The majority of the TNs in our series appear to be of donor origin with a possible association with chronic hepatitis C infection. Of the remaining retransplant cases due to bile duct stricture formation, three cases demonstrated neural abnormalities in the form of hyperplasia, which may represent early, yet symptomatic lesions. We conclude the incidence may be significantly higher than what has been previously reported in the literature and should be considered in the differential when managing post-operative bile duct strictures.

1651 Intrapancreatic Cholangiocarcinomas: A Clinicopathological and Immunohistochemical Analysis

J Shen, I Konstantinidis, CR Ferrone, V Deshpande. Massachusetts General Hospital, Boston, MA.
Background: Intrapancreatic cholangiocarcinomas (ICC) are distal common bile duct (CBD) tumors that may be indistinguishable from pancreatic ductal adenocarcinomas (PDAC). The diagnosis of ICC is dependant on the pattern and extent of bile duct involvement, including the presence of dysplasia. However, there have been no prior attempts to explore ICC pathologically and genetically. The aim is to characterize the pathological features of ICC and their association with a panel of tumor suppressors or oncogenes.
Design: We reviewed 100 resections in which the tumors were located adjacent to the CBD. The tumor microscopically involved the CBD in 64 cases, and these formed the study group. Two patterns of tumor growth were recognized: type I tumors demonstrated circumferential and symmetrical involvement of the bile duct, whereas in type II tumors the epicenter of the tumor located away from the CBD. Pathological correlates were analyzed and compared between the two subtypes. A tissue microarray (TMA) was constructed, and immunohistochemical studies for p16, p53, EGFR, INI1, Her2/Neu, and B-catenin were evaluated and compared between two subtypes. A positive staining was recorded when more than 5% of cells are stained, and only nuclear positivity is recorded for B-cateinin, p16, INI1, and p53.
Results: We first classified 37 patients as type I and 27 as type II. Type I lesions were associated with bile duct dysplasia, (46% vs 11%, p=0.03) whereas type II lesions were statistically more likely to be associated with high-grade PanIN (41%vs 8%, p=0.002). Of these patients, 22 from type 1 and 7 from type 2 showed reliable results for immunohistochemical studies on TMA and were included for analysis. Type I showed more staining than type 2 for p53 (82% vs 29%;p=0.016), and p16 (45% vs 14%;p=NS). Neither nuclear positivity for B-cateinin nor loss of INI1 was observed in either group.

	p53	p16	EGFR	Her2/Neu
Type 1 (n=22)	18 (82%)	10 (45%)	7 (32%)	1 (5%)
Type 2 (n=7)	2 (29%)	1 (14%)	2 (29%)	0 (0%)
p value	p=0.016	p=0.202	p=1.000	p=1.000

Conclusions: Intrapancreatic cholangiocarcinoma is a heterogeneous group. Type 2 peribiliary intrapancreatic adenocarcinomas are pathologically more related to PDACs, while type 1 tumors likely represent true cholangiocarcinomas. The differential expression of P53 raises the possibility that the mutational profile of ICCs differs from PDACs.

1652 Dramatic Pancreatic Duct Strictures Secondary to Small Endocrine Neoplasms: A Manifestation of Serotonin Production?

C Shi, SS Siegelman, S Kawamoto, CL Wolfgang, RD Schulick, A Maitra, RH Hruban. Johns Hopkins School of Medicine, Baltimore, MD.
Background: We observed six pancreatic endocrine neoplasms (PENs) associated with stenosis of the pancreatic duct out of proportion to the size of the tumors on computed tomography (CT). In this study, we attempted to elucidate if serotonin production by PENs is associated with this pattern of pancreatic duct stenosis.
Design: Clinical presentations and radiographic findings of these six patients were reviewed. Gross findings and histology of the resected pancreata were also assessed. Formalin-fixed, paraffin-embedded tumor sections were immunolabeled with an antibody to serotonin. Tissue microarrays constructed from 47 PENs in our bank were used as control. Histology and serotonin immunoreactivity were compared between the two groups.
Results: Four of 6 PENs with associated pancreatic duct stricture had prominent stromal fibrosis. Serotonin immunoreactivity was present in 5 cases (5/6, 83%), and this labeling was very strong and diffuse in the 4 cases with prominent fibrosis. By contrast, stromal fibrosis was minimal in the non-immunoreactive case. Only 3 of 47 control PENs (6%) were immunoreactive for serotonin ($P<0.01$, X^2 test).
Conclusions: These data suggests that serotonin produced by PENs may be associated with local fibrosis and stenosis of the pancreatic duct. Clinicians should be aware that small PENs can produce pancreatic duct stenosis resulting in dramatic ductal dilatation and/or upstream pancreatic atrophy out of proportion to the size of the tumor.

1653 Extensive Fatty Replacement of the Pancreas: Its Clinicoptahological Features

M Shimizu, H Yamaguchi, K Nagata, L Jin, S Sannohe, T Ichimura, T Sakurai, Y Shimizu, A Sasaki, S Murata, M Yasuda. Saitama Medical University, Saitama International Medical Center, Hidaka City, Saitama, Japan.
Background: Fatty replacement is also known as lipomatosis, which results from a partial replacement of the acini by fatty tissue, without any significant inflammation or scarring. When it shows a significant replacement of the exocrine elements by adipose tissue, it may be called "lipomatous psuedohypertrophy." However, these lipomatous lesions are not fully described in the literature.
Design: In this study, we use the term "extensive fatty replacement." Here, we defined extensive fatty replacement of the pancreas as an entity in which "macroscopically at least two of the three segments (pancreatic head, body, and tail) are replaced by fatty tissue, and microscopically more than 50% of the section is replaced by fatty tissue". We reviewed eight cases of extensive fatty replacement of the pancreas, including one surgical case and seven autopsy cases. We investigated the clinicopathological features of these cases.
Results: The average age of the patients studied ranged 49 to 89 years, and most cases were female. Three cases had a pancreatic mass in the head, and obstructive jaundice was noted. Another four cases revealed diabetes mellitus. One case showed alcoholic liver cirrhosis. In all cases, the pancreatic duct either had disappeared or was obstructed. Most cases revealed fatty replacement of the pancreatic body and tail. Microscopically, mature adipose tissue replaced the acini and most of the ducts. The islets were mostly preserved, but parts of the acini and ducts were also preserved. Arteriosclerosis was noted in half of the cases. There was no significant inflammatory infiltrate, nor was there any scar formation.
Conclusions: Extensive fatty replacement of the pancreas is predominantly found in females with an average age of 70. It is also associated with diabetes mellitus as well as pancreatic head tumors. Entrapped islets within the fatty tissue are a histopathological clue to rule out congenital defect of pancreatic body and tail.

1654 Nodular Elastosis of the Liver: An Under-Recognized Pseudotumor Associated with Segmental Atrophy

AD Singhi, HR Makhlouf, A Mehrotra, Z Goodman, RA Anders, U Drebber, H Dienes, M Torbenson. Johns Hopkins, Baltimore, MD; AFIP, Washington, DC; AIPL, Washington, DC; University of Cologne, Cologne, Germany.
Background: Elastotic nodules within the liver are a rare type of pseudotumor that can be associated with areas of segmental or lobar atrophy. These pseudotumors are under-recognized as a diagnostic entity and can be diagnostic challenges because they can present as mass lesions, can demonstrate a range of histological appearances,

and because the associated atrophy may not be evident on imaging studies or gross examination. To better understand the full clinicopathological spectrum of this lesion, cases were collected from 3 academic centers.

Design: 16 cases were identified including resections (3), wedge biopsies (10), and needle biopsies (3). Clinical and histological features were evaluated.

Results: A modest female predominance (12/17, 71%) was seen. Ages at presentation ranged from 14 to 91 years (median 65 years). The most common clinical presentation was right upper quadrant abdominal pain (13/17, 76%). All cases showed evidence of a mass lesion. The majority of lesions were subcapsular (14/17, 82%) and ranged in size from 1.8 to 10.0 cm. Based on size, most cases appeared to involve a segment of the liver and only rarely the entire lobe. A striking feature in all cases was the presence of abnormally thick-walled and often thrombosed vessels, typically at the edge of the lesion. Both arteries and veins were affected. Examination of the histological findings for the entire series of cases suggested a sequences of changes, with early lesions (N=4) composed of collapsed hepatic parenchyma with occasional islands of residual hepatocytes and brisk bile ductular proliferation. These cases showed relatively mild elastosis. Other cases (N=10) showed little or no ductular proliferation but had increased levels of elastosis. Finally, 3 cases were composed almost solely of elastosis with small scattered islands of unremarkable hepatocytes. Biliary cysts were also a common finding (6/17, 35%).

Conclusions: Segmental atrophy of the liver is typically subcapsular and is strongly associated with evidence of vascular injury. The lesion appears to have multiple stages marked initially by parenchymal collapse and ductular proliferation, followed by a stage showing resolution of the ductular reaction and increased levels of elastosis. In its final stage, segmental atrophy can present as essentially a pure elastotic nodule of liver.

1655 Mucinous Carcinoma (MC) of the Gallbladder (GB): Clinicopathologic Analysis of 14 Cases Identified among 606 GB Carcinomas

O Tapia, JC Roa, A Cakir, N Dursun, I Coban, O Basturk, J Cheng, J Sarmiento, H Losada, NV Adsay. U de La Frontera, Temuco, Chile; Emory U, GA; NYU, NY.

Background: There is virtually no data in the literature regarding the incidence, subtypes & clinicopathologic characteristics of MC of GB.

Design: 606 primary invasive GB carcinomas were reviewed. Extracellular mucin production of variable degrees & patterns was identified in 40(6%). Those with ≥50% of the tumor showing *stromal* mucin deposition (14 cases, 2.3%) were classified as *MC*. Remainders (26 cases, 3%) were excluded as *adenocarcinoma with focal mucinous differentiation*.

Results: **Clinical:** Mean age=64. F/M=1.6 (*vs* 3.8 of usual GB carcinomas; UCa). **Pathology:** Mean & median tumor sizes were larger than those of UCas (4.8 & 3.4 *vs* 2.7 & 2.4 cm, respectively; p=0.034). MCs revealed 3 histologic patterns: **I.**Colloid(2/14): >90% composed of well-defined stromal mucin nodules, some containing scanty ca cells, mostly floating within the mucin. **II.**Mixed-mucinous(7/14): Substantial amount (up to 50%) of other Ca component in addition to at least 50% mucinous pattern. **III.** Mucinous signet-ring cell(5/14): Both the cells within the mucinous component and those infiltrating into the stroma (individually or in cords) are mostly of signet-ring morphology. 3/14 MCs were associated with an intramucosal papillary neoplasm of villous-intestinal pattern. **IHC:** MCs lacked the gastric-pancretobiliary differentiation marker(MUC6) and some of the intestinal differentiation markers(CDX2/CK20); although colloid marker(MUC2) was expressed.

CK7	CK20	MUC1	MUC2	MUC5AC	MUC6	CDX2	p53
4/7	2/7; F	3/7	6/7	6/7	0/7	1/7 F	3/7 (1; F)

F:Focal

MLH1 and MSH2 was retained in all 7 tested. **Outcome:** F/U was available in 11: 10 died of disease (1-37 mos), 1 was alive (23 mos). Median survival was worse than that of UCas (13.7 *vs* 49.8 mos); however, the difference in estimated survival probabilities was not significant, due to small number of MCs (p=0.09).

Conclusions: Focal/aberrant mucinous differentiation is noted in 6% of GB carcinomas; however, MCs (defined as >50% with stromal mucin) constitute 2.3% and typically present as large tumors. Most are mixed type (not pure colloid), which goes along with their aggressive behavior; their prognosis appears to be even worse than usual GB carcinomas. Immunophenotypically, they are different from usual GB carcinomas by MUC6 negativity, from intestinal carcinomas by an inverse CK7/20 profile, and pancreatic MCs by CDX2 negativity. Unlike gastrointestinal MCs, they appear to be microsatellite stable.

1656 IHC for Foxp3, CD4 and CD8 Lymphocytes Aid in the Diagnosis of Acute Rejection vs. HCV Recurrence in Liver Transplant Biopsies

A Tholpady, G Krueger, B Zhao, RE Brown, N Tatevian. UT Health Science Center at Houston, Houston, TX.

Background: End-stage liver disease due to Hep C is the most common indication for liver transplantation. Fresh donor liver transplant is inevitably doomed to recurrent HCV (rHCV) in these patients, which is further complicated by the risk of acute rejection (AR). Distinguishing between the two can be a diagnostic challenge by H & E alone. In this study, we used the IHC markers CD4, CD8 and Foxp3-a marker for regulatory Tcells (Tregs)-to aid in diagnosis.

Design: Biopsies from explant liver and donor pre- and post-transplant over the course of 132 weeks were stained with H&E and scored for rHCV and AR by the Scheuer system and rejection activity index (RAI). IHC was performed with Foxp3, CD4 and CD8. Average numbers of positive cells were calculated in 10 high power fields in liver lobules (LL) and in 10 portal areas (PA) in each biopsy.

Results: As seen here:

Quantity of Foxp3 and CD8 cells in PAs and LL

Diagnosis	Time (weeks)	CD8/hpf	CD8/PA	Foxp3/hpf	Foxp3/PA
Explant (cirrhotic liver, S 3-4)	0	2.2	32.2	0.8	7
No AR, no rHCV	1.4	3.6	29.4	0.4	3
Donor pre-transplant	0	3.8	8	0.2	3.8
rHCV (G 2/4, S 1/4) no AR	132	4.8	81.3	1.8	7.6
rHCV (G 2/4, S 1/4), AR?	111	8.3	50	3.7	9
rHCV (G 2/4, S 1/4), AR?	85.7	10	88	1.8	23.9
rHCV (G 3/4, S 3/4), RAI=6/9	60	28.9	206	4.3	33.5
rHCV (G3/4, S 1/4), RAI=5/9	128	33.2	138	6.1	33.8
RAI 7/9	9	33.7	102.5	0.9	2.2

hpf=40x mag., rHCV=grade and stage

CD8 cells are markedly increased in LL from biopsies with AR alone or concurrent AR and rHCV (>28/hpf) in comparison to biopsies without AR (<10/hpf). Foxp3 cells in LL were decreased in AR alone (<1/hpf) vs. rHCV (>1.7/hpf). The distribution of both CD8 and Foxp3 in PAs showed a similar but less correlative trend. A striking pattern was observed in biopsies with both AR and rHCV where CD4 cells formed nodules in portal areas while CD8 cells remained predominantly in the periphery.

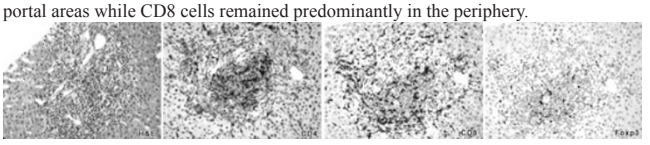

Conclusions: In cases with AR, CD8 lymphocytes were remarkably increased in a diffuse manner. Foxp3 lymphocytes were rarely seen in AR but increased in # when rHCV occured. Our preliminary results show these immunohistochemical markers to be useful in diagnosing AR and rHCV.

1657 Repression of E-Cadherin by the Polycomb Group Protein EZH2 in Pancreatic Cancer

AD Toll, A Dasgupta, M Potoczek, CG Kleer, JR Brody, AK Witkiewicz. Thomas Jefferson University Hospital, Philadelphia, PA; University of Michigan, Ann Arbor, MI.

Background: Pancreatic ductal adenocarcinoma (PDA) is the fourth leading cause of cancer deaths in the United States. Single-agent gemcitabine remains the standard treatment for advanced PDA, which has shown improvement in disease-related symptoms and a modest benefit in survival. A recently discovered histone methyltransferase termed enhancer of zeste homologue 2 (EZH2) was found to be overexpressed in a variety of carcinomas including PDA. Silencing of E-cadherin was proposed as a mechanism by which EZH2 mediates tumor aggressiveness. Furthermore, in-vitro studies showed EZH2 depletion sensitizes pancreatic cancer cells to gemcitabine. In this study we correlated EZH2 with E-cadherin expression in PDA, and evaluated response to gemcitabine in relation to EZH2 expression.

Design: 43 PDAs, 14 intraductal papillary mucinous neoplasms (IPMNs), and 5 chronic pancreatitis (CP) cases were stained with EZH2 (BD Bioscience; 1:25) and E-cadherin (Zymed; 1:1,000). Cases with diffuse weak staining, or strong staining in less than 30% of tumor nuclei were considered to have low EZH2 expression. High EZH2 expression was defined as strong nuclear staining in >30% of tumor cells. E-cadherin expression was scored on membrane positivity as follows: 0 (0-10%); 1 (10-25%); 2 (25-75%), and 3 (>75%). E-cadherin scores were considered normal at 3, reduced at 2, and negative at 1 or 0. Statistical analysis was performed using Fisher's exact and Kruskal-Wallis tests, depending on the discrete or continuous nature of the other factors. A Kaplan-Meier curve was stratified by EZH2 expression to assess survival.

Results: High EZH2 expression in PDA was significantly associated with decreased E-cadherin expression (70% vs. 35%), node-positivity (82% vs. 40%), and larger tumor size (4 cm vs. 2.4 cm). There was a trend for longer survival (35 vs. 15 months) in gemcitabine treated patients with low vs. high EZH2 expression. High EZH2 expression was detected in IMPN with moderate-severe dysplasia, however not in CP.

Conclusions: Our study suggests that E-cadherin downregulation may lead to EZH2-mediated invasion and metastasis. While strong diffuse EZH2 expression is seen in PDA, overexpression may be present in IPMN.

1658 Identification of Gastrointestinal Contamination in Pancreatic FNA

AD Toll, M Bibbo. Thomas Jefferson University Hospital, Philadelphia, PA.

Background: Endoscopic ultrasound-guided pancreatic FNA has become increasingly used in the diagnosis of pancreatic lesions. A common diagnostic dilemma occurs with the presence of suspected gastrointestinal epithelial contamination (GIC). Gastric contamination is more problematic due to its similar appearance to low-grade mucinous lesions. B72.3 showed promise in the differentiation between benign and malignant ductal epithelium in a baseline study of direct smears obtained from surgical specimens (Nawgiri, 2007). Immunohistochemical staining for CEA distinguished non-malignant cyst lining of intraductal papillary mucinous neoplasm (IPMN) from contaminating duodenal and gastric epithelium in a tissue microarray analysis (Pitman, 2009). The goal of the present study is to determine whether B72.3 and CEA can identify both duodenal and gastric contamination in cell blocks of clinically proven cases of pancreatic ductal carcinoma, IPMN, and mucinous cystic neoplasm (MCN).

Design: Cell blocks of pancreatic FNAs from 19 ductal adenocarcinomas, 8 IPMNs, 5 MCNs, and 22 cases containing GIC (7 gastric, 15 duodenal) were obtained. The material aspirated for the cell block had been immediately placed in Sacomanno fixative (containing ethanol, methanol, isopropyl alcohol and carbowax) and fixed in 10% formalin following centrifugation. The slides was stained with antibody to CEA (Dako) and B72.3 (Santa Cruz Biotechnology).

Results: CEA was positive in 89% of adenocarcinomas and 92% of mucinous lesions. It was never expressed in gastric contamination, and positive in 2/15 (13%) duodenal contaminants. B72.3 was positive in 95% of adenocarcinomas and 85% of mucinous

lesions. It was positive in 2/7 (28%) gastric and 7/15 (47%) duodenal contaminants.
Conclusions: In contrast to previous work, our preliminary results indicate B72.3 expression cannot be reliably used to identify GIC. A lack of CEA expression, however, may be used to identify both gastric and duodenal contamination. This represents an important diagnostic aid in the evaluation of suspected low-grade mucinous lesions.

1659 The Potential Role of bcl-2 and Bax Expression, Apoptosis and Cell Proliferation, after Partial Hepatectomy with and without Ischemia, on Cholestatic Livers in Rats: An Experimental Study

AC Tsamandas, J Maroulis, N Siassos, D Karavias. University of Patras Medical School, Patras, Greece.

Background: Liver regeneration after partial hepatectomy (PHx) is regulated by several factors that activate or inhibit hepatocyte proliferation. Apoptosis seems to play an important role in cellular proliferation and liver regeneration. Bax and Bcl-2 oncogenes regulate apoptotic process. This study investigates the expression of bcl-2 and bax, and the presence of apoptosis and cell proliferation (Ki67+ cells) after partial hepatectomy with and without ischemia, on cholestatic livers in rats.
Design: Sixty male Wistar rats were randomly divided into four groups (15 rats each): group I: controls, group II: common bile duct ligation (BDL) for 10 days, group III: total liver ischemia (total occlusion of hepatic artery and portal vein-TLI) for 30 minutes, and group IV: BDL for 10 days followed by TLI for 30min. After all procedures (BDL or TLI or both) were completed all 60 rats underwent PHx (68%). All rats were sacrificed 24 and 48 hrs after PHx was completed. Liver tissues were evaluated for **a)** Bax, Bcl-2 mRNA levels (real time RT-PCR) and distribution (in situ hybridization, **b)** Bax, Bcl-2 protein levels (Western blot), and distribution (immunohistochemistry), **c)** cell proliferation (Ki67+ cells-immunohistochemistry) and **d)** apoptosis (TUNEL method). Results were expressed following image analysis.
Results: Before hepatectomy, bcl-2 and bax levels (protein/mRNA), and apoptotic body index (ABI) were higher in jaundiced rats (groups II and IV) compared to non-jaundiced rats (groups I and III) ($p<0.01$ in each case). After hepatectomy, there was an early (at 24 hrs) decrease in bcl-2 levels (protein/mRNA), and a late (at 48 hrs) increase of bax levels (protein/mRNA) and of ABI in jaundiced rats (groups II and IV) compared to non-jaundiced rats (groups I and III) ($p<0.01$ in each case). Proliferation of hepatocytes (Ki67+ hepatocytes) was lower in group V (BDL + TLI), compared to that of groups II (BDL only) implying that superimposed ischemia impairs regeneration that follows PHx in cholestatic livers.
Conclusions: This study shows that hepatocyte apoptosis takes place in cholestatic livers with or without superimposed ischemia. This process may contribute to the impaired regenerative response observed in livers of jaundiced rats after partial hepatectomy.

1660 Involvement of the VHL Pathway in the Pathogenesis of Sporadic Pancreatic Endocrine Neoplasms

E Veras, L Tang, D Klimstra. Memorial Sloan-Kettering Cancer Center, New York, NY.

Background: Pancreatic endocrine neoplasms (PENs) can arise sporadically or on the basis of hereditary syndromes, including von Hippel Lindau (VHL); PENs in these patients may have clear cell features. The VHL gene is known to be involved in the development of PENs in patients with VHL syndrome but is not typically abnormal in sporadic PENs. However, the possibility that other components of the VHL pathway may be more commonly involved in the pathogenesis of sporadic PENs has not been fully explored.
Design: VHL pathway molecules were characterized by immunohistochemistry using tissue-microarray (TMA) technology in 154 PENs retrieved from our pathology archives (1973-2008). In addition to these were 8 PENs with clear cell features, including 3 from VHL patients and 5 sporadic PENs. Antibodies included hypoxia-inducible factor 1(HIF-1), carbonic anhydrase IX (CA IX), vascular endothelial growth factor (VEGF), and GLUT-1. The following scoring system was used for HIF-1 (nuclear), CAIX (membranous), VEGF (cytoplasmic) and GLUT-1 (membranous): score 1: ≤5% (+) staining; score 2: 6-50% (+) staining or diffuse, but weak staining, and score 3: >50% (+) staining. A score 2 or 3 was considered (+) and a score 1, (-). Staining results were correlated with clinical outcome.
Results: The findings are summarized in tables 1 and 2.

Table 1. VHL-related markers in PEN with / without clear cell features (CCF)

PEN	HIF 1	CAIX	GLUT-1
Without CCF	26/154 (17%)	8/154 (5%)	16/154 (10%)
With CCF	7/8 (88%)	2/8 (25%)	4/8 (50%)

Among the PEN without CCF, 4/154 (2.5%) showed concomitant positivity for CAIX, HIF-1 and GLUT-1; 6/154 (4%) were (+) for GLUT-1 and HIF-1, and 1/154 (0.6%) was (+) for CAIX and HIF-1 only. Among the PEN with CCF, 1/8 (12.5%) case showed concomitant positivity for CAIX, HIF-1 and GLUT-1 and 3/8 (38%) were (+) for HIF-1 and GLUT-1. The 3- and 5-year DSS for PENs (+) and (-) for VHL markers was 47% and 32%; 70.5% and 45%, respectively.

Table 2. Clinical data for 32 cases in which at least one VHL-related marker was reactive.

Status / Follow up (mean,mos)	Positive for any VHL-related marker
NED (44.5)	12/32* (38%)
AWD (21.7)	14/32* (44%)
DOD (63)	6/32* (19%)

Clinical data was not available in 3/35 cases.

Conclusions: The VHL pathway does not play a pivotal role in the pathogenetic development of most sporadic PENs (without CCF), with 35/154 (23%) of cases showing immunohistochemical expression of one or more molecules in this pathway. PENs (+) for VHL markers may be associated with a less favorable outcome.

1661 Leptin and Adiponectin Expression in Hepatocellular Carcinoma: Correlation with Proliferation and Prognostic Parameters

J Wang, A Page, D Lawson, C Cohen. Emory University, Atlanta, GA.

Background: Obesity, a risk factor for hepatocellular carcinoma (HCC), results in increased serum leptin and decreased serum adiponectin. *In vitro* studies show that leptin, the key regulator of energy balance and body weight, increases proliferation and induces invasion of HCC cells via JAK/STAT, ERK, and PI3K/AKT signaling pathways, and is blocked by inhibitors of these pathways. This suggests that leptin plays a crucial role in the growth, invasion, and migration of HCC. Adiponectin, however, inhibits HCC growth with a decrease in proliferation and increase in apoptosis through AMPK-JNK and AMPK-mTOR signaling pathways.
Design: 140 HCCs in 3 tissue microarrays with 2 1mm cores of each tumor were assessed for leptin and adiponectin expression. Stains, scored as intensity 0-4+ and % (+) cells, were compared to proliferation (mitoses/10HPF, MIB-1 labeling index [LI], and phosphohistone-3 [PPH3] LI using the ACIS III Image Cytometer [Dako]) and prognostic parameters (size, grade, stage, vascular invasion, metastases, and focality).
Results: Of the 140 HCCs, 105 (75%) had 3-4+ leptin expression while 42 (30%) had 3-4+ adiponectin expression. Mean mitotic count was 3.7/10HPF, MIB-1 LI was 3.7%, and PPH-3 LI was 3.6%. Leptin expression correlated significantly with proliferation (MIB-1 [p=0.038] and PPH3 [p=0.01] LIs), and stage (p=0.02), and tended to correlate with metastases (p=0.062); no other correlation was found. Adiponectin expression correlated significantly and inversely only with tumor size ($p<0.001$).

Adiponectin

Adiponectin	**0-2+**	**3-4+**	**p-value**
Size (mean)	6.3 +/- 4.6	4.0 +/- 2.5	<0.001

Leptin

Leptin	**0-2+**	**3-4+**	**p-value**
MIB-1 LI	4.7 +/- 3.9	3.4 +/- 3.1	0.038
PPH3 LI	5.0 +/- 4.3	3.1 +/- 3.3	0.01
Stage 1-2	21 (61.7%)	68 (64.8%)	
Stage 3-4	11 (32.4%)	36 (34.3%)	0.02
Mets -	23 (67.6%)	75 (71.4%)	
Mets +	3 (8.8%)	20 (19.0%)	0.062

Conclusions: In accordance with *in vitro* studies, leptin expression in human HCC sections correlated significantly with proliferation, as evaluated by MIB-1 and PPH3 LIs, but not by mitotic count, and with stage, and tended to correlate with metastases. These are congruent with its suggested role in HCC growth, invasion, and migration. Adiponectin expression correlated significantly with tumor size, consistent with its proposed role of HCC growth inhibition. Additional correlations with adiponectin may be lacking due to strong leptin effect.

1662 Peritumoral Hyperplasia of the Liver with Expression of Glutamine Synthetase – A Report of 6 Cases Adjacent to Metastatic Endocrine or Colon Carcinoma, Hepatocellular Carcinoma, or Hepatocellular Adenoma

IR Wanless, KE Fleming, TA Arnason. Dalhousie University, Halifax, NS, Canada.

Background: Peritumoral hyperplasia (PTH) has been described in liver adjacent to FL-HCC as a single case report (Wanless 2000).
Design: Since this initial report we have discovered 2 cases associated with metastatic endocrine carcinoma (EC) and single cases associated with HCC, hepatocellular adenoma (HCA), or metastatic colon carcinoma (CC). This prompted a review of 8 metastatic EC yielding an additional case of PTH. Thus we report here 6 cases of PTH present adjacent to metastatic endocrine carcinoma (3), CC (1), ordinary HCC (1), and HCA (1). These cases were stained with H&E and trichrome. Immunohistochemical stains for CD34 and glutamine synthetase were performed.
Results: The PTH width varied from minimal to 5 mm. In all cases, the central tumor deposit was hypervascular with prominent CD34 positive capillaries or sinusoids. There was evidence of hepatic vascular invasion in all cases with metastatic disease. The PTH was strongly positive for hepatocellular GS in 5/5 lesions tested with a diffuse pattern including periportal hepatocytes. CD34 was strongly expressed in PTH sinusoidal endothelial cells in 3/5 tested.
Conclusions: PTH may be seen adjacent to many types of vascular neoplasms, especially endocrine carcinoma. GS is normally found in a narrow rim of perivenous hepatocytes. However, in PTH GS is strongly expressed in perivenular and periportal hepatocytes. Recently, GS expression has been reported to be increased in perivenous hepatocytes of FNH with a map-like pattern (Bioulac-Sage 2009). Because FNH is widely believed to be a response to increased arterial blood flow, our observation indicates that PTH and FNH may be physiologically related with increased blood flow as a common factor. In addition, our observation may help to illuminate the control mechanisms of GS expression.

1663 Liver Pathology in Adult Patients with Multidrug Resistance 3 Protein Deficiency (ABCB4 Gene Mutations): Some Patients Have Small Duct Sclerosing Cholangitis

D Wendum, O Rosmorduc, V Barbu, L Arrive, J-F Flejou, R Poupon. APHP, Hopital St Antoine, Paris, France; APHP, Hopital StAntoine, Paris, France; APHP, Hôpital St Antoine, Paris, France.

Background: The multidrug-resistant P-glycoprotein 3(MDR3) encoded by the ABCB4 gene acts as a phospholipid flippase. ABCB4 gene mutations result in a spectrum of cholestatic liver diseases including progressive familial intrahepatic cholestasis type 3 (PFIC-3), low phospholipid associated cholelithiasis (LPAC) and intrahepatic cholestasis of pregnancy (ICP) or unexplained anicteric cholestasis. The aim of this study was to describe the pathological features associated with ABCB4 gene mutations in adult patients.

Design: All adult patients of our institution with an ABCB4 gene mutation who have had a liver sample with pathological analysis were included. Patients with other causes of liver disease (heavy alcohol intake, viral hepatitis) were excluded. The pathological features were analyzed without knowledge of the clinical phenotype or the type of gene mutation.
Results: 12 patients (13 liver samples) were included . Six patients had a typical LPAC syndrome : 3 had normal liver histology and 3 patients had a mild ductular reaction without fibrous septa. In one case there was ductopenia. Three patients had hepatolithiasis without sclerosing cholangitis on magnetic resonance cholangiography . On liver samples these patients had a ductular reaction with or without few septa . In 2 cases there were fibro-obliterative lesions of the interlobular bile ducts. Two patients had a biliary cirrhosis, one developed an hepatocellular carcinoma. One patient had unexplained cholestasis and liver cytolysis with, on the liver biopsy, a fibro-obliterative lesion of some interlobular bile ducts and mild ductular reaction without fibrous septa. Magnetic resonance cholangiography was normal. The patient with LPAC and ductopenia had a homozygous ABCB4 gene mutation. The patient with hepatolithiasis and small duct sclerosing cholangitis and the patient with unexplained cholestasis and small duct cholangitis had a compound heterozygous ABCB4 gene mutation All the other patients had a heterozygous ABCB4 mutation.
Conclusions: In this study we show that some adult patients with ABCB4 gene mutation have small duct sclerosing cholangitis. These lesions did not seem to be associated with a severe fibrosis. There could be an association between compound heterozygous ABCB4 mutations and small duct sclerosing cholangitis.

1664 Spectrum of Disease in Liver Biopsies from Patients with Neonatal Jaundice

M Westerhoff, RK Pai, CH Mziray-Andrew, L Hovan, A El-Gendi, R Azzam, J Hart. University of Chicago, Chicago; Washington University, St. Louis.

Background: Liver biopsy is an essential component of the diagnostic work-up of jaundiced infants. Unfortunately, there is considerable histological overlap among the various diseases that can cause jaundice in this population.
Design: The pathology database was searched for liver biopsies performed on infants under 4 months of age. Biopsies were assessed for degree of inflammation, bile duct paucity, cholestasis, steatosis, fibrosis, and giant cell change (GCC). After histological assessment, clinical records were correlated with biopsy findings.
Results: 55 cases (61% male, average age 2.5 months) had follow-up ranging 2 - 36 months. Neonatal iron (Fe) storage disease (n=8) could be identified by the presence of marked GCC, extensive pericellular fibrosis, and Fe deposition in multinucleated hepatocytes. Alagille patients (5) exhibited duct loss but little GCC, cholestasis, or inflammation. Biliary atresia (BA) was correctly identified in all 7 cases by the presence of portal fibrosis, bile ductular proliferation with bile plugs, and cholestasis. Total parenteral nutrition cases (4) also showed these features, but also exhibited macrovesicular steatosis. Biopsies from idiopathic neonatal hepatitis (NH) (17), α-1-antitrypsin deficiency (4), progressive familial intrahepatic cholestasis (2), bile acid metabolism defect (1) and pan-hypopituitarism (PHP) (6) were histologically similar, but all PHP cases exhibited bile duct paucity. The biopsy of 1 patient with established coxsackie infection exhibited prominent portal and lobular inflammation; these findings were also seen in 3 NH cases. Chart review indicated that these 3 also had sepsis, but an infectious agent was not identified in 2. All patients with idiopathic NH recovered spontaneously. 2 with neonatal Fe storage disease expired and 2 underwent transplantation, as did 1 with bile acid metabolic defect. BA patients underwent Kasai procedure.
Conclusions: Multiple disorders cause neonatal jaundice, many of which have distinctive histological features. PHP produces typical non-specific features of NH, but in addition usually exhibits bile duct paucity, which can serve as a histological marker of this disorder. Although PHP is usually thought of as a rare disorder, it accounted for 11% of the biopsies performed to evaluate neonatal cholestasis in this series. The presence of significant portal and lobular inflammation should suggest an infectious etiology, as this feature is not typical of other disorders causing neonatal jaundice.

1665 Drug-Induced Ductopenia: Natural History and p16^{INK4} Expression

M Westerhoff, L Hovan, G Yoshiba, R Pierce, J Hart. University of Chicago, Chicago.

Background: Many medications have been documented in case reports to cause cholestasis due to bile duct damage and loss, but the histological features have not been reported for a large case series. Recently, biliary p16 expression has been noted to be a marker of cellular senescence and to be important in the pathogenesis of bile duct loss in primary biliary cirrhosis (PBC). The role of p16 expression in drug-induced ductopenia has not been reported to date.
Design: The pathology database was searched for all liver biopsies with duct loss attributable to drugs; chart reviews were then performed. Biopsies (18) were stained immunohistochemically with p16. For comparison, PBC (15) and normal liver (5) were also stained. Combined nuclear and cytoplasmic staining of bile duct epithelium was scored as positive or negative.
Results: All drug-induced ductopenia patients had elevated total bilirubin (TB) (mean 22.6 mg/dL) and alkaline phosphatase (AP) levels (mean 600 U/L) at time of biopsy. Follow-up ranged from 3 - 84 months. Table 1 displays their clinical outcomes.

Table 1

		Following cessation of drug				
Drug Class	n	Re-biopsy showed resolution of duct loss (n)	Labs and symptoms improved (n)	TB or AP remained elevated; symptoms continued (n)	Expired or transplant (n)	p16 positivity (n=6)
Antibiotic	2		2			
Anti-depressant	3	2		1		1
Anti-psychotic	1			1		
Anti-seizure	3		2	1		
ACE-inhibitor	1				1	1
Weight loss	1			1		
NSAID	1	1				
Multiple drugs, no established agent	6		1	2	3	4

On average, biopsies sampled 14 portal tracts with 58% bile duct loss. 8 patients improved clinically, 1 underwent transplantation, and 3 expired. Degree of duct loss and ductular proliferation did not correlate with liver function tests (LFTs) or outcome. 3 of 4 patients improved with ursodiol treatment in addition to stopping the offending drug. All normal livers were p16 negative. 13 of 15 PBC cases had positive bile duct staining. In 6 of 18 drug-induced ductopenia cases, damaged ducts exhibited p16 reactivity. All 6 of these patients did poorly (2 deaths, 2 developed biliary cirrhosis, 2 with persistent elevated LFTs). In contrast, 8 of 12 patients with negative p16 staining improved their LFTs or showed resolution of duct loss on re-biopsy.
Conclusions: This is the largest series reporting histological features and clinical follow-up on drug-induced ductopenia. Degree of bile duct loss did not correlate with clinical severity or outcome. 44% had histological or clinical resolution by discontinuing the offending drug. However, p16 reactivity, which occurred in 33% of ductopenia cases, was associated with poor prognosis ($p<0.01$).

1666 Liver and Gallbladder Pathology in Small Duct Primary Sclerosing Cholangitis: Is There a Risk for Neoplasia?

TT Wu, S Shah, JJ Poterucha, SC Abraham. Mayo Clinic, Rochester; MD Anderson Cancer Center, Houston.

Background: The elevated risk for cholangiocarcinoma (CCA) in primary sclerosing cholangitis (PSC) is well known. Small duct PSC (i.e., biochemical and histologic evidence of PSC but normal cholangiography) forms a minor subgroup with a favorable prognosis. In particular, it is thought that small duct PSC never develops CCA outside of radiologic progression to large duct PSC. However, due to the small number of cases requiring transplant, neither the biliary nor gallbladder pathology of small duct PSC has been well characterized.
Design: We investigated the presence of metaplastic and dysplastic lesions of bile ducts and gallbladder mucosa in patients with end-stage small duct PSC who underwent liver transplant (n=8) and concomitant cholecystectomy (n=5). Extensive sections of biliary mucosa were taken (mean 14/case) and evaluated for the following: intestinal metaplasia, mucinous metaplasia, pyloric metaplasia, and dysplasia (low or high grade, papillary or flat). Small duct PSC was compared to 2 previously-characterized control groups (100 liver explants with PSC and 164 with cirrhosis from alcohol or hepatitis C).
Results: Bile duct metaplasia was found in 6 (75%) small duct PSC. Low grade dysplasia involved intrahepatic bile ducts of 3 (38%) patients, one with extensive papillary dysplasia, one with extensive flat dysplasia and one with several (7) dysplastic ducts. There was no hilar dysplasia, high grade dysplasia or CCA. None of the accompanying gallbladders had lymphoplasmacytic chronic cholecystitis. Comparison to controls is shown in Table 1.
Conclusions: Low grade biliary lesions (metaplasia and low grade dysplasia) in small duct PSC are similar to large duct PSC in frequency, but without progression to high grade dysplasia or CCA. Since most PSC-associated CCAs involve the hilum, the lack of hilar bile duct dysplasia in small duct PSC might play a protective role.

Table 1

	Small duct PSC (8)	**PSC (100)**	**Alcohol/hepatitis C cirrhosis (164)**
Intestinal metaplasia	3 (38%)	26 (26%) (ns)	8 (5%) (p=0.009)
Pyloric metaplasia	4 (50%)	73 (73%) (ns)	3 (2%) (p<0.001)
Mucinous metaplasia	7 (88%)	77 (77%) (ns)	152 (93%) (ns)
Biliary dysplasia (any)	3 (38%)	50 (50%) (ns)	85 (52%) (ns)
High grade dysplasia	0 (0%)	26 (26%) (ns)	8 (5%) (ns)
CCA or gallbladder carcinoma	0 (0%)	34 (34%) (p=0.05)	6 (4%) (ns)
Lymphoplasmacytic cholecystitis	0 of 5 (0%)	35 of 72 (49%) (p=0.06)	--

ns, not statistically significant

1667 Molecular Characteristics and Biological Behavior of Intraductal Papillary-Mucinous Neoplasm, Oncocytic Type (IPMN-O)

HD Xiao, H Yamaguchi, D Dias-Santagata, Y Kuboki, S Akhavanfard, T Hatori, M Yamamoto, K Shiratori, M Kobayashi, M Shimizu, M Mino-Kenudson, T Furukawa. Massachusetts General Hospital, Boston; Saitama Medical University, Saitama, Japan; International Research and Educational Institute for Integrated Medical Sciences, Tokyo, Japan; Tokyo Women's Medical University, Tokyo, Japan.

Background: Both IPMN-O and the pancreatobiliary type of IPMN (IPMN-PB) are usually diagnosed to have high-grade dysplasia with or without invasive components. However, since KRAS mutation has been reported to be absent in IPMN-O, some consider that IPMN-O is distinct form other types of IPMN. The aim of this study was to compare molecular alterations and biologic behavior between IPMN-O and IPMN-PB.
Design: Our cohort consisted of 12 IPMN-PBs and 18 IPMN-Os that were diagnosed and classified based on histologic and immunohistochemical evaluation. Point mutations of KRAS, BRAF and PIK3CA were studied using either multiplex PCR or by direct sequencing. Nuclear expression of p53 and ß-catenin, and loss of SMAD4 nuclear

staining were assessed by immunohistochemistry. (Table 1) The results of molecular profile and clinical outcome were compared between the 2 types.
Results: KRAS mutation was identified in 17% of IPMN-Os and in 58% of IPMN-PBs. BRAF mutation was identified only in one IPMN-O. Loss of SMAD4, overexpression of p53 and nuclear ß-catenin expression were also found in a fraction of both types (IPMN-PB ≥ IPMN-O) (Table 1).

Table 1

	IPMN-PB	IPMN-O
KRAS	7(58%)*	3(17%)*
BRAF	0	1(6%)
PIK3CA	0	0
SMAD4[a]	4(33%)	2(12%)
TP53[b]	7(58%)**	1(6%)**
β-catenin[c]	2(17%)	3(17%)

a: any loss of nuclear expression, b: presence of expression in > 30% of tumor cells, c: any nuclear expression, *: p<0.05, **: p<0.01.

92% of IPMN-PB and 50% of IPMN-O contained invasive adenocarcinoma. At the end of follow-up (1 to 165 months after resection), 4 patients with IPMN-PB and 2 with IPMN-O died of the disease. All showed invasive carcinoma. Although the overall survival was better in IPMN-O than in IPMN-PB (Kaplan-Meier survival analysis, $p < 0.05$), there was no difference in survival of cases with invasive components between the 2 types ($p = 0.16$).
Conclusions: The results of our study indicate that molecular alterations as well as biological behavior are not significantly different between IPMN-O and IPMN-PB, especially in those with invasive components. In addition, it is the first report demonstrating KRAS mutation in IPMN-O, thus supporting the notion that IPMN-O is not distinct from the other types of IPMN.

1668 Arginase-1, a New Immunohistochemical Marker of Hepatocytes and Hepatocellular Neoplasms

BC Yan, C Gong, J Hart. University of Chicago Medical Center, Chicago, IL.
Background: The distinction of hepatocellular carcinomas (HCCs) from metastatic tumors to the liver often presents a diagnostic challenge that carries significant impact on subsequent prognostication and therapeutic management. The number of immunohistochemical markers for pathologic identification of hepatocytes remains limited to HepPar-1, polyclonal CEA and CD10, with alpha-fetoprotein and glypican-3 labeling HCCs. The HepPar-1 antigen was recently shown to correspond to the urea cycle enzyme carbamoyl phosphate synthetase [Butler SL, Dong H, Cardona D, Jia M, Zheng R, Zhu H, Crawford JM and Liu C. (2008) Lab. Invest. 88: 78-88]. Previous immunohistochemical studies have established that arginase-1 (ARG1), another enzyme involved in the urea cycle, is also expressed in normal human liver with a high degree of specificity [Multhaupt H, Fritz P and Schumacher K. (1987) Histochemistry 87: 465-470].
Design: We examined the expression of ARG1 in 24 HCCs, 15 macroregenerative nodules (MRNs), 3 dysplastic nodules (DNs), 4 intrahepatic cholangiocarcinomas, 23 breast carcinomas, 15 pulmonary adenocarcinomas, 15 prostate carcinomas, 99 colonic adenocarcinomas and 111 salivary gland tumors by immunohistochemistry using a commercially available antibody (Sigma Aldrich) and heat retrieval methods for antigen unmasking to determine its viability as a hepatocellular marker.
Results: We found that ARG1 demonstrated strong, diffuse, nuclear and cytoplasmic expression in both normal hepatocytes and hepatocellular neoplasms: 23 of 24 HCCs (95%) exhibited strong, diffuse immunoreactivity for ARG1. All examined MRNs and DNs showed similar reactivity. In contrast, biliary epithelium, endothelial cells and Kupffer cells were non-reactive. A single combined HCC-cholangiocarcinoma exhibited ARG1 positivity only in the HCC component. In addition, one prostatic adenocarcinoma was also reactive. All other tumors examined were non-reactive.
Conclusions: ARG1 appears to be a specific marker of hepatocytes and, as such, can be used to distinguish hepatocellular carcinomas from metastatic tumors in the liver. The identification of ARG1 as a specific immunohistochemical marker of hepatocytes may lead to its development as a useful diagnostic adjunct in routine surgical pathology practice.

1669 The Effect of Tumor Heterogeneity on the Prognostic Value of Ki67 Labeling Index in Well-Differentiated Neuroendocrine Tumors (NETs) Metastatic to the Liver

Z Yang, LH Tang, DS Klimstra. Memorial Sloan-Kettering Cancer Center, New York, NY.
Background: The Ki67 labeling index correlates with survival in patients with NETs. A proposed grading scheme classifies well-differentiated NETs into two categories based on Ki67 index: low grade (<3%), and intermediate grade (3-20%). Metastatic NETs to the liver are often diagnosed by random needle core biopsy, and the Ki67 index is thus determined on this limited sample. The reliability of the Ki67 index has been questioned based on possible intratumoral heterogeneity.
Design: Forty-three resected cases of NET metastatic to the liver were collected. Triplet tissue cores from three random sites in the paraffin blocks were used to construct a tissue microarray, representing simulated biopsies. Immunohistochemical staining for Ki-67 was performed, and the labeling index was determined by image analysis. The overall Ki67 index was determined for each core triplet, and heterogeneity was defined as the presence of grade discordance among the 3 samples. The mitotic count of the original slides was also determined: low grade <2/10 HPF, and intermediate grade 2-20/10 HPF.
Results: Thirty-four cases had a low Ki67 index, while 8 cases had an intermediate Ki67 index; these included one case that showed an intermediate Ki67 index in one block and low in another. By Kaplan-Meier survival analysis, intermediate overall Ki67 index predicted worse overall, disease-free, and progression-free survival ($p<0.005$), compared to a low Ki67 index. Intermediate mitotic activity predicted worse progression-free survival ($p<0.05$), but not overall and disease-free survival. Thirty-eight cases (83%) were considered homogenous for Ki67 index (34 low grade and 4 intermediate grade) on simulated random biopsy, and 8 cases (17%) had heterogeneity. Statistically, there were significantly more overall intermediate grade cases showing Ki67 heterogeneity (Fisher's exact test, $p=0.02$), and in those cases, the Ki67 indices were close to the 3% cutoff value (range 2.1-3.6%). One of three cases also showed significant Ki67 heterogeneity between different metastatic foci.
Conclusions: By imaging analysis, Ki67 labeling index has significant prognostic value for patients with NETs metastatic to the liver. In most cases in particular the low grade ones, random sampling has no clear effect on the prognostic value of the Ki67 index. Ki67 staining of core biopsies usually provides an adequately reliable method of proliferation assessment for prognosis.

Neuropathology

1670 Distinction between Complete and Partial 1P/19Q Losses in Gliomas: A Novel User-Friendly Approach

A Ariza, C Carrato, MD Lopez, M Domingo-Sabat, MT Lopez, K Beyer. Hospital Germans Trias i Pujol, Autonomous University of Barcelona, Badalona, Barcelona, Spain.
Background: Complete loss of both 1p and 19q has been associated with oligodendrogliomas, whereas partial 1p loss has been related to aggressive astrocytomas. However, the two most frequently used methods for 1p and/or 19q loss determination (fluorescent in situ hybridization and microsatellite amplification) focus on 1p34-36 and 19q13 only and are thus unable to accurately distinguish between complete and partial arm losses.
Design: In an attempt to discriminate between the types of arm loss, we used semiquantitative real-time PCR of telomeric and centromeric sequences on 1 p (SPAG17, ATG4), 19q (DPY19L3, RPS9), 1q (PYGO2 and GREM2), and 19p (COPE, FUT3) in a series of 69 astrocytomas and 10 oligodendrogliomas. The deltadeltaCt method was used for relative quantification of PCR products. Conventional LOH study of 1p and 19q by microsatellite amplification was also performed in all cases.
Results: Among astrocytomas, of the 11 instances showing 1p loss and the 12 instances showing 19q loss by microsatellite amplification, our approach demonstrated the loss to be complete for 1p in just 1 instance and for 19q in just 4 instances. In contrast, each of the 10 oligodendrogliomas, all showing both 1p and 19q loss by microsatellite amplification, revealed both complete 1p and complete 19q loss by our method.
Conclusions: The rapid and easy-to-use approach herein described is a useful complementary tool for accurately determinating whether chromosome losses are complete or partial in gliomas. Of practical interest, it abolishes the need for patient's normal tissue or peripheral blood as control.

1671 Atypical Mycobacterial Brain Abscess Presenting as Spindle Cell Lesion in an Immunocompetent Patient

K Arkun, DA Gordon, C Lincoln, M Levi, J Bello, CE Keller, KM Weidenheim. Montefiore Medical Center, Bronx, NY; Albert Einstein College of Medicine, Bronx, NY.
Background: Mycobacterium Avium Complex (MAC) organisms are important secondary infections in immunocompromised patients and are usually seen in patients with AIDS. Disseminated and focal MAC infections usually involve the lungs, gastrointestinal tract and peripheral lymph nodes. It is unusual to see involvement of the central nervous system, where MAC produces imaging findings similar to tuberculoma.
Design: We present a 52-year-old HIV-negative man with a previous history of non-caseating pulmonary granulomata and lung carcinoma treated with radiotherapy, who presented with 6 month history of slowly progressive dizziness, headache,and gait disturbance with frequent falls. Tissue obtained at subtotal resection was cultured and paraffin sections were examined with the light microscope.
Results: Neuroimaging revealed a large, complex, multiloculated, ring-enhancing cystic lesion centered in the left tentorium with extension into supratentorial and infratentorial compartments. Compression of the fourth ventricle resulted in hydrocephalus that required subtotal resection of the mass and aspiration of caseous yellow material. The specimen consisted of a variably cellular proliferation of CD68-positive spindle cells arranged in bands, fascicles and ill-defined nodules. A few lymphocytes and plasma cells were seen, and a single giant cell was present. Delicate rod-shaped organisms were faintly positive using methenamine silver, Brown-Brenn Gram staining and Ziehl-Neelsen staining. The bacilli were strongly positive with Fite and Kinyoun staining, and DNA probes confirmed their identification as MAC. M. tuberculosis was not present on DNA analysis.
Conclusions: This MAC brain abscess presented as a complex mass with differential diagnosis that includes infections and tumor. Its exuberant spindle cell proliferation had a pseudosarcomatous appearance and produced difficulty in diagnosis because granulomatous features were found only focally. Clinical correlation and culture results were critical in obtaining the correct diagnosis. In the appropriate clinical setting, infectious processes including MAC-related brain abscess, should be ruled out before making the diagnosis of a spindle cell neoplasm.

1672 Expression of SALL-4 Distinguishes Intracranial Germ Cell Neoplasms from Other Central Nervous System Tumors

JK Deisch, D Rakheja, P Shang, CL Hladik, CL White, J Raisanen. University of Texas Southwestern Medical Center, Dallas, TX; Children's Medical Center, Dallas, TX.
Background: Germ cell neoplasms are relatively uncommon intracranial tumors accounting for 0.3-0.6% of primary intracranial neoplasms in the Western hemisphere and 2-3% in Eastern Asia. Most occur in children and young adults, most in males, and